

MoDOT

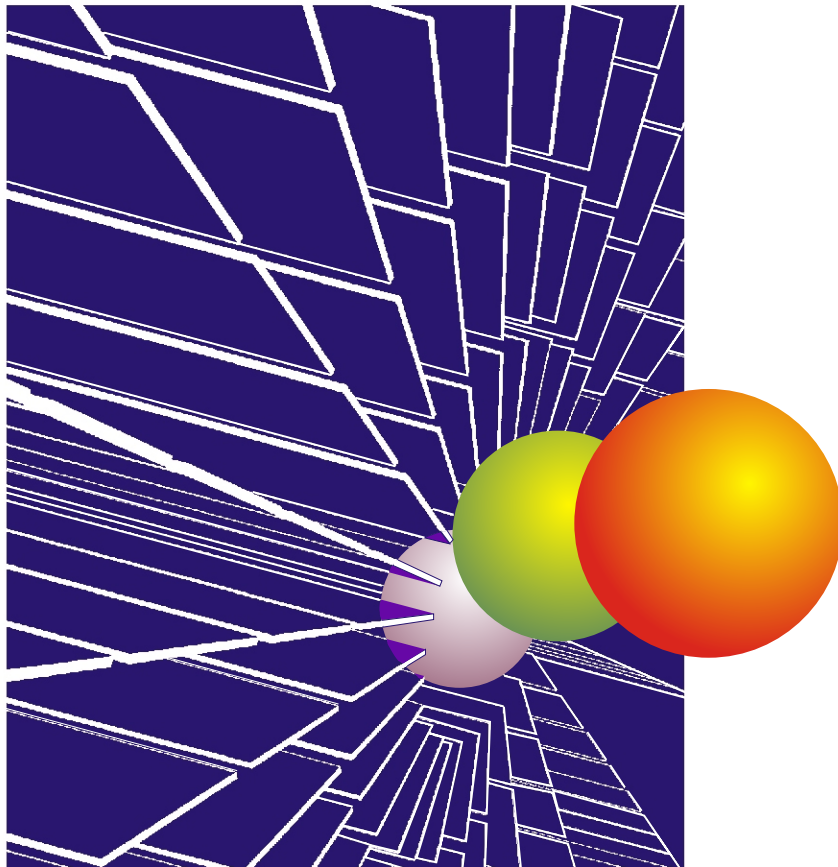
Research, Development and Technology

University of Missouri-Columbia

RDT 03-019

Evaluation of Recycled Plastic Products in Terms of Suitability for Stabilization of Earth Slopes

RI 98-007C



November, 2003

TECHNICAL REPORT DOCUMENTATION PAGE

1. Report No. RI98-007C/RDT 03-019	2. Government Accession No.	3. Recipient's Catalog No.	
4. Title and Subtitle Evaluation of Recycled Plastic Products in Terms of Suitability for Stabilization of Earth Slopes		5. Report Date November 2003	
		6. Performing Organization Code	
7. Author(s) John J. Bowders, J. Erik Loehr and Cheng-Wei Chen		8. Performing Organization Report No.	
9. Performing Organization Name and Address University of Missouri-Columbia; Columbia, MO 65211-2200		10. Work Unit No. RDT 03-019	
		11. Contract or Grant No.	
12. Sponsoring Agency Name and Address Missouri Department of Transportation Research, Development and Technology Division P. O. Box 270-Jefferson City, MO 65102		13. Type of Report and Period Covered Final Report	
		14. Sponsoring Agency Code	
15. Supplementary Notes This report is based on work supported by the Federal Highway Administration under Cooperative Agreement No. DTFH61-98-X-00095 through the Recycled Materials Resource Center at the University of New Hampshire, Durham, New Hampshire.			
16. Abstract Slender recycled plastic pins (RPPs) can be used to stabilize earthen slopes by driving the RPPs into the face of the slope to intercept the sliding surface and "pin" the slope. For RPP technology to become widely applied, a specification for accepting or rejecting particular products is required. In this work, engineering properties and field performance of four types of RPPs were evaluated and a draft specification was developed. Compressive strengths ranged from 1600 psi to 3000 psi and compressive moduli ranged from 80 ksi to 190 ksi at one percent strain. Flexural strengths ranged from 1300 psi to 3600 psi and flexural moduli varied from 90 ksi to 250 ksi at one percent strain. Arrhenius modeling showed creep failure ranged from 45 to 2000 years at field temperature and stress levels. Installation stresses did not alter the strengths of the RPPs. A draft specification for RPPs to be used to stabilize slopes includes "design" compressive (1500 psi) and flexural (1200 psi) strengths for RPPs tested at the field strain rate (0.00003 in/in/min); or establishing a compressive strength versus strain rate behavior and estimating the compressive strength at the field strain rate; or a minimum compressive strength of 3750 psi at a strain rate of 0.03 in/in/min. The "design" flexural strength is 1200 psi at two percent center strain, when tested in four-point flexure using a crosshead displacement rate of 0.02 in/min or 2000 psi if displaced at 1.9 in/minute. To ensure durability to environmental exposures, the RPPs must consist of more than 60 percent polymeric material or exposure testing must be performed. Finally, the RPP should not fail (break) under a cantilever bending load that generates an extreme fiber stress of at least 50 percent of the design compressive strength when subjected to the load for 100 days. Exposure testing and Arrhenius modeling are offered as alternate means to qualify the durability a material.			
17. Key Words Geotechnical, Slope Stability, Reinforced Slopes, Maintenance, Repair, Recycled Plastic Pins, Stabilization, Material Properties, Specification		18. Distribution Statement No restrictions. This document is available to the public through National Technical Information Center, Springfield, Virginia 22161	
19. Security Classification (of this report) Unclassified	20. Security Classification (of this page) Unclassified	21. No. of Pages 125	22. Price

Final Report

RDT 03-019

Research Investigation 98-007C

**Evaluation of Recycled Plastic Products in Terms of
Suitability for Stabilization of Earth Slopes**

PREPARED FOR:

MISSOURI DEPARTMENT OF TRANSPORTATION
RESEARCH, DEVELOPMENT AND TECHNOLOGY
JEFFERSON CITY, MISSOURI

BY:

Dr. John J. Bowders, PE
Professor of Civil Engineering

Dr. J. Erik Loehr, EIT
Assistant Professor of Civil Engineering

Mr. Cheng-Wei Chen
Graduate Research Assistant

Department of Civil & Environmental Engineering
University of Missouri-Columbia

DATE SUBMITTED: November 2003

The opinions, findings, and conclusions expressed in this publication are those of the principal investigators and the Missouri Department of Transportation; Research, Development and Technology. They are not necessarily those of the U.S. Department of Transportation, Federal Highway Administration. This report does not constitute a standard or regulation

Acknowledgements

The encouragement and support of Mr. Thomas Fennessey, technical liaison for this project, Missouri Department of Transportation, is always appreciated.

This program would not have been possible without the kind cooperation of Bedford Technology, LLC (Ms. Rachel Aanenson), Epoch Composite Products (Mr. Randy Jolitz), and Resco Plastics (Ms. Sabine Zink). These manufacturers provided their products for testing and evaluation.

Support for the field installations at the I435 sites in Kansas City was received from MoDOT District 4. Mr. Bill Billings was exceptionally supportive of this effort.

The Judy Company, Mr. Pat Carr, president, contributed construction and installation services for the field sites.

This report is based on work supported by the Federal Highway Administration under Cooperative Agreement No. DTFH61-98-X-00095 through the Recycled Materials Resource Center at the University of New Hampshire, Durham, New Hampshire.

Executive Summary

An ongoing demonstration project has shown the feasibility of using slender recycled plastic pins (RPPs) for in situ reinforcement of earthen slopes. The technique uses RPPs driven into the face of the slope in a grid pattern to intercept the sliding surface and “pin” the slope. The compressive, tensile, and flexural strength along with creep behavior dictate the design. Constituent materials and manufacturing processes are highly variable among the US manufacturers. In order for RPP technology to become widely applied, it is imperative to have a suitable specification for accepting or rejecting particular products. The specification must consider both the installation and performance requirements of the pins. Test methods were established and the engineering properties and driving performance of four different types of RPPs were evaluated.

Compressive strengths ranged from 1600 psi to 3000 psi (11 MPa to 21 MPa) with extruded products about 20 percent lower than compression molded products. Compressive moduli ranged from 80 ksi to 190 ksi (552 MPa to 1310 MPa) at one percent strain and the fiberglass-reinforced products were about 60 percent stiffer than unreinforced products. The flexural strengths ranged from 1300 psi to 3600 psi (9 MPa to 25 MPa), but there was significant variability. The flexural moduli varied from 90 ksi to 250 ksi (621 MPa to 1724 MPa) at one percent strain. Although the RPPs are creep sensitive, Arrhenius modeling indicated that at field temperature and stress levels, creep failure ranged from 45 to 2000 years. Installation stresses did not alter the strengths of the RPPs.

A draft specification for RPPs includes requirements for: (A) minimum compressive strength, (B) flexural strength, (C) durability to environmental exposures

and (D) durability to creep bending loads. The minimum compressive strength tested at field strain rates is 1500 psi and minimum flexural strength is 1200 psi for RPPs to be used in stabilization of slopes. Ideally, these strengths should be determined using the field strain rate (0.00003 in/in/min); however, this rate is too slow for production facilities. Therefore, alternatives for qualifying an RPP material are provided. Two alternatives for compressive strength include: Alternate A1 -establishing a compressive strength versus strain rate behavior and estimating the compressive strength at the field strain rate, or Alternate A2 - a compressive strength of 3750 psi (25.9 MPa) or better when tested at the ASTM D6108 strain rate of 0.03 in/in/min (0.03 mm/mm/min). The latter value represents the increase in strength realized by the 3-order of magnitude increase in strain rate, i.e., above the field strain rate of 0.00003 in/in/min (0.00003 mm/mm/min), using a reasonable upper-bound for strain rate effects. The “design” flexural strength is 1200 psi (8.3 MPa) at less than or equal to two percent center strain, when tested in four point flexure using a crosshead displacement rate of 0.02 in/min (0.51 mm/min). The alternative for the flexural strength (Alternative B1) allows for the use of ASTM D6109 crosshead deformation rate of 1.9 in/min (48.3 mm/min); however, the required flexural strength is 2000 psi (13.8 MPa) at less than or equal to two percent center strain. To ensure durability to environmental exposures, the RPPs must consist of more than 60 percent polymeric material or exposure testing must be performed. Finally, the RPP should not fail (break) under a cantilever bending load that generates an extreme fiber stress of at least 50 percent of the design compressive strength when subjected to the load for 100 days. Exposure testing and Arrhenius modeling are offered as alternate means to qualify the durability a material.

Due to the potential for a wide variability in manufacture-supplied products, additional materials should be obtained, evaluated and findings incorporated into the RPP material property database in order to strengthen the specification.

TABLE OF CONTENTS

ACKNOWLEDGEMENTS	iii
EXECUTIVE SUMMARY	iv
TABLE OF CONTENTS.....	vii
LIST OF TABLES	x
LIST OF ILLUSTRATIONS.....	xii
CHAPTER	Page
1. INTRODUCTION	1
1.1 Background.....	1
1.2 Objectives	1
1.3 Scope of Work	2
2. LITERATURE REVIEW	4
2.1 Introduction.....	4
2.2 Slope Stability.....	4
2.3 Stabilizing Methods	4
2.4 Recycled Plastic Pins Method.....	5
2.5 Sources and Manufactured Processes of Recycled Plastic Pins	7
2.6 Engineering Properties of Recycled Plastic Lumber	9
2.7 Summary	14
3. MATERIALS AND METHODS.....	16
3.1 Overview.....	16
3.2 Materials	16
3.3 Laboratory Methods.....	18

3.3.1	Uniaxial Compression Test.....	18
3.3.2	Four-Point Flexure Test	21
3.3.3	Flexural Creep Test and Compressive Creep Test.....	25
3.3.3.1	Flexural creep test.....	25
3.3.3.2	Compressive Creep Test	29
3.4	Field Methods: Drivability Analyses	31
4.	RESULTS AND DISCUSSION	38
4.1	Overview.....	38
4.2	Uniaxial Compression Tests	38
4.2.1	Stress-Strain Curves.....	38
4.2.2	Uniaxial Compression Strength	41
4.2.3	Modulus of Elasticity	47
4.2.4	Strain Rate Effects	50
4.3	Four-Point Flexure Tests.....	56
4.3.1	Flexural Stress- Center Strain Curves.....	56
4.3.2	Flexural Strengths	57
4.3.3	Flexural Modulus	59
4.4	Creep Behavior	60
4.4.1	Flexural Creep Tests	60
4.4.2	Compression Creep Tests	68
4.5	Field Installation Behavior.....	71
4.5.1	Introduction.....	71
4.5.2	I70-Emma Site	72

- 4.5.3 I435-Wornall Site and Holmes Site74
- 4.5.4 US36-Stewartsville and US54-Fulton Site79
- 4.5.5 Installation Performance for all Demonstrated Sites81
- 5. DRAFT SPECIFICATION FOR RPPs TO BE USED IN THE SLOPE STABILIZATION84
 - 5.1 The Need for A Specification84
 - 5.2 Draft Specification84
- 6. CONCLUSIONS AND RECOMMENDATIONS89
 - 6.1 Conclusions89
 - 6.2 Recommendations93
- 7. APPENDICES95
 - A Test Results for Uniaxial Compression Tests94
 - B Test Results for Four-Point Flexure Tests102
 - C Test Results for Flexural Creep and Compressive Creep Tests105
 - D RPP Penetration Rate Frequency Distribution for Field Installations ...114
 - E Draft Provisional Specification (AASHTO) for RPPs118
- 8. REFERENCES124

LIST OF TABLES

Table	Page
2.1 Cost Comparison for Slope Stabilization Methods.....	7
2.2 Common Recycled Plastics for Recycled Plastic Lumber (Osman, 1999).....	8
2.3 ASTM Standard Test Methods for Plastic Lumber	11
2.4 Engineering Properties of Plastic Lumber Products (Breslin et al., 1998)	13
2.5 Specific Gravity and Results of Compression Tests on Recycled Plastic Lumber (Lampo and Nosker, 1997)	14
3.1 Details of RPPs Tested in this Project	17
3.2 Temperatures and Loadings Detail for Flexural Creep Tests	27
3.3 Detail of Seven Slopes Using RPPs for Stabilization.....	33
4.1 Uniaxial Compression Strength from Uniaxial Compression Test on RPPs.....	43
4.2 Secant Moduli from Uniaxial Compression Test on RPPs.....	47
4.3 Results of Four-Point Flexure Tests on RPPs.....	58
4.4 Summary of Flexural Creep Tests on Recycled Plastic Specimens	62
4.5 Loading Conditions and Results of the Flexural Creep Tests on the RPPs	64
4.6 Summary Results of the Compressive Creep Tests on the RPPs.....	70
4.7 Penetration Performance of RPPs at I-70 Emma Site.....	73
4.8 Penetration Performance of RPPs at I-435 Wornall and Holmes Site.....	74
4.9 Penetration Rates and Material Properties for RPPs Installed at I435-Wornall and I435-Holmes Sites.....	77
4.10 Penetration Rates of “Test Pins” and “Nearest Neighbors”.....	79
4.11 Driving Performance of RPPs at US36-Stewartsville and US54-Fulton Site.....	80
4.12 Results of Subdivided Groups for RPPs at Seven Slide Sites	82

5.1 Draft Specification For RPPs to Be Used in Slope Stabilization Applications85

6.1 Draft Specification for RPPs to Be Used in Slope Stabilization Applications91

LIST OF ILLUSTRATIONS

Figure	Page
1.1	Surficial slope failures in highway embankment.....2
1.2	Three types of failures of reinforcing members in the field slopes2
2.1	(a) Profile view of Recycled Plastic Pins (RPPs) stabilizing a potential sliding surface. (b) Installing RPP in a slope at I70 Emma Slide3, Missouri (January 2003)6
3.1	Setup for uniaxial compression tests.....19
3.2	Typical stress-strain curve (a) and average strain rate calculation (b).....20
3.3	Loading diagram of the four-point flexure test.....22
3.4	RPPs in the four-point flexure test.....22
3.5	Flexural stress versus center strain (a) and average deformation rate calculation (b) for flexural test on RPPs (Batch A5). Secant flexural modulus (E_b) is shown for secant points at one and two percent center strain23
3.6	Setup for testing flexural creep of RPPs26
3.7	Deflection versus time response of RPPs with five 10-Lb loads at even spacing in 56°C environment. Specimen failed after 210 days27
3.8	Arrhenius plot of inverse reaction rate versus inverse temperature29
3.9	Setup for compressive creep test of recycled plastic specimen30
3.10	An idealized creep curve.....31
3.11	Initial equipment used for installation of RPPs at the I70 Emma slide 134
3.12	Crawler mounted drilling rig used for installation of RPPs at the I70 Emma slide 1 and slide 234
3.13	Ingersoll Rand ECM350, 100-psi air compressor and Daken Farm King hitter series, impact hammer used for installation of RPPs at the I70 Emma slide 3.....35
3.14	Ingersoll Rand CM150, 100-psi air compressor used for installation of RPPs at the I435 Wornall site.....37

4.1	Typical compressive stresses versus axial strain behavior for recycled plastic pins (RPPs) (a) Stress-strain curve typical of RPPs exhibiting failure planes (All Mftg A) (b) Stress-strain curve typical of RPPs exhibiting bulging failure (Mftg B and C).....	39
4.2	Failure modes of RPPs during uniaxial compression tests: (a) Typical failure planes shown by compression molded RPPs from Mftg A (b) Typical bulging failure has shown by extruded products from Mftg B and Mftg C.....	40
4.3	Difference calculated from measured perimeter versus axial strain during compression tests (Mftg A, B, and C).....	42
4.4	Comparison of average compressive strengths with and without cross-sectional area corrections for materials from all manufacturers	45
4.5	Average compressive strength versus average unit weight for materials from all manufacturers.....	46
4.6	Comparison of average secant modulus at 1% axial strain ($E_{1\%}$) for all manufacturers.....	48
4.7	Comparison of average secant modulus at 5% axial strain ($E_{5\%}$) of all manufacturers.....	49
4.8	Compressive strength versus strain rate for tests on RPPs (Mftg A – virgin specimens).....	51
4.9	Compressive strength versus strain rate for materials from Mftg A (virgin specimens versus disturbed specimens).....	52
4.10	Compressive strength versus strain rate for tests on RPPs (Mftg B and C)	53
4.11	Standard compressive strength (σ_{std}) for tests on RPPs (Batch A10)	54
4.12	Ratio of compressive strength to standard compressive strength versus strain rate for RPPs.	55
4.13	Typical flexural stresses versus center strain behavior for RPPs	57
4.14	Comparison of average flexural strengths for all manufacturers.....	59
4.15	Comparison of average secant flexural modulus at one percent center strain ($E_{1\%}$) and two percent strain ($E_{2\%}$) of RPPs	60

4.16	Deflection versus time response for RPP loaded with 50 lbs at the free end of a simple cantilever (Figure 3.6) under various temperatures	61
4.17	Typical Arrhenius Plot for flexural creep test on 2 in x 2 in x 24 in RPP loaded with a 50-lbs weight at the end of a cantilever under various temperatures.....	63
4.18	Method for estimating time to failure resulting from flexural creep of RPP.....	65
4.19	Maximum mobilized bending moments from instrumented RPPs at I70-Emma site (Parra et al., 2003)	66
4.20	Typical deflection under constant axial stress versus time of a recycled plastic specimen from batch B7	69
4.21	Deflections versus time of the compressive creep tests on RPPs	71
4.22	Penetration rate frequency distribution for RPPs and trial steel pipe reinforcements in slope stabilization site, I435-Wornall	76
4.23	Analysis of penetration rate “test pin” to the average driving rate for its “nearest neighbors”	78
4.24	Penetration rate analysis by subdividing RPPs as four groups from top to bottom of slope.....	81
4.25	Average penetration rate versus installation sequence of seven slopes	83

CHAPTER 1: INTRODUCTION

1.1 Background

In situ reinforcement techniques show a great deal of promise for stabilization of surficial slope failures. Reinforcing members made from plastic wastes offer an economic and environmentally attractive alternative to traditional materials for stabilizing such failures. In an on-going demonstration project, slopes at five different sites (all located in the state of Missouri) have been stabilized using recycled plastic pins (RPPs) and, for comparative purposes, steel pipe. All five sites have experienced surficial failures in embankments or cut slopes before installing RPPs (Figure 1.1).

1.2 Objectives

The engineering properties of the reinforcing members are of paramount importance because of the potential for structural failure of the pins due to the loads imposed by the moving soil and due to the stresses imparted on the members during field installation (Figure 1.2). Due to the variety of manufacturing processes and constituent mixes used in the manufacture of recycled plastic products, the engineering properties of commercially available members could vary substantially.

In order for the RPP technology to become widely applied, it is imperative to have a suitable specification for accepting or rejecting particular products. The specification must consider both the installation and performance requirements of the pins, since there is currently little agreement on testing protocols and few tests directly applicable to the slope stabilization application.



Figure 1.1 Surficial slope failures in highway embankment.

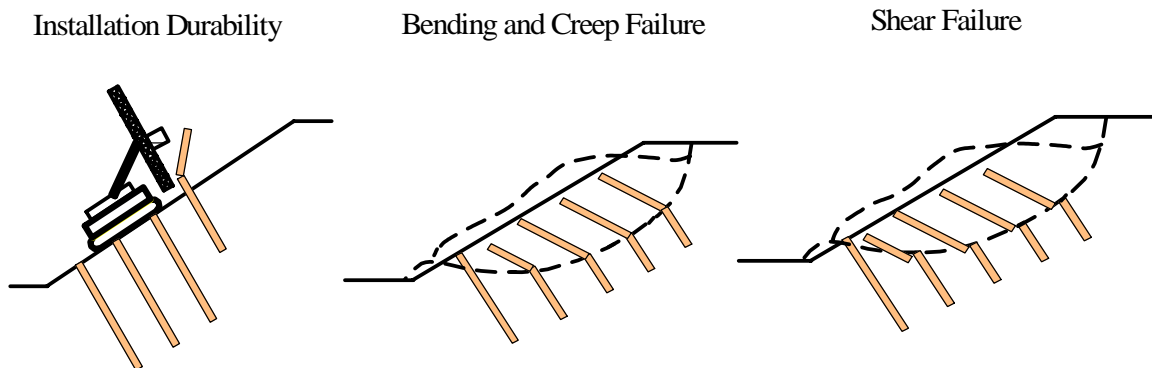


Figure 1.2 Three types of failures of reinforcing members in the field slopes.

1.3 Scope of Work

In order to gain a proper perspective of the engineering properties of RPPs, an extensive testing and analysis program is being undertaken. The program includes: (a) determining the basic engineering and material properties of RPPs; (b) determining the potential variability of these properties within one product and among various products and manufacturers; and (c) determining how these properties change when the material is

subjected to various potentially detrimental environments. The scope of this report is limited to points (a) and (b), in order to provide background data for developing a draft specification for RPPs in slope applications. A draft specification is presented in the text and in the format of a provisional specification for the American Association of State Highway and Transportation Officials (AASHTO).

CHAPTER 2: LITERATURE REVIEW

2.1 Introduction

In this chapter, the general concepts and methods for slope stability are introduced, as well as use of recycled plastic pins (RPPs) for slope stabilization. The source and manufacturing process of the RPPs and existing methods to measure the engineering properties are presented.

2.2 Slope Stability

Slope failure on public and private transportation routes is an all too common occurrence. Based on previous research (TRB, 1996), total direct costs for maintenance and repair of landslides involving major U.S. highways alone have been estimated to exceed \$100 million annually. Costs attributed to routine maintenance and repair of “minor ” failure slopes are largely neglected. The slope types and geometric dimensions of minor slopes failures vary, but most are characterized by relatively shallow sliding surfaces that are less than 10 feet (3 m) deep (Figure 1.1). The costs for repair a minor slope failure are quite low, but the cumulative costs for many minor slopes failures are extremely large (TRB, 1996). If not properly maintained, these minor sliding failures often progress into more serious problems and require more costly repairs.

2.3 Stabilizing Methods

There are various methods of slope stabilization available. Some methods include the use of soil and rock fill, drilled shaft walls, and tieback walls. The most common slope stabilization method is based on using soil and rock (or aggregates) fill to rebuild the slope. This method is used to provide sufficient dead weight near the toe of the slope,

thus preventing driving force of the failure slope. This is a practical way to arrest further movement of an unstable slope when resources of the soil and rock fill are available and can be found locally. However, the repair cost becomes relative high to replace the failure when using aggregates. Drilled shaft walls and tieback walls are not economical for minor slopes failure application. The construction costs can be very high and the installation process affects the road user.

Using small diameter in-situ reinforcement techniques is a relatively new approach for stabilization of slopes. For example, soil nailing is one of these similar techniques. It generally consists of steel bars, metal tubes, or other metal rods that can be either driven or grouted in predrilled boreholes. The repair cost is still high for minor slope failures. Since minor slope failures often have relatively shallow sliding surfaces, the load imposed on in-situ reinforcement members is expected to be small. A major advantage of this method is that the reinforcing member will control the design (Loehr et al., 2000b). The uncertainties associated with the soil properties and field conditions can be reduced and the reliability of the design can be improved. Small and mobile equipment allows for easy access to remote sites and reduced mobilization costs for small diameter stabilization techniques. In addition, installation costs for this application may be significantly lower than costs for other stabilization methods.

2.4 Recycled Plastic Pins Method

A new technique for slope stabilization has been developed that uses recycled plastic pins (RPPs), comparable to soil nailing. The RPPs are driven in a grid pattern on the failure sliding surfaces. The schematic design concept for stabilization slope is illustrated in Figure 2.1. The pins are typically 3.5 in. x 3.5 in. x 8 feet (90 mm x 90 mm

x 2.4 m) in length; however, the dimensions can be readily changed in the manufacturing process. This method offers a cost-effective alternative to current slope repair methods. Table 2.1 provides a cost comparison for using RPPs technique, rock armor, and soil nailing. The costs were calculated on a unit area basis (the total cost was divided by the total area of the slope face). Based on these estimated costs, the RPP stabilization method is the least costly. As experience is gained and installation technology improves, the costs for RPP slope stabilization are expected to decrease (Loehr et al., 2000a).

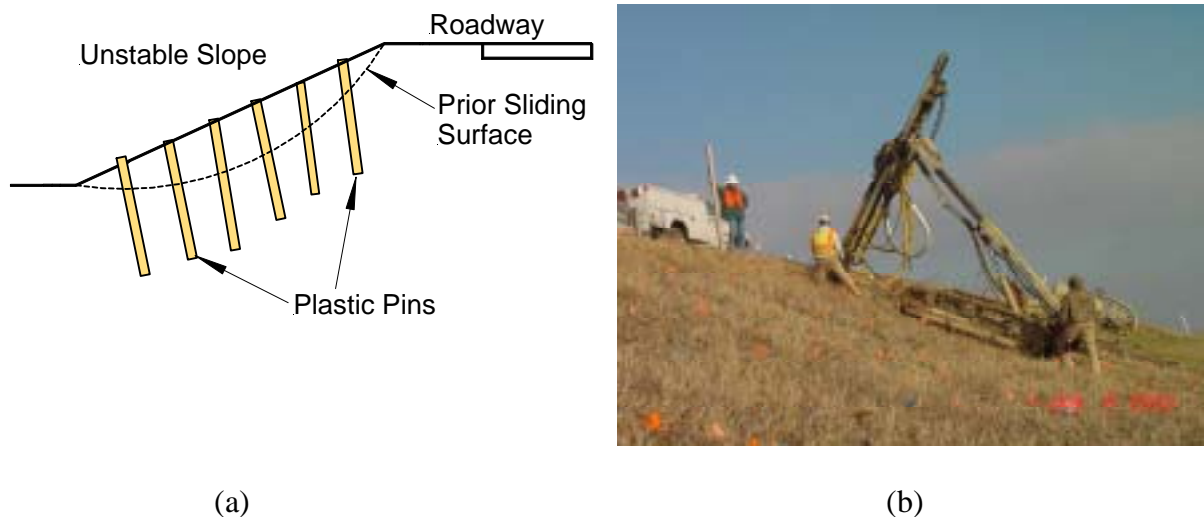


Figure 2.1(a) Profile view of Recycled Plastic Pins (RPPs) stabilizing a potential sliding surface. (b) Installing RPP in a slope at I70-Emma slide 3, Missouri (January 2003).

The first full-scale demonstration in which RPPs were used to stabilize two slope failures (Loehr et al., 2000b) indicated that the strengths of the RPPs control the design of stabilization. Having the pin capacity control the design also reduces the necessity of applying a highly accurate theory for predicting the loads imposed by the soil on reinforcing members. The importance of accurately knowing soil properties is diminished; however, the reliability of the design is improved. Therefore, knowing the

engineering properties of the RPPs becomes important and can help to fit the main requirement of the slope stabilization design.

Table 2.1 Cost Comparison for Slope Stabilization Methods

Stabilization Method	Cost/ Unit area of Slope Face ^[1]	
	(\$/ ft ²)	(\$/ m ²)
Recycled Plastic Pins (RPPs)	3.9	42
Rock Armor ^[2]	5.4	58
Soil Nailing	19.0	200

^[1]: Results from I70-Emma Slide1 and Slide2, reported on Loehr et al., 2000a

^[2]: Technique that uses a surface layer of large rocks to hold soil in place

2.5 Sources and Manufactured Processes of Recycled Plastic Pins

Recycled plastic pins (RPPs) are manufactured from industrial or post-consumer waste consisting predominantly of polymeric materials (usually high or low density polyethylene). Typically, recycled plastic lumber is composed of the following resins (McLaren, 1995): High Density Polyethylene (HDPE) (55 percent to 70 percent), Low Density Polyethylene (LDPE) (5 percent to 10 percent), Polystyrene (PS) (2 percent to 10 percent), Polypropylene (PP) (2 percent to 7 percent), Polyethylene-terephthalate (PET) (1 percent to 5 percent), and varying amounts of additives (sawdust, fly ash, and other waste materials) (0 percent to 5 percent). Table 2.2 shows the common resins, their major advantages, typical and recycled uses, and recycling rate for 2001. In the United States, post-consumer waste has increased at a faster rate than industrial waste. The post-consumer plastic bottle recycling increased by 80 million pounds in 2001 to an all time high of 1,591 million pounds (APC, 2002). The HDPE raw material comes from post-consumer milk jugs and PET comes from post-consumer soda bottles. Assuming 50 percent of recycling rate for all waste plastics, the total production of the recycled plastic

lumber is estimated to approach 25 billion board feet (6254 m³) per year (McLaren, 1995). Therefore, the importance of the recycled plastic lumber industry in recycling of plastics cannot be overemphasized.

Table 2.2 Common Recycled Plastics for Recycled Plastic Lumber (Osman, 1999)

Resin Type	Major Advantages	Typical Original Uses	Typical Recycled Uses	Millions pounds Bottle Recycled^[1] (Recycled rate^[2], %)
Polyethylene terephthalate (PET)	High strength, excellent moisture barrier, good clarity	Soft drink bottles, juice containers, food packaging	Bottles, paint brushes, geotextiles, carpeting	834.3 (22.1%)
High Density Polyethylene (HDPE)	High strength and melting point, good ductility	Milk containers, oil bottles, films and pipes	Plastic lumber, motor oil containers, bottles, drainage pipes	750 (23.2%)
Low Density Polyethylene (LDPE)	Excellent clarity, toughness and flexibility, easy to process	Bottles, trash bags, cable sheathing, sheets and films	Films, plastic bags, bottles	0.2 (0.5%)
Polypropylene (PP)	Low density, high melting point, and excellent chemical resistance	Carpeting, netting, geotextiles, heavy-duty bags	Flexible packing containers	5.7 (3.8%)
Polystyrene (PS)	Low cost, low density, good weathering resistance	Cups, water bottles, outdoor furniture	Egg cartons, video tape cases	0.1 (1.1%)

^[1]: Data from American Plastic Council survey results (APC, 2002)

^[2]: Percentages shown for PET and HDPE are based on virgin resin sales plus the recycled resin used in the manufacture of bottles.

Manufacturers also use different processes to produce their product (Bruce et al., 1992). The two main processes commonly used are compression molding and extrusion forming. In compression molding, the constituent waste streams are pulverized, blended together, heated until partially melted, and then compression formed in molds. In this process, the raw material is compressed into desired shapes and dimensions and is cured

with heat and pressure. Extrusion forming includes similar steps; however, the molten composite material is forced through a die of the desired cross-section for the member being produced in lieu of compression into a mold. An advantage of the extrusion process is that it is relatively easy to manufacture members of any desired length while the compression molding process requires different molds for each different member length. It is also easy to make more products than compression molding process. Owing to the endless variety of possible constituents and manufacturing processes, the resulting recycled plastic products (often seen in park benches, picnic tables, and decks for homes and marine setting) can have very different engineering properties, even among apparently similar materials and sections.

2.6 Engineering Properties of Recycled Plastic Lumber

There are many manufacturers of recycled plastic lumber in the United States. The number is currently more than 30, but is variable due to the nature of start-up businesses. Each manufacturer uses proprietary blends of constituents, which can vary at their source, and different manufacturing methods to products. Therefore, the engineering properties also vary. In order for the RPP stabilization technology to gain wide spread acceptance and application, both of which are tied to the costs of the technique, a specification for the RPPs in terms of required minimum engineering properties must be established.

In order to develop a specification for RPPs in slope stabilization applications, the key variables must be identified and their behavior documented for the application. In the slope stabilization application, key variables include strength and stiffness (axial and bending), and resistance to installation stresses. Compressive and flexural strength and

stiffness can readily be measured by most manufacturers. Several ASTM standards relative to plastic lumber along with comments on the testing procedures are given in Table 2.3. Uniaxial compression and four-point flexure tests are common and easy performed in material testing. ASTM D6108 (ASTM, 1997a) recommends using a minimum or effective original cross-sectional area to calculate compressive stress. A calculation of the effective cross-sectional area is listed in ASTM D6111 (ASTM, 1997c), which outlines a method of obtaining the specific gravity and bulk density of plastic specimens by water displacement. With the density, length, and weight by the following equation (ASTM, 1997c).

$$area, cm^2 = \frac{(a + w - b)}{(0.9976 * length, cm)} \quad (2.1)$$

where a = overall weight of specimen, without wire or sinker, in air (mg), b = over weight of specimen (and of cage and sinker) completely immersed and of the wire partially immersed in liquid (mg), w = overall weight of totally immersed sinker, cage, and partially immersed wire (mg). The effective cross-sectional area can be calculated. Note, the ASTM-recommended standard strain rate is 0.03 in/in/min (0.03 mm/mm/min) and the testing time is approximately one minute to five minutes. In slope stabilization applications, the RPPs resist sustained soil movement as bending loads over time; a loading condition is likely to be very slow on the order of weeks or months. Therefore, the ASTM-recommended strain rate might be too fast for this slope stabilization design.

Table 2.3 ASTM Standard Test Methods for Plastic Lumber

ASTM No. & Title	Test Method	Main Comments
D6108 Standard Test Method for Compressive Properties of Plastic Lumber and Shapes	Uniaxial Compression Test	<ul style="list-style-type: none"> • Specimens: length = 2 x minimum width. • Compressive stress = compressive load divided by minimum or effective original cross-sectional area. • Choose 3 % strain as compressive strength if no clear a yield point. • Strain rate = 0.03 ± 0.003 in/in/min (mm/mm/min) and testing time ~ 1 to 5 min. • Secant Modulus @ 1% strain.
D6109 Standard Test Method for Flexural Properties of Unreinforced and Reinforced Plastic Lumber	Four-point Flexure Test	<ul style="list-style-type: none"> • Specimens: support span (length) divided by minimum width = 16 (nominally). • Calculated rate of crosshead motion by equation that list in the standard. • Flexural strength = maximum stress at the moment of ruptured specimen. • Secant Modulus of elasticity in flexure from equation provided.
D6112 Standard Test Methods for Compressive and Flexural Creep and Creep-Ruptured of Plastic Lumber and Shapes	Compressive Creep and Flexural Creep	<ul style="list-style-type: none"> • Uniaxial type of loading for compressive creep. • Plot successive creep modulus versus time at various stresses for linear viscoelasticity materials. • Four-point flexure testing set-up for flexural creep. • Approximate time schedule for compressive or flexural creep tests: 1, 6, 12, and 30 min; 1, 2, 5, 20, 100, 200, 500, 700, and 1000 hours. • Able to predict the creep modulus and strength of material under long-term loads from testing data.

The testing procedures of the four-point flexure test are listed in ASTM D6109 (ASTM, 1997b). The length of specimens needs to follow the ratio of support span to minimum width, equal to 16. The ASTM-recommended rate of crosshead motion, R (in/min), as provided by equation 2.2.

$$R = 0.185ZL^2/d \quad (2.2)$$

where L = support span (inch), d = depth of the beam (inch), and $Z = 0.01$, rate of straining of the outer fibers (in/in/min). The flexural strength is equal to the maximum stress in the outer fibers at the moment of break (ruptured).

Although durable with respect to environmental degradation, polymeric materials can exhibit higher creep rates than other structural materials such as timber, concrete, or steel. In the slope stabilization application, the RPPs will be subjected to lateral (bending) forces and their ability to resist deformation (either mechanical or creep) will strongly influence the success of the RPPs for stabilizing slopes. Accordingly, determining the creep behavior of the plastic pins is important for establishing this stabilization technology. ASTM D6112 (ASTM, 1997d) outlines the testing procedures for compressive and flexural creep tests. Data from these tests are necessary to predict the creep modulus and strength of materials under long-term loads.

Table 2.4 shows the composition and engineering properties of plastic lumber from various manufacturers. Manufacturers use materials including virgin plastics, post-consumer waste plastics, and various plastics mixtures. Breslin et al. (1998) concluded that the engineering properties of plastic lumber vary depending on the composition of the polymers and additives used in lumber manufacturing. The unit weight ranged from 47 pcf to 60 pcf (7 KN/m^3 to 9.5 KN/m^3) for different manufacturers. The compressive strength varied from 1700 psi to 3800 psi (11.7 MPa to 26.2 MPa). The use of a single polymer (HDPE) and glass fiber additive resulted in significantly higher the modulus of elasticity for plastic lumber (Breslin et al., 1998).

Table 2.4 Engineering Properties of Plastic Lumber Products (Breslin et al., 1998)

Product	Composition	Specific Gravity	Unit Weight ^[1] (lb/ft ³)	Compressive Strength (psi)	Modulus of Elasticity (ksi)	Tensile Strength (psi)
TRIMAX	HDPE/Glass fibers	0.75	46.80	1740	450	1250
Lumber last	Commingled recycled plastic	0.86	53.66	3755	140	1453
Earth care recycle maid	Post-consumer milk jugs	0.79	49.30	3205	93 - 102.5	2550
Earth care products	HDPE	0.909	56.72	-- ^[2]	173.4	--
Supperwood Selma, Al	33% HDPE, 33% LDPE, 33% PP	0.82-0.87	51.2-54.3	3468	146.2	--
Rutgers University	100% Curb tailings	0.944	58.9	3049	89.5	--
	60% Milk bottles, 15% Detergent bottles, 15% Curb tailings, 10% LDPE	0.883	55.1	3921	114.8	--
	50% Densified PS	0.806	50.3	4120	164	--
BTW Recycled plastic lumber	Post-consumer	0.88-1.01	54.9-63.0	1840-2801	162	--

^[1]: calculated by the present author

^[2]: data not available

Conversion: 1MPa = 145 psi, 1ksi = 6.9 MPa

Lampo and Nosker (1997) performed the compression tests on recycled plastic lumbers from multiple manufacturers. Table 2.5 contains the average for the specific gravity and material properties from each manufactures. It shows the different materials in terms of their material properties will perform differently among various manufacturers. Overall, the moduli of elasticity ranged from 38 psi to 191 psi (400 MPa to 1320 MPa). The significant variation in moduli proves that these materials cannot be considered identical, and they cannot be assumed to perform similarly in many applications (Lampo and Nosker, 1997).

Table 2.5 Specific Gravity and Results of Compression Tests on Recycled Plastic Lumber (Lampo and Nosker, 1997)

Sample	Specific Gravity	Unit Weight ^[1] (lb/ft ³)	Yield Strength (at 2 % strain) (psi)	Ultimate Strength (at 10 % strain) (psi)	Modulus of Elasticity (ksi)
51A	0.28	17.4	709	785	38.0
1B	0.70	43.8	1381	1885	61.9
2D (br)	0.86	53.9	1668	2321	85.3
2D (g)	0.81	50.5	2103	2857	116.0
1E	0.86	53.8	1769	2422	80.8
1F	0.79	49.2	2190	2814	108.2
1j (b)	0.75	47.0	1900	2364	93.3
1j (w)	0.91	56.7	2161	2828	110.1
23L	0.79	49.0	1711	1929	191.4
1M	0.57	35.3	964	1226	57.9
1S	0.91	56.7	1668	2045	80.5
1T	0.88	54.9	2248	3118	117.9
9U	0.77	48.3	1827	2408	86.7
Range	0.28-0.91	17.4-56.7	709-2248	785-3118	38-191.4
Mean	0.76	47.4	1715	2231	94.5
Std. Dev.	0.17	10.8	465	666	37.6

^[1]: Calculated by the present author

Conversion: 1MPa = 145 psi, 1ksi = 6.9 MPa

2.7 Summary

Maintenance and repair costs due to slope failure on public or private infrastructure are significant portions of annual expenditures for government and private agencies. Many slope stabilization methods are available, but the most economic but effective solution is always desired. Preliminary demonstration sites (Loehr et al., 2000a) showed that using the RPP stabilization method is the least costly when compared to rock armor and soil nailing. In this application and based on parametric studies, the designing method requires better knowledge of the engineering properties of the RPPs. However, the existing testing methods for recycled plastic lumber and data are not directly

applicable for slope stabilization application. Modifications of the testing procedures are necessary to obtain the engineering properties for slope at stabilization applications. Installation performance tests directed toward RPPs slope stabilization are needed. Results from extensive laboratory tests and field performance are helpful for developing a specification for RPPs to be used in slope stabilization applications. The materials and engineering properties are also needed for RPPs to be readily adopted as a slope stabilization technique.

CHAPTER 3: MATERIALS AND METHODS

3.1 Overview

Extensive laboratory tests were performed to evaluate the engineering properties of recycled plastic pins (RPPs) from three different manufacturers. Laboratory tests included uniaxial compression, four-point flexure, compressive creep, and flexural creep tests. Field tests included drivability analyses. The materials and methods used in the testing program are described in this chapter.

3.2 Materials

Tests were performed on specimens from three manufacturers denoted A, B, and C, as shown in Table 3.1. All of the members were nominally 3.5 in. x 3.5 in. (90 mm x 90 mm) in cross-section by 8 feet (2.4 m) in length. A detail of the RPPs composition and manufacturing processes for each manufacturer were not provided. Measured unit weights for all batches are not identical and ranged from 52 pcf to 68 pcf (8 kN/m³ to 11 kN/m³). One manufacturer (manufacturer A) provided pins manufactured in seven different batches, denoted batches A1 through A6 and A10, over a period of three years. Members in batches A1 through A4 were compression-molded products while members from batches A5, A6 and A10 were extruded products. The constituent formula among the first five batches (A1 to A5) was similar with approximately 60 percent low-density polyethylene (LDPE) and 40 percent filler material (primarily sawdust). Batches A6 and A10 were produced using a higher percentage of high-density polyethylene (HDPE). Two additional manufacturers (manufacturers B and C) provided specimens of unreinforced members composed of HDPE with negligible filler and additives. These specimens are

denoted as batches B7 and C9. Manufacturer B also provided specimens composed of HDPE reinforced with cut-strand fiberglass reinforcement (batch B8). The specimens from batches A1 through A6, A10, B7, B8 and C9 were manufactured at company facilities and shipped to the University of Missouri-Geotechnical Laboratories for testing or to the contractor for installation at the field test sites. They all are considered “virgin” materials (undisturbed).

Table 3.1 Details of RPPs Tested in this Project

Specimen Batch	Principal Constituent	Mftg. Process	Source	Depth (in)	Width (in)	Length ^[1] (in)	Unit weight (lb/ft ³)
A 1	LDPE	Compression	Lab (virgin)	3.6	3.6	7.0	61.2
A 2	LDPE	Compression	Lab (virgin)	3.5	3.5	6.9	63.4
A 3	LDPE	Compression	Lab (virgin)	3.6	3.6	7.1	64.5
A 4	LDPE	Compression	Lab (virgin)	3.6	3.4	7.0	64.6
A 5	LDPE	Extruded	Lab (virgin)	3.4	3.4	7.1	58.9
A 6	HDPE	Extruded	Lab (virgin)	3.4	3.4	7.0	60.9
A10	HDPE	Extruded	Lab (virgin)	3.5	3.5	7.0	67.6
A11	HDPE	Extruded	Field (disturbed)	3.5	3.5	7.0	68.3
A12	HDPE	Extruded	Field (disturbed)	3.5	3.5	7.0	68.5
A13	HDPE	Extruded	Field (disturbed)	3.5	3.5	7.0	66.8
B 7	HDPE	Extruded	Lab (virgin)	3.4	3.4	6.9	52.9
B 8	HDPE + Fiber glass	Extruded	Lab (virgin)	3.4	3.4	6.9	51.9
C 9	HDPE	Extruded	Lab (virgin)	3.5	3.5	7.0	67.9

^[1]: for uniaxial compression tests.

Conversion: 1 in = 2.54 cm, 1 lb/ft³ = 0.1572 kN/m³

Batches A11, A12 and A13 were taken from the portion of the RPPs that remained above the ground surface after installation. They were all manufactured at the same period as batch A10, thus have a similar constituent formula; however, these specimens are considered “disturbed”. Batches A11 and A12 were installed in the I70-Emma Slide³ in January 2003. Different installation equipment was used between the two batches. Batch A13 was installed in the US54-Fulton site in January 2003.

3.3 Laboratory Methods

3.3.1 Uniaxial Compression Test

Uniaxial compression tests were performed on specimens cut from full size RPPs. Their cross-section was square with side dimensions of 3.5 inches (90 mm) and a nominal length of 7 inches (180 mm), twice the minimum width. The tests were conducted using a stress controlled universal compression machine. The compression test is shown in Figure 3.1. A steel plate was placed on top of the specimen to make sure the compressive load was uniformly distributed over the whole cross-sectional area of the specimen. A dial gage was placed beneath the steel plate to measure the displacement during the test.



Figure 3.1 Setup for uniaxial compression tests.

The axial strain was computed by dividing the incremental displacement of the loading head by the initial height of each specimen. A strain rate was determined by dividing the incremental strain by the elapsed testing time. Secant moduli at one percent strain and five percent strain were determined as shown in Figure 3.2. The secant moduli were calculated using the slope of the straight line connecting zero percent strain to the corresponding stresses at one percent and five percent strain, as shown in Figure 3.2a. The average strain rate was determined by taking the average of all strain rates before peak stress was reached, as illustrated in Figure 3.2b. An average strain rate of approximately 0.006 in/in/min (mm/mm/min) was used through out this analysis.

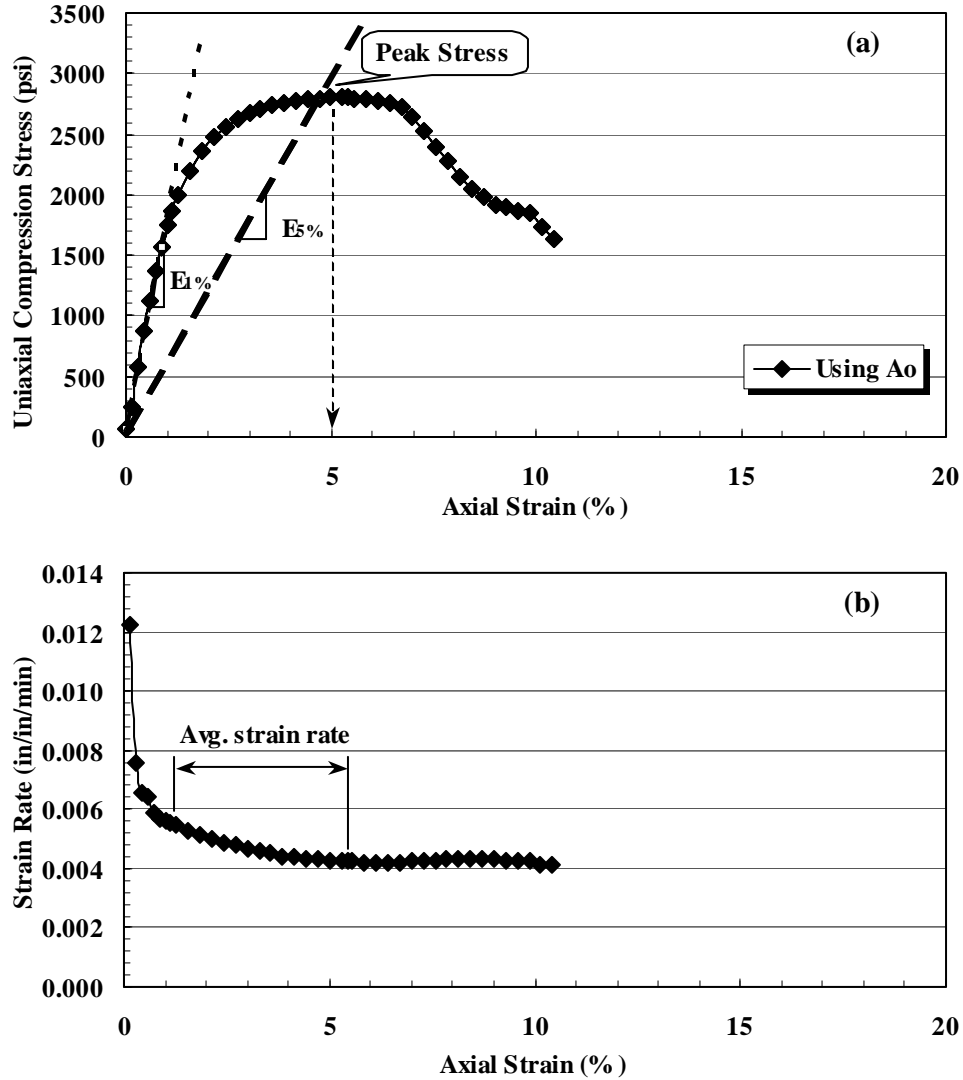


Figure 3.2 Typical stress-strain curve (a) and average strain rate calculation (b) (Batch A3).

Two failure criteria were used to determine the compressive strength of the RPPs in this project. The first one was based on using the original cross-sectional area (A_0) of the specimen to calculate the compressive stress and using five percent strain limit as the baseline to choose the compressive strength. The second criterion was based on using a

corrected cross-sectional area (A_C) based on measured perimeter of the specimen to calculate the compressive stress and choosing the peak stress as compressive strength.

A tape measurement was used to measure the perimeter of the middle section of specimens during the compression test (Figure 3.1). The corrected cross-sectional area (A_C) was calculated by assuming the measured perimeter was that of a square section, so that

$$A_C, \text{ Corrected Cross Sectional Area} = \left(\frac{\text{Measured Perimeter}}{4} \right)^2 \quad (3.1)$$

3.3.2 Four-Point Flexure Test

Four-point flexure tests were used to determine the flexural strength and stiffness of the RPPs. Specimens were cut into testing length, approximately 6 feet (~2 m). The support span to depth ratio used was 16:1 (ASTM, 1997b). A schematic drawing of the setup is shown in Figure 3.3 and a photograph of the setup in the laboratory is shown in Figure 3.4. The tests were conducted using a stress controlled universal testing machine with a four-point bending attachment. The support span length (L) ranged from 4 feet to 5 feet (1.2 m to 1.5 m) with load span ($L/3$) of 16 inches to 20 inches (0.4 m to 0.5 m). The rate of crosshead motion ranged from 1.2 in/min to 1.9 in/min (30 mm/min to 48 mm/min) was calculated by following the standard. Again, the ASTM-recommended crosshead rate might be too fast for slope stabilization application. The overhanging length was 6 inches (15 cm) on each end. The deflection at the middle point of the load span and corresponding load applied to the specimen were recorded.

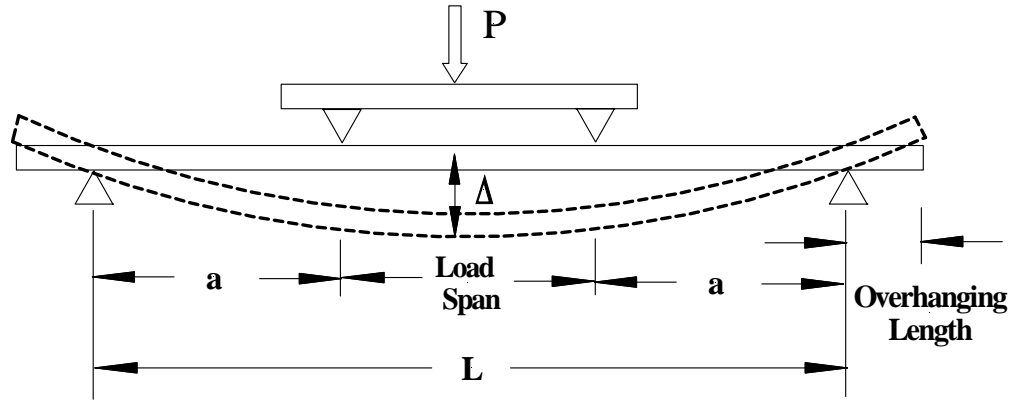


Figure 3.3 Loading diagram of the four-point flexure test.



Figure 3.4 RPPs in the four-point flexure test.

The typical response observed in the four-point flexure tests is shown in Figure 3.5. The flexural stress is plotted as a function of the extreme fiber strain at the center of the specimen ("center" strain). These data points were derived from the applied loads and measured deflections as follows.

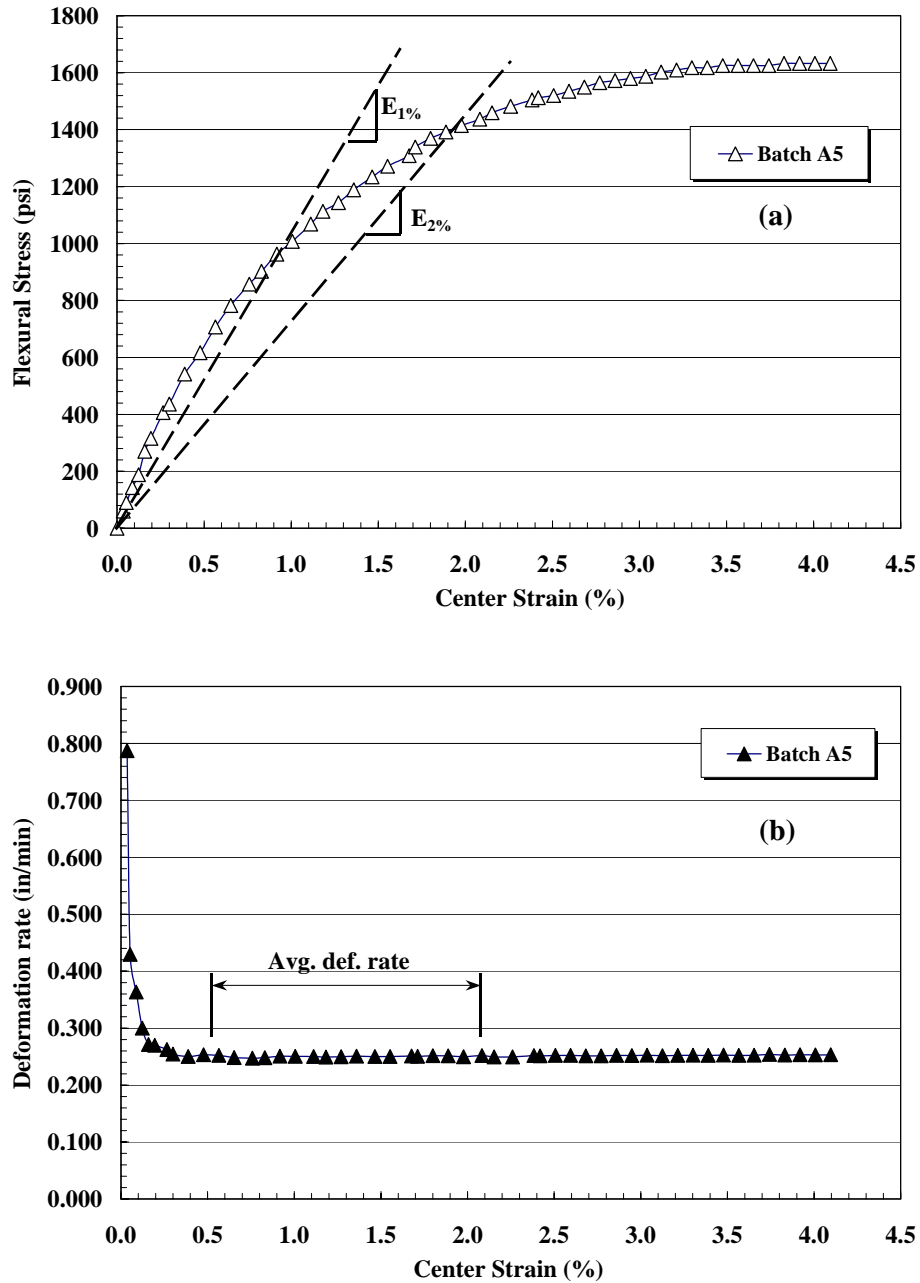


Figure 3.5 Flexural stress versus center strain (a) and average deformation rate calculation (b) for flexural test on RPPs (Batch A5). Secant flexural modulus (E_b) is shown for secant points at one and two percent center strain.

The flexural stress (or bending stress), σ_b , was calculated as

$$\sigma_b = \frac{Mc}{I} \quad (3.2)$$

where M is the bending moment, c is distance from the neutral axis to the extreme fiber, and I is the moment of inertia of the whole cross-sectional area of the RPPs. The maximum deflection at the center of load span, Δ_{\max} , is given as:

$$\Delta_{\max} \text{ (at center)} = \frac{\left(\frac{P}{2}\right) a \left(3L^2 - 4a^2\right)}{24E_b I} \quad (3.3)$$

where P is the applied load, L is the total span length, a is the distance from the outer support to the loading point ($L/3$), Δ is the deflection at the center of load span, and I is the moment of inertia. Equation 3.3 is merely a modification of the general equation for the center deflection (Δ) of a beam being tested in four-point flexure test (Timoshenko and Gere, 1972). Therefore, the flexural or bending modulus for each specimen was calculated from the results of the four-point bending tests as:

$$E_b = \frac{\left(\frac{P}{2}\right) a \left(3L^2 - 4a^2\right)}{24 * \Delta * I} \quad (3.4)$$

If the material is elastic with a linear stress-strain relationship, Hooke's law can be used to calculate the strain. In these tests, the center strain, ε_b , was calculated as:

$$\varepsilon_b = \frac{\sigma_b}{E_b} = \frac{12 * \Delta * h}{\left(3L^2 - 4a^2\right)} \quad (3.5)$$

where h is the depth of the specimen, L is the total span length, and a is the distance between the loading supports ($L/3$). A deformation rate is calculated by dividing the central deflection by the elapsed testing time. The average deformation rate was

computed by taking the average of all deformation rates before the flexural stress at center strains of two percent, as illustrated in Figure 3.5b. A nominal deformation rate for the four-point flexure tests was 0.2 in/min (5.1 mm/min).

Because the members tended to soften with increasing strain, secant values of the flexural modulus were computed at center strains of one and two percent, as shown in Figure 3.5a.

3.3.3 Flexural Creep Test and Compressive Creep Test

3.3.3.1 Flexural creep test

Flexural creep response testing was performed on scaled RPPs having nominal dimensions of 2 in. x 2 in. x 24 in. (51 mm x 51 mm x 61 cm). A cantilever setup was conceived to achieve the desired field loading. The creep frame that was designed and built resembled a pommel horse; a schematic drawing is shown in Figure 3.6. Two steel channels (C8 x 14) were welded together with the channels facing in. A gap of approximately two inches was left between channels for a fastening position. The channels were welded to a two-inch (51 mm) steel pipe stand that was threaded together to accommodate moving the creep frame from place to place. The overall dimensions of the frame are approximately 41-inch (104 cm) long by approximately 42-inch (107 cm) tall. Fixing the specimens to the frame was achieved using several all thread bolts approximately nine-inch (23 cm) long, 1 in. x 6 in. (25 mm x 152 mm) wood boards and a 1 in. x 6 in. (25 mm x 152mm) steel plate with the same length as that of the creep frame. The wooden boards and steel plate had holes drilled in them at the positions that the all thread bolts would be used to clamp the specimens. A wood board was placed on the creep frame and on top of the creep specimens to protect the specimens from melting

on the steel at high temperatures. The 1 in. x 6 in. (25 mm x 152 mm) steel plate was place on top to provide rigidity to the clamping mechanism. The creep frame was designed to hold eight specimens at various loads.

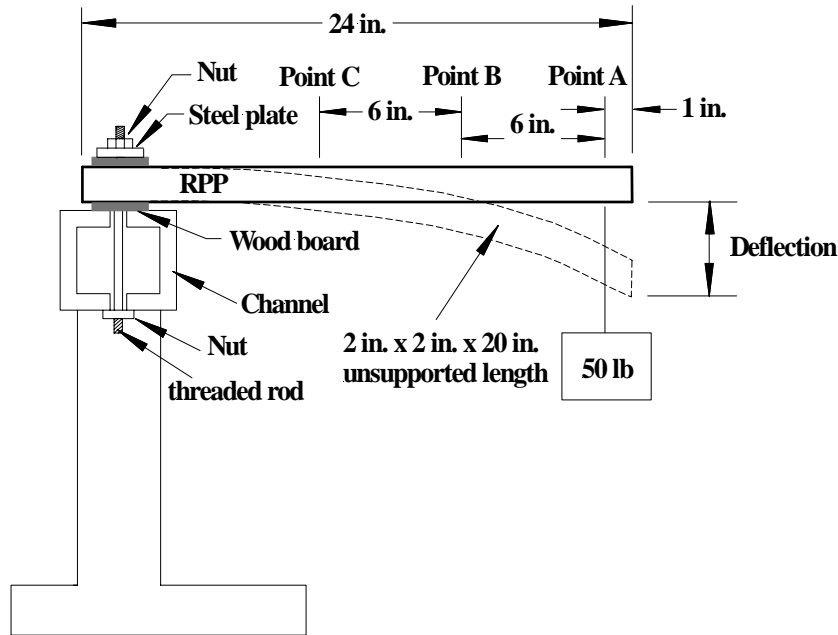


Figure 3.6 Setup for testing flexural creep of RPPs.

Table 3.2 shows the temperature and loading setup for the flexural creep tests. It was determined that five temperatures would be needed to achieve continuity throughout testing. Temperatures of 21°, 35°, 56°, 68°, and 80° Celsius (70°, 95°, 133°, 154°, and 176° Fahrenheit) were easily obtained in the elevated temperature controlled environmental rooms. Humidity levels were not monitored. Eight specimens at each temperature were tested for a total of thirty-six specimens with the exception that only four specimens were tested at 35°C (95°F). Two specimens were equally loaded at the same temperature to assure reproduction. Specimens were loaded with either single (21 lbs, 35 lbs or 50 lbs) or multiple point loads along their length (five 10-Lb loads distributed evenly). The deflections at three points (points A, B, C as shown in Figure

3.6) along the cantilever were measured and recorded over time. Typical results are shown in Figure 3.7, which shows the creep deflection versus time response.

Table 3.2 Temperatures and Loadings Detail for Flexural Creep Tests

Temperature (°C)	# Specimens Tested	Point Load (lbs)	Disturbed Load (lbs)
21	8	21, 35, 50	10 lbs @ 5 points
35	4	50	-- ^[1]
56	8	21, 35, 50	10 lbs @ 5 points
68	8	21, 35, 50	10 lbs @ 5 points
80	8	21, 35, 50	10 lbs @ 5 points

^[1]: data not available

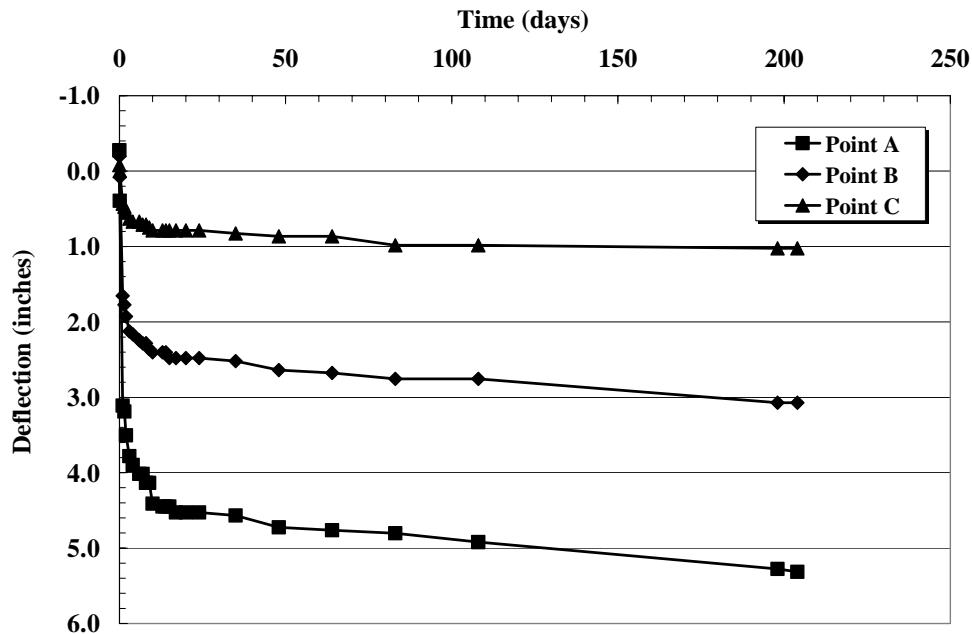


Figure 3.7 Deflection versus time response of RPPs with five 10-Lb loads at even spacing in 56°C environment. Specimen failed after 210 days.

By its very nature, creep is a long-term phenomenon. For example, the RPPs being tested at 21°C (70°F) have been under load for more than five years but have not

failed. Failure was defined as breakage of the RPP. The tests at elevated temperatures were established in order to accelerate the creep process. Results from the accelerated testing were used along with the Arrhenius method (Koerner et al., 1990) to estimate the long-term creep behavior for the RPPs in the field.

Arrhenius modeling provides a method to accelerate the creep rate of materials and to predict performance at field temperatures. An example of an Arrhenius plot is shown in Figure 3.8. The following steps explain the method:

Step 1: Results from flexural creep tests at several different temperatures are presented in a plot of the natural logarithm of the inverse of the time required for the RPP to break (failure) versus the inverse of the temperature at which the test was conducted (Figure 3.8).

Step 2: The negative slope of the line on the Arrhenius plot is known as the activation energy (E_{act}) divided by the universal gas constant ($R = 8.314 J/mol - ^\circ K$).

Knowing the value of negative slope ($-\frac{E_{act}}{R}$), the reaction rate intercept on the Arrhenius plot ($\ln A$) and the temperature of the actual site (T_{site}), we can estimate the time for the RPP to reach the breaking point under field conditions for a RPP stressed to the same level as those used to develop the Arrhenius plot.

Step 3: The reaction rate for the field condition, $\ln(R_{site})$, was calculated as:

$$\ln\left(\frac{1}{t}\right) = \ln A - \left(\frac{E_{act}}{R}\right)\left(\frac{1}{T_{site}}\right) \quad (3.6)$$

For this project, flexural creep tests at different temperatures were completed and the parameters for the Arrhenius model were calculated. Estimations of the time for the RPPs to deform to reach failure can now be performed.

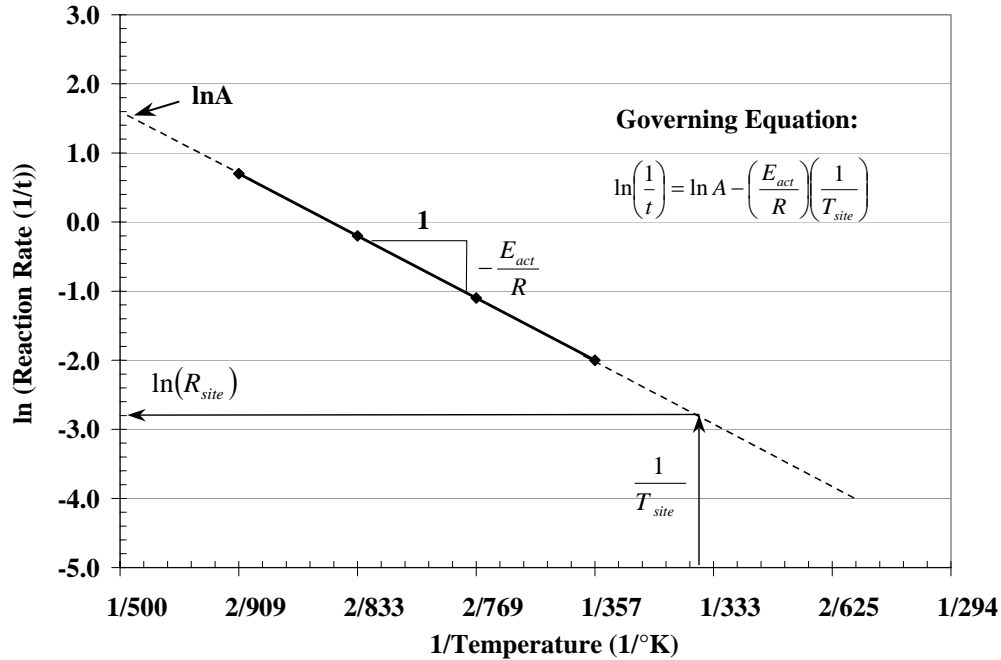


Figure 3.8 Arrhenius plot of inverse reaction rate versus inverse temperature (Koerner, 1998).

3.3.3.2 Compressive Creep Test

The 3.5-inch squares by 7-inch height specimens were cut from the manufactured RPPs for the compressive creep tests, as shown in Figure 3.9. A 0.42-inch (10.7 mm) diameter hole was drilled at the center of specimen. The compressive load was applied through a spring with an 800 lb/in (44.1 KN/m) spring constant. Two dial gages were used; one measured the deformation of the spring for controlling the applied load. The other measured the deflection of the specimen. All specimens were tested at room temperature. (21°C (70°F)).



Figure 3.9 Setup for compressive creep test of recycled plastic specimen.

Measurements of deflection on both dial gages over time were recorded. This data was necessary because creep is a time dependent phenomenon under sustained loads. During compression creep testing, the dimensional changes that occurred during the time, the specimen was under a constant static load were measured. Plotting deflection versus time reveals the different stages of creep. An idealized creep curve is shown in Figure 3.10. Primary creep occurs upon loading after which the creep rate decreases rapidly with time. Secondary creep occurs after primary creep and is distinguished by the flattening of the deformation versus time curve (the steady-state value). Tertiary creep is the final stage of creep, which is noted by a rapid increase in the deformation with time. It is common to define failure as the deformation/time when the specimen transitions from secondary to tertiary creep. In this work, failure was taken as the time to ultimate rupture.

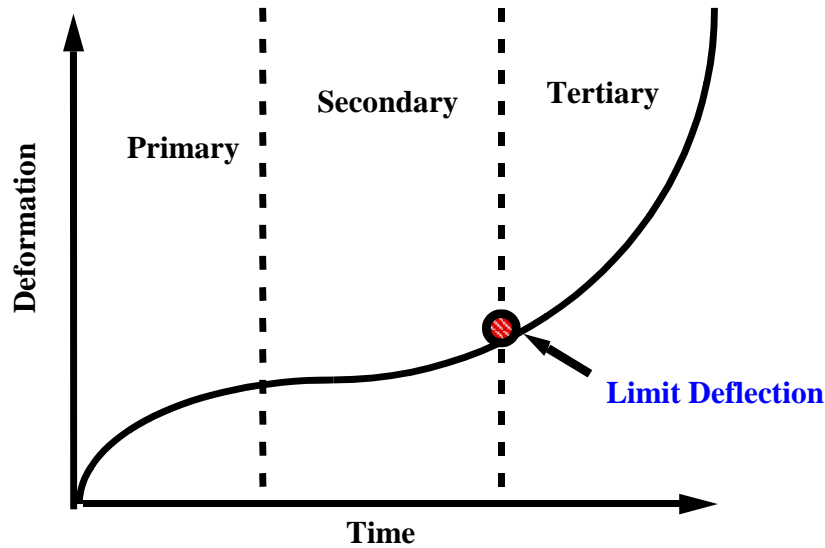


Figure 3.10 An idealized creep curve.

3.4 Field Methods: Drivability Analyses

Installation characteristics for the different members were monitored at five slope stabilization sites. During installation, the time required to drive the RPP to full depth, 8 feet (2.4 m), or until refusal, was recorded and a penetration rate (ft/min) was calculated for each member. Refusal was defined when the penetration rate drop to three inches per minute. The penetration rate was calculated by dividing the penetration length by the corresponding time, excluding set up time.

Table 3.3 describes the seven slopes at five different sites with workdays, total RPPs installed, and driving equipment. The first demonstrated site (man-made, compacted fill) is an approximately 22-feet (6.8 m) high embankment with 2.5:1 (horizontal:vertical) side slopes that forms the eastbound entrance ramp to Interstate 70 near Emma Missouri (the I70-Emma site). This site was stabilized with RPPs in November and December 1999. The site includes two separate stabilized areas (slide 1 and slide 2) and two control area (unstabilized), denoted slide 3 and slide 4, all of which

had experience repeated surficial slides over the past decade or more (Loehr et al., 2000a). A total of 362 RPPs (includes trial installation) were installed in slide 1 and slide 2 during October and November 1999. The initial installation equipment used at the site consisted of an Okada OKB 305 1250 ft-lb (1695 N-m) energy class hydraulic hammer mounted on a Case 580 backhoe (Figure 3.11). This equipment was used for trial installation and 45 RPPs were installed in I70-Emma slide 1. It proved unsuccessful as the penetration rate was deemed unacceptable and installation was halted (Loehr et al., 2000a, Sommers et al., 2000). Installation at slide 1 and slide 2 resumed on November 11, 1999 using a Davey-Kent DK 100B crawler mounted drilling rig supplied by the Judy Company of Kansas City, Kansas (Figure 3.12). The crawler system caused much less damage to the slope than the rubber-tired equipment. The crawler system did become marginally stable when operating on the steepest parts of the embankment (>2H:1V) and had to be tethered to the top of the slope in some locations.

Subsequently, the I70-Emma slide 3, which was one of the control areas, was stabilized with RPPs and finished installation on January 7, 2003. A total 166 RPPs were installed using Ingersoll Rand ECM350 system (Figure 2.1b and Figure 3.13). An additional new installation equipment was the Daken Farm King hitter series II, Case XT90 skid steer loader (impact-hammer equipment) that used for trials installation in this site (Figure 3.13). Only two workdays were needed to finish the stabilization using RPPs on January 7, 2003.

Table 3.3 Detail of Seven Slopes Using RPPs for Stabilization

Stabilized Slope	Slope Inclination	Slope Height (ft)	Work Days	# Pin Installed	Installation Equipment
I70 Emma slide 1	2.5 (H): 1 (V)	22	1	45 ^[1]	Okada OKB 305(1250 ft-lb) 1695 N-m energy class hydraulic hammer
	2.5 (H): 1 (V)	22	2	154	Davey-Kent DK 100B crawler mounted drilling
I70 Emma slide 2	2.5 (H): 1 (V)	20	3	163	Davey-Kent DK 100B crawler mounted drilling
I70 Emma slide 3	2.5 (H): 1 (V)	20	2	166	Ingersoll Rand ECM350, IR 300 CFM, 100 psi air compressor
	2.5 (H): 1 (V)	20	1	32 ^[1]	Daken Farm King hitter series II, Case XT90 skid steer loader
I435 Wornall	2.2 (H): 1 (V)	31.5	2	33	Davey-Kent DK 100B crawler mounted drilling
	2.2 (H): 1 (V)	31.5	10	583	Ingersoll Rand CM150, IR 350 CFM, 100 psi air compressor
I435 Holmes	2.2 (H): 1 (V)	15	5	262	Ingersoll Rand CM150, IR 350 CFM, 100 psi air compressor
US36 Stewartsville	2.2 (H): 1 (V)	27	5	360	Ingersoll Rand CM150, IR 350 CFM, 100 psi air compressor
US54 Fulton	3.2 (H): 1 (V)	43	4	377	Ingersoll Rand ECM350, IR 300 CFM, 100 psi air compressor

^[1]: trial installation



Figure 3.11 Initial equipment used for installation of RPPs at the I70-Emma slide 1.



Figure 3.12 Crawler mounted drilling rig used for installation of RPPs at the I70-Emma slide 1 and slide 2.



Figure 3.13 Ingersoll Rand ECM350, 100-psi air compressor and Daken Farm King hitter series, impact hammer used for installation of RPPs at the I70 Emma slide 3.

The second slope stabilized with RPPs located at the intersection of Interstate 435 at Wornall Road in southern Kansas City, Missouri near the Missouri-Kansas border (the I435-Wornall site). The compacted fill (man-made) embankment is an approximately 31.5-feet (9.6 m) high with side slope of 2.2:1 (horizontal:vertical). The Davey-Kent DK 100B crawler mounted drilling rig was used for trial installation and only 33 RPPs were installation during the first two workdays. Observations showed that the equipment was too heavy and could easily damage the slope faces during installation even if was tethered to the top of slope in some locations. Therefore, an Ingersoll Rand CM150 air crawler plus the air-track (air compressor) system supplied by the Judy Company was used for the subsequent installation (Figure 3.14). This type of installation equipment is lighter than the Davey-Kent DK 100B crawler rig and could easily operate on the slope (>2H:1V). It also made driving the RPPs with correct alignment and placement fairly

easy and quick. A total of 583 RPPs were installed with the Ingersoll Rand CM150 system in ten workdays and the work was finished on December 7, 2001.

An additional stabilized slope located at the southeast side of intersection between Interstate 435 and Holmes Road, Kansas City (the I435-Holmes site). The compacted fill (man-made) is an approximately 15-feet (4.6 m) high embankment with 2.2:1 (horizontal:vertical) slope face. The same equipment, Ingersoll Rand CM150 air crawler plus 100-psi air compressor, were used for five workdays to install a total of 254 steel pipes. The 3.5-inch (90 mm) diameter steel pipes were used at this location to provide for a wider range of reinforcing member properties.

A cut slope located at Route US36, near Stewartville Missouri (the US36-Stewartville site) has been stabilized using RPPs since May 7, 2002. The slope is approximately 27-feet (8.2 m) high with side slope of 2.2:1 (horizontal:vertical). A total of 360 RPPs were installed using the same equipment as that used at the I435-Wornall and Holmes sites.

The last stabilized site (cut slope) located at Route US54, near Fulton Missouri (the US54-Fulton site). It is approximately 43-feet (13.1 m) high embankment with 3.2:1 (horizontal:vertical) slope face. The slope was stabilized using 377 RPPs and work was finished on January 15, 2003 for four workdays. The same installation machine was used for this site (Figure 2.1b). All seven slopes at five sites were instrumented for performance monitoring.



Figure 3.14 Ingersoll Rand CM150, 100-psi air compressor used for installation of RPPs at the I435-Wornall site.

CHAPTER 4: RESULTS AND DISCUSSION

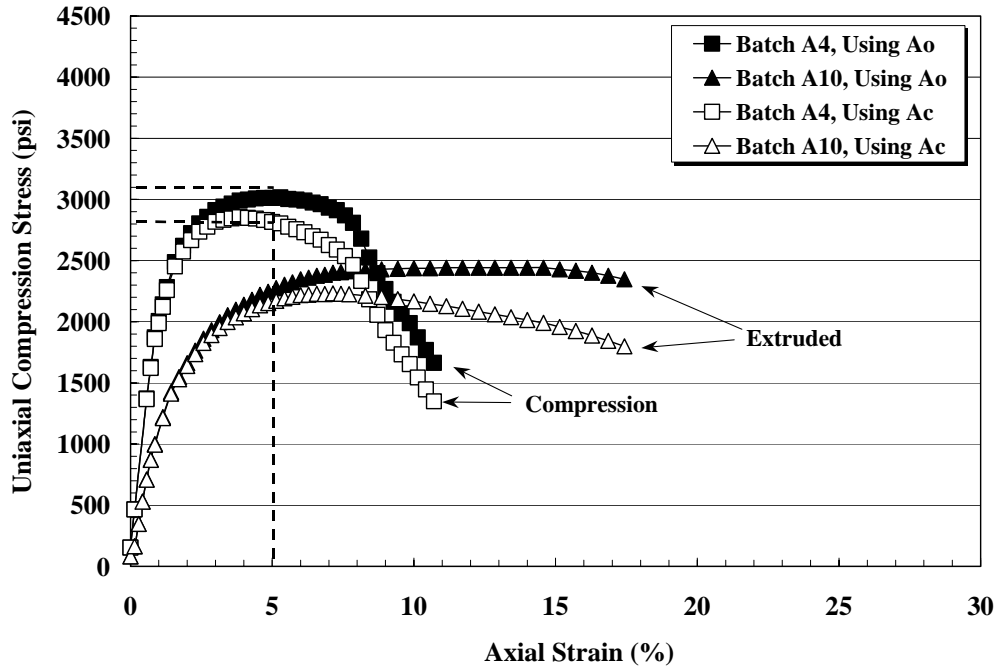
4.1 Overview

The results of the laboratory tests and field drivability analyses are presented in this chapter. Tests performed included uniaxial compression, four-point flexure, flexural creep, and compressive creep. Arrhenius modeling was used to predict the time to reach creep failure for RPPs installed in the field. Field tests included drivability performance for seven stabilized slopes are also presented and discussed in this section.

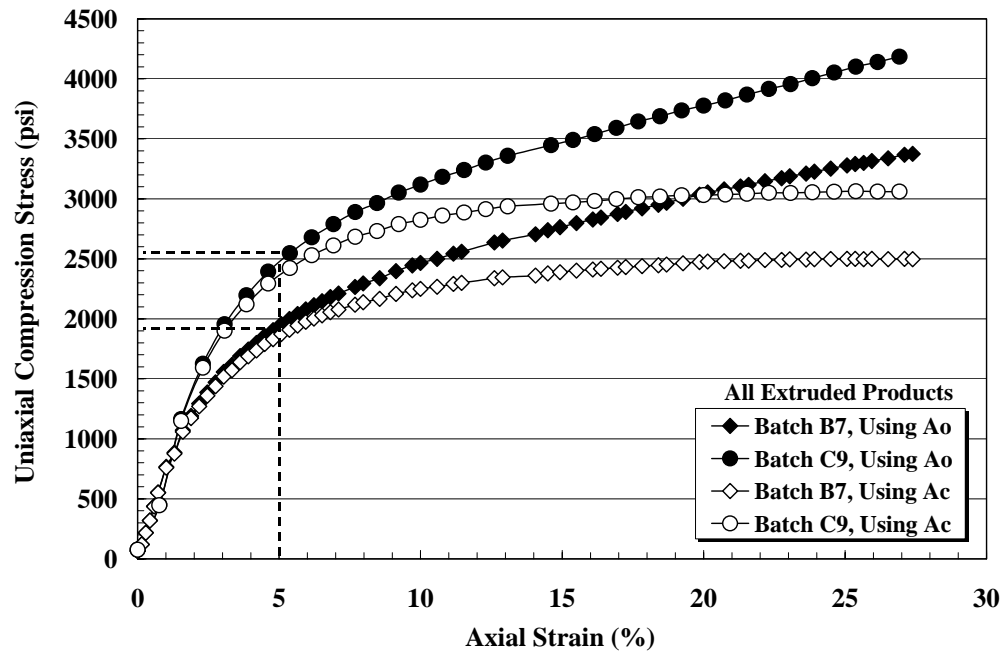
4.2 Uniaxial Compression Tests

4.2.1 Stress-Strain Curves

Typical compressive stress-axial strain curves determined for the recycled plastic pins (RPPs) are shown in Figure 4.1 for specimens from manufacturer A (Figure 4.1a) and manufacturers B and C (Figure 4.1b). As shown in the figures, specimens provided by manufacturer A exhibited a clear peak in the stress-strain response, whereas specimens from manufacturers B and C produced no clear peak in the stress-strain curves when the original cross-sectional area (A_0) was used to compute the stress. The peak stress occurred after exceeding five percent axial strain for compression materials from manufacturer A. The compression-molded specimens show a small strain (about 10 percent strain) to reach total failure, and the extruded products show at least about 18 percent strain until the appearance of failure planes.



(a) Stress-strain curve typical of RPPs exhibiting failure planes (All Mftg A).



(b) Stress-strain curve typical of RPPs exhibiting bulging failure (Mftg B and C).

Figure 4.1 Typical compressive stresses versus axial strain behavior for recycled plastic pins (RPPs).

The extruded products from manufacturers B and C exhibited no peak stress in the stress-strain curve. The stress increased with increasing strain up to about 30 percent strain when using the original cross-sectional area (A_0) to calculate compressive stress. Figure 4.2 shows typical deformed specimens after compression tests. These photographs reveal that specimens from manufacturer A developed clearly defined failure planes, while specimens from manufacturers B and C developed no clear failure planes, but exhibited a bulging type of failure mode.



(a) Typical failure planes shown by compression molded RPPs from Mftg A.



(b) Typical bulging failure has shown by extruded products from Mftg B and Mftg C.

Figure 4.2 Failure modes of RPPs during uniaxial compression tests.

4.2.2 Uniaxial Compression Strength

Observations from the laboratory testing results suggest that a corrected cross-sectional area should be used in the determination of the compressive strengths, but no standard area correction has been established. If one assumes a constant volume and that the cross-section remains uniform during compression, a corrected cross-sectional area can be computed as:

$$A_e = \frac{A_0}{(1 - \varepsilon)} \quad (4.1)$$

where A_e is the corrected cross-section area calculated from Equation 4.1, A_0 is the original cross-sectional area, and ε is the axial strain. However, observations of the specimens during testing indicate that the cross-sectional areas do not remain uniform and the volume is not constant during deformation, thus invalidating the use of Equation 4.1 for area corrections. Since no consistent area correction has been agreed upon, the compressive strengths reported subsequently were taken to be the compressive stress at five percent axial strain for all specimens without area corrections. The five percent strain limit serves to limit the magnitude of errors associated with the specimen area and provides a consistent basis for comparison of strengths for different specimens. The five percent strain limit also serves as a basis for limiting deformation in the field applications.

The difference between the corrected cross sectional area (A_c) calculated from the measured perimeter during the compression test and the original area (A_0) versus axial strain during compression test for three different manufacturers is shown in Figure 4.3. In general, the cross-sectional area is a function of axial strain. The area increased

with axial strain for all RPP specimens from all three manufacturers. The cross sectional area for batches A4 (compression molded) rapidly increases within 11 percent axial strain while the cross sectional area for batches B7, B8, and C9 increased at a lower rate. The cross sectional areas for batches A5, A6, and A10 (all extruded products from manufacturer A) have intermediate increase within 15 percent axial strain. Application of this correction produces a more clearly defined peak in the stress-strain response for specimens from manufacturers A, B, and C (Figure 4.1).

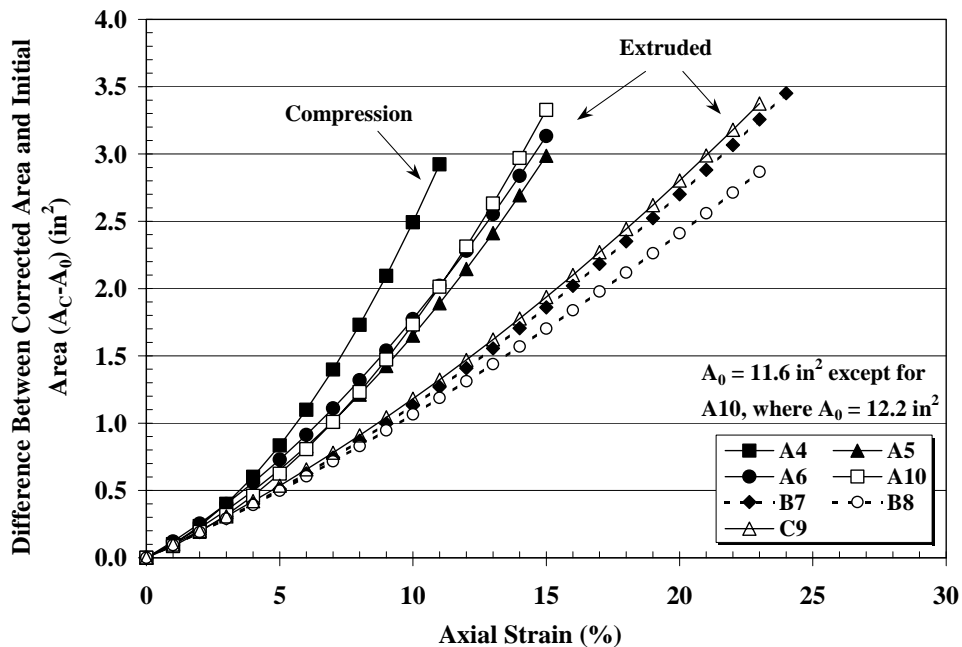


Figure 4.3 Difference calculated from measured perimeter versus axial strain during compression tests (Mftg A, B, and C).

The average and standard deviation of the compressive strengths determined for each batch of specimens are given in Table 4.1. Overall, the measured compressive strengths range from 1600 psi to 3000 psi (11 MPa to 21 MPa) based on original cross-sectional area calculation at a nominal strain rate equal to 0.006 in/in/min (0.006 mm/mm/min).

Table 4.1 Uniaxial Compression Strength from Uniaxial Compression Test on RPPs

Specimen Batch	# Specimens Tested	Nominal Strain rate (in/in/min)	Uniaxial Compression Strength ^[1] (psi)		Uniaxial Compression Strength ^[2] (psi)	
			Avg.	Std. Dev.	Avg.	Std. Dev.
A1	10	NA	2784	128	-- ^[3]	--
A2	7	0.005	2948	117	--	--
A3	6	0.005	2824	88	--	--
A4	6	0.005	2621	295	2486	271
A5	6	0.007	1634	200	1578	189
A6	14	0.007	1602	105	1521	102
A10	15	0.006	2219	154	2152	136
A11	15	0.006	2301	139	2217	140
A12	8	0.007	2085	84	1931	199
A13	15	0.007	2380	330	2310	318
B 7	15	0.007	2080	69	2331	134
B 8	15	0.006	2500	191	2505	195
C 9	15	0.007	2315	209	2556	322

^[1]: Use original cross-sectional area (A_0) to calculate stresses

^[2]: Use corrected cross-sectional area (A_c) to calculate stresses

^[3]: Data not available

Conversion: 1 MPa = 145 psi

Specimens from batches A1 to A4 are compression-molded products with dates of manufacture spanning two years. The average strength of these specimens is 2800 psi (19 MPa) with a standard deviation of about 150 psi (1 MPa). This shows a good consistency of product over the two-year period. Specimens from batches A5 and A6 were manufactured using the extrusion process with a slightly lower amount of “filler” material (primarily sawdust). The average compressive strength of these specimens was 1600 psi (11 MPa), approximately 40 percent lower than specimens from batches A1 to A4. Most of the reduction in strength among specimens in batches A1-A4 and batches

A5-A6 is attributed to the manufacturing process. However, specimens in batches A5 and A6 represent the initial attempts by manufacture A at extruded products. Specimens from batches A10 to A13 were also manufactured using the extrusion process. The average strength of these specimens is 2200 psi (15 MPa), approximately 20 percent lower than specimens from batches A1 to A4. The subsequent products (Batches A10 to A13) show about a 30 percent increase in the average compressive strength of the batch A5 and A6. This demonstrates that the manufacturer can modify the process and the constituent mixture to produce materials with comparable strengths to the compression-molded product.

The specimens used to represent the strength for batches A11, A12 and A13 were taken from the portion of the RPPs that remained above the ground surface after installation. Thus, these specimens are considered “disturbed” (Table 3.1). Batch A10 specimens were delivered directly to the laboratory and are considered “virgin” materials. Note, there is no discernable change in the average compressive strength between the specimens in the virgin condition and those in the disturbed condition indicating that the installation process does not have a deleterious effect on the compressive strength of the RPPs. Batches A11 and A13 are disturbed specimens that were installed using an air-compression hammer (Figure 3.13). Batch A12 specimens were installed using the impact hammer (Figure 3.13). In one instance, Batch A12 has slightly lower strengths (about 10 percent lower) than the virgin specimens from batch A10. The reasons may be associated with the different installation equipment or different number of specimens tested. The variation in strength between the three batches is not significant to indicate

that either driving method is more or less deleterious to the compressive strength of RPPs.

The average compressive strength for manufacturer B and C ranged from 2000 psi to 2500 psi (14 MPa to 17 MPa), approximately 10 percent to 30 percent lower than specimens from batches A1 to A4. Batch B8 with the fiberglass-reinforced specimens shows about 20 percent increase in compressive strength when compare to the unreinforced specimens (Batch B7).

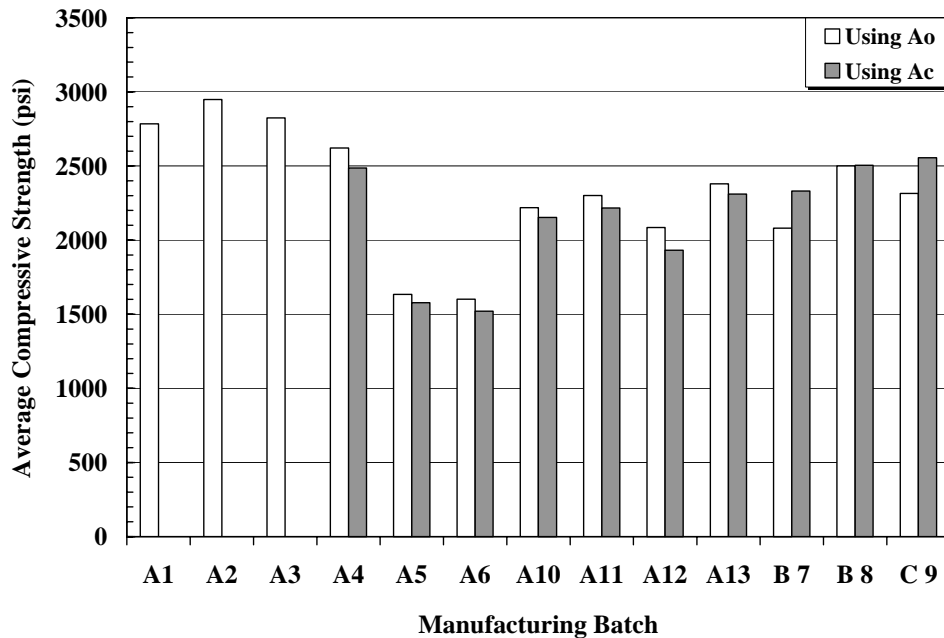


Figure 4.4 Comparison of average compressive strengths with and without cross-sectional area corrections for materials from all manufacturers.

The average compressive strengths for materials from the three manufacturers determined at five percent strain with no area correction (A_0) and at the peak stress with area correction (A_c) are shown as bar graph in Figure 4.4. In general, the strengths at A_0 (5%) are higher than those with area correction (A_c). The difference is approximately five

percent. In two instances, batches B7 and C9, the strength with the area correction was higher (by approximately 10 percent) than the specimens without area correction. The close agreement between the strengths indicates that using the strength at five percent strain without corrected cross-sectional area provides a reasonable value for the peak strength.

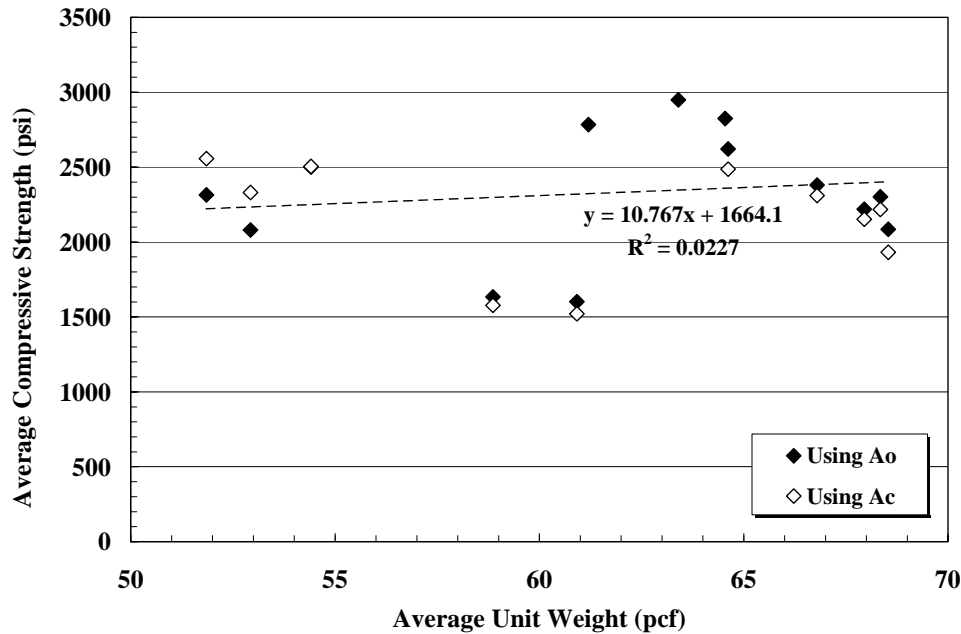


Figure 4.5 Average compressive strength versus average unit weight for materials from all manufacturers.

Figure 4.5 shows a plot of the average compressive strength versus average unit weight for materials from three manufacturers. The solid data points represent strengths calculated based on original cross-sectional area (A_o), and open data points represent strengths calculated from corrected cross-sectional area (A_c). The average strengths ranged from 1500 psi to 3000 psi (10 MPa to 21 MPa) within a unit weight range of 50 pcf to 70 pcf (8 kN/m³ to 11 kN/m³). There is little correlation between strengths and unit weights. The reasons could be associated with the principal constituents and the

manufacturing processes. Therefore, the unit weights of the RPPs play a small role in influence on the compressive strengths.

4.2.3 Modulus of Elasticity

Average values and standard deviations of the secant modulus of elasticity, E , determined from the uniaxial compression tests at one percent strain and five percent strain are shown in Table 4.2.

Table 4.2 Secant Moduli from Uniaxial Compression Test on RPPs

Specimen Batch	# Specimens Tested	Nominal Strain rate (in/in/min)	Secant Modulus, $E_{1\%}^{[1]}$ (ksi)		Secant Modulus, $E_{5\%}^{[1]}$ (ksi)		Secant Modulus, $E_{1\%}^{[2]}$ (ksi)		Secant Modulus, $E_{5\%}^{[2]}$ (ksi)	
			Avg.	Std. Dev.						
A1	10	NA	134	8	57	4	-- ^[3]	--	--	--
A2	7	0.005	184	9	55	3	--	--	--	--
A3	6	0.005	164	29	57	3	--	--	--	--
A4	6	0.005	186	20	52	4	185	20	49	4
A5	6	0.007	84	16	33	4	84	16	31	3
A6	14	0.007	93	8	32	2	92	8	30	2
A10	15	0.006	114	12	45	3	113	12	43	3
A11	15	0.006	119	11	47	3	119	11	45	3
A12	8	0.007	108	11	40	4	107	11	38	4
A13	15	0.007	110	21	48	6	110	21	45	6
B 7	15	0.007	87	10	42	2	85	11	39	3
B 8	15	0.006	138	27	49	4	136	26	47	4
C 9	15	0.007	87	12	46	4	86	12	45	4

^[1]: Use initial cross-sectional area (A_0) to calculated stresses

^[2]: Use corrected cross-sectional area (A_c) to calculated stresses

^[3]: Data not available

Conversion: 1 MPa = 145 psi, 1 ksi = 6.9 MPa

The moduli were calculated using original cross-sectional area and corrected cross-sectional area. The moduli determined at one percent strain generally ranged from 80 ksi to 190 ksi (552 MPa to 1310 MPa) for both failure criteria. The moduli of the extruded products was generally on the order of one half that determined for the compression-molded products. For example, batch B8 (fiberglass-reinforced specimens) show the stiffness about 20 percent lower than the compression-molded products. Average secant modulus at one percent axial strain of batch B8 (fiber-reinforced materials) was 138 ksi (951 MPa), approximately 60 percent higher than specimens from batch B7 (unreinforced materials).

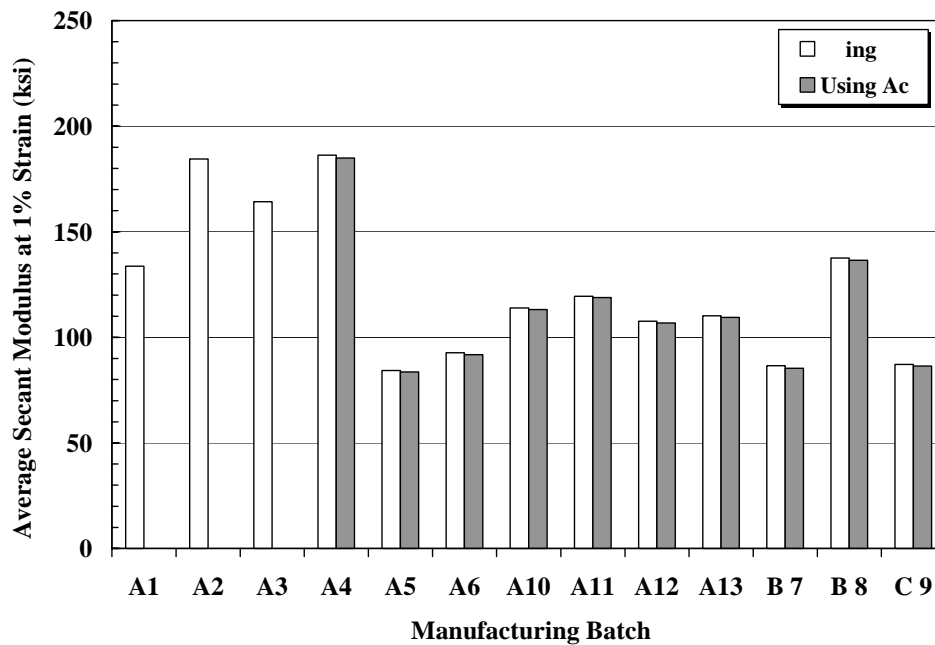


Figure 4.6 Comparison of average secant modulus at 1% axial strain ($E_{1\%}$) for all manufacturers.

The average results and range for each batch are shown as bar graph in Figure 4.6 ($E_{@1\% \epsilon}$) and Figure 4.7 ($E_{@5\% \epsilon}$). The secant moduli at one percent axial strain show no difference between original and corrected area. At five percent axial strain (Figure 4.7),

the moduli calculated using the original cross-sectional area are about five percent greater than those calculated using the corrected area. This behavior is similar to that for the compressive strength and further indicates that the strength and modulus calculated using the original area at five percent strain is a reasonable representation of the peak strength.

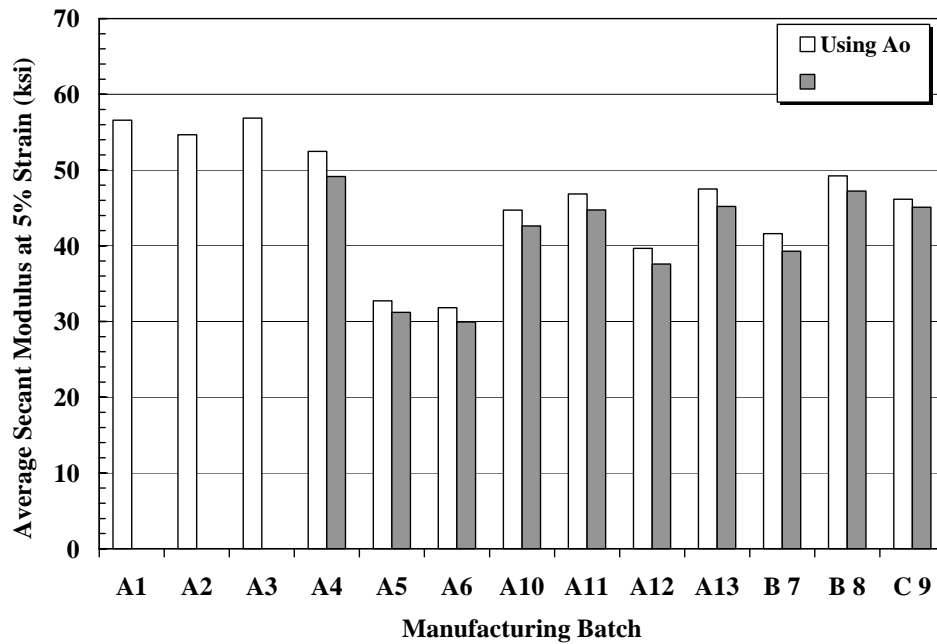


Figure 4.7 Comparison of average secant modulus at 5% axial strain ($E_{5\%}$) of all manufacturers.

The average secant moduli at one percent strain for batches A10 – A13 ranged from 110 ksi to 120 ksi (758 MPa to 827 MPa). For Batches A5 and A6 the average secant moduli at one percent strain ranged from 80 ksi to 90 ksi (552 MPa to 621 MPa). The secant moduli at one percent strain for batches B7 and B8 were quite different from manufacturer A. The secant moduli at one percent strain for batches B7 and C9 were almost identical and both are unreinforced material. The unreinforced material (Batch B7) had a secant modulus of 90 ksi (621 MPa) while the reinforced material (Batch B8)

had a secant modulus of 140 ksi (965 MPa). Obviously, the reinforcing fibers significantly stiffened the material.

The modulus values determined at five percent strain ranged from 30 ksi to 60 ksi (207 MPa to 414 MPa), indicating that all of the products exhibited significant softening (decreasing stiffness) with increasing strain. The secant moduli at five percent strain were similar for batches A10 through A13, manufacturer B, and manufacturer C, and were in the range of 40 ksi to 50 ksi (276 MPa to 345 MPa).

4.2.4 Strain Rate Effects

The properties of plastic materials are dependent on the rate of loading (Birley et al, 1991). The behavior of the recycled plastic lumber (viscoelastic) is that the more rapidly it is loaded, the stronger and stiffer the material behaves (McLaren, 1995). To evaluate this effect, a series of tests were performed for a range in strain rates for specimens provided by all three manufacturers. All results of the compressive strengths were calculated using the original cross-sectional area (A_0). The results of these tests from the “virgin” specimens from manufacturer A are plotted in Figure 4.8. It is of interest to see that the trend line of batch A4 (compression molded) is almost parallel to the trend line of batch A10 (extruded products). Batch A4 shows that the measured compressive strength increased from 2100 psi to 2900 psi (14 MPa to 20 MPa) (a 30 percent change) as the strain rate was varied from 0.0006 in/in/min to 0.02 in/in/min (0.0006 mm/mm/min to 0.02 mm/mm/min). This corresponds to a drop in compressive strength of approximately 18 percent for each log cycle reduction in strain rate. Batch A10 had a drop in compressive strength of approximately 22 percent for each log cycle reduction in strain rate. Batches A5 and A6 had slightly smaller differences in strength

and moduli shows that they had the same strain rate effect. They all had a drop in compressive strength of approximately 16 percent for each log cycle reduction in strain rate. In these tests, the specimen tested at the lowest strain rate (0.0006 in/in/min) reached its peak stress in about two hours while the specimen tested at the highest strain rate (0.021 in/in/min) reached failure in approximately 6 minutes. Because of the significance of strain rate effects and practical issues involved with developing a specification, a strain rate of approximately 0.006 in/in/min (testing time of approximately 20 minutes) was chosen as a baseline for comparing the remaining test specimens.

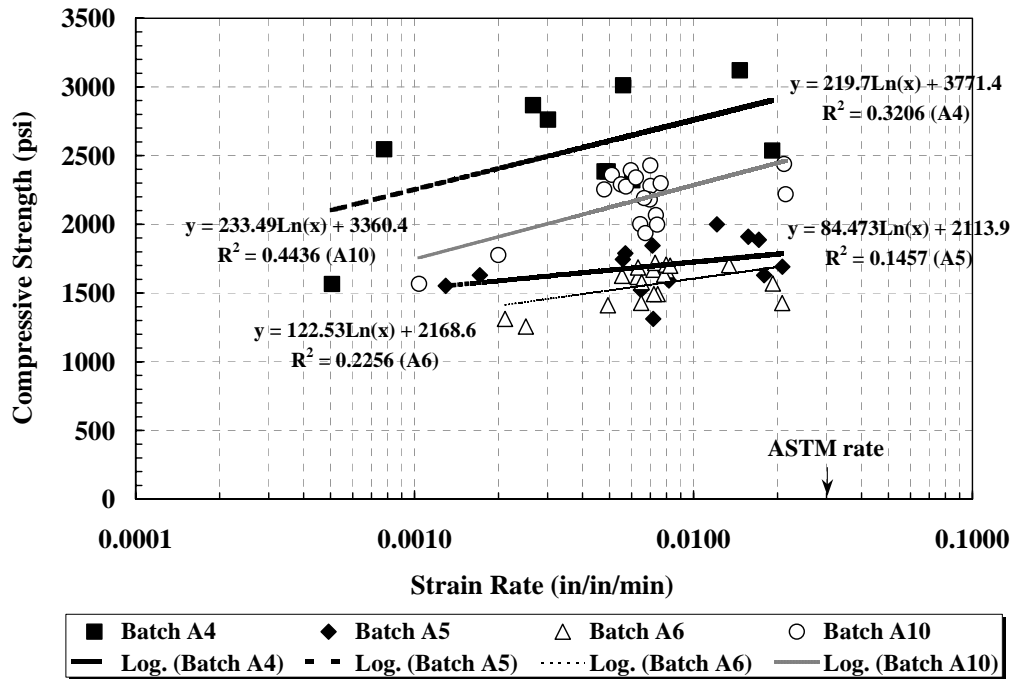


Figure 4.8 Compressive strength versus strain rate for tests on RPPs (Mftg A – virgin specimens).

Figure 4.9 shows that the compressive strength versus strain rate for batch A10 (virgin specimens) and for batches A11 to A13 (disturbed specimens). In general, the differences in the slopes of each batch were small. Batches A11 and A13 were installed using the same types of equipment and show that the measured compressive strength

increased from 1800 psi to 2500 psi (12 MPa to 17 MPa) (a 30 percent change) as the strain rate was varied from 0.0003 in/in/in to 0.02 in/in/min (0.0003 mm/mm/min to 0.02 mm/mm/min). This corresponds to a drop in compressive strength of approximately 15 percent for each log cycle reduction in strain rate, which is lower than that for batch A10 that had a 22 percent decrease in strength for each log cycle reduction in strain rate. The variation in stain rate effects between the three disturbed batches is not significant to indicate again that either driving method is more or less deleterious to the RPP strength.

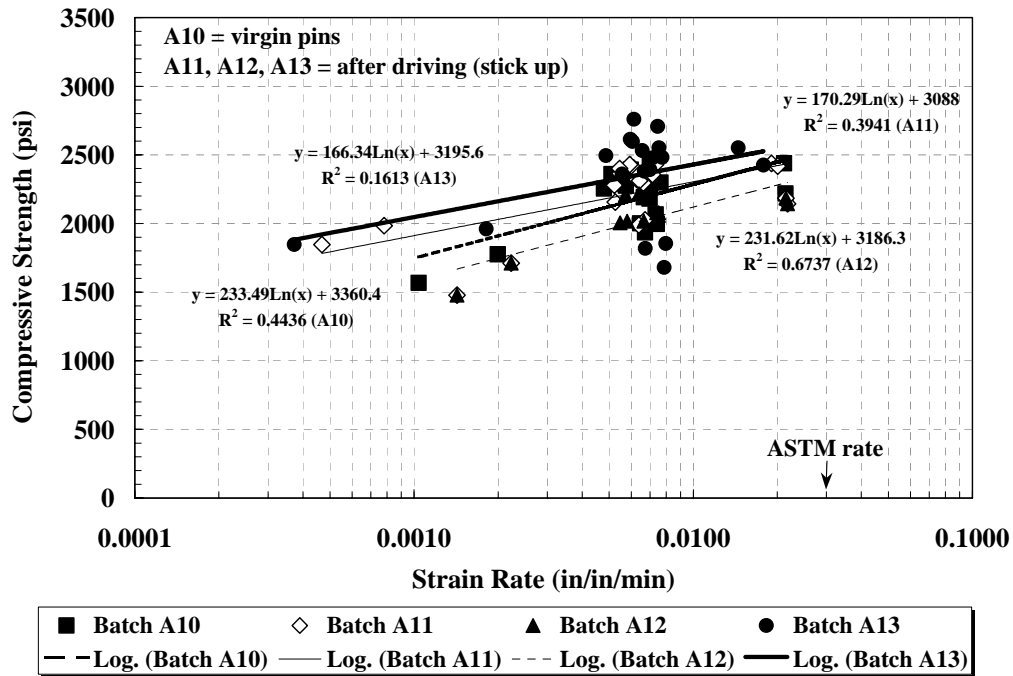


Figure 4.9 Compressive strength versus strain rate for materials from Mftg A (virgin specimens versus disturbed specimens).

Figure 4.10 shows the compressive strength versus strain rate batches from manufacturer B and manufacturer C. Note that the slope of strain rate relationships are almost identical, although these materials come from different manufacturers. In general, these three batches show that the strength increased from 1800 psi to 2700 psi (12 MPa

to 19 MPa) (a 30 percent change) as the strain rate was varied from 0.0003 in/in/min to 0.02 in/in/min (0.0003 mm/mm/min to 0.02 mm/mm/min). This corresponds to a drop in compressive strength of approximately 20 percent for each log cycle reduction in strain rate. It can be concluded that the drop in compressive strength for RPPs from all three manufacturers ranged from 15 percent to 25 percent for each log cycle reduction in strain rate.

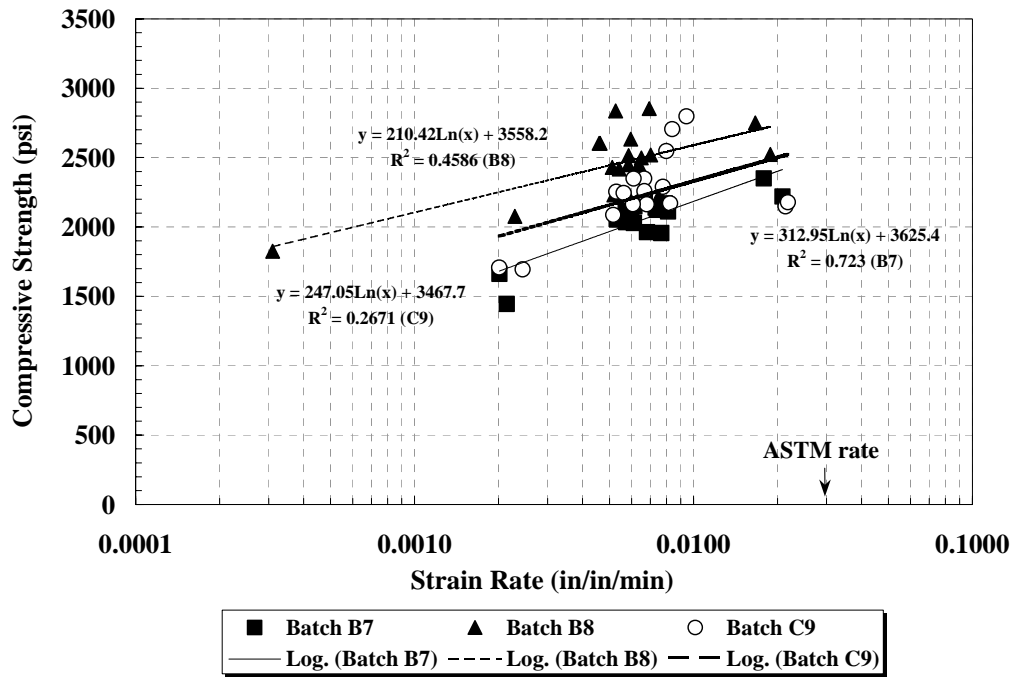


Figure 4.10 Compressive strength versus strain rate for tests on RPPs (Mftg B and C).

Standard compression strength (σ_{std}) was defined by the compressive strength at 0.03 in/in/min (ASTM, 1997a), based on the compressive strength versus strain rate plot (Figure 4.11). For example, results of the compressive strengths versus strain rates from batch A10 were plotted in Figure 4.11. The standard compression strength was taken equal to 2540 psi at a strain rate equal to 0.03 in/in/min (0.03 mm/mm/min). Note that,

every batch has a different standard compressive strength as measured at a strain rate of 0.03 in/in/min (0.03 mm/mm/min).

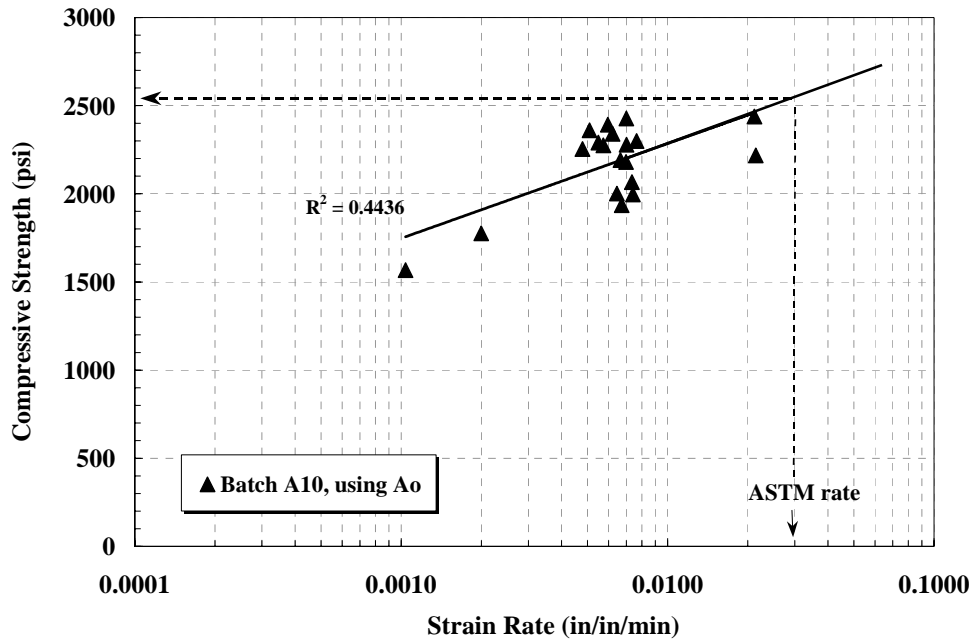


Figure 4.11 Standard compressive strength (σ_{std}) for tests on RPPs (Batch A10).

The ratio of the compressive strength (at a given strain rate) to the standard compression strength (σ_{std}) as a function of strain rate for the RPPs from all three manufacturers is plotted in Figure 4.12. As shown in this figure, the compressive strength decreases with decreasing strain rate in terms of the standard compressive strength (σ_{std}) of percentage reduction. Batch A5 has the flatter slope and serves as “upper-bound” reduction. Batch B7 has the steepest slope and serves as “lower-bound” reduction. The average slope was computed by taking average value of all the data. Thus making it easy to compare all possible strain rates that might occur in the field in terms of reductions of the standard compression strength (σ_{std}). For example, the compressive strengths decrease by approximately 30 percent (average slope) of standard strengths at one-day

testing rate, while the strengths reduce about 60 percent (average slope) of standard strengths at one-week testing rate. From this strain rate relationship (Figure 4.12), we can test specimens at any strain rate and find their corresponding compressive strengths at field strain rate.

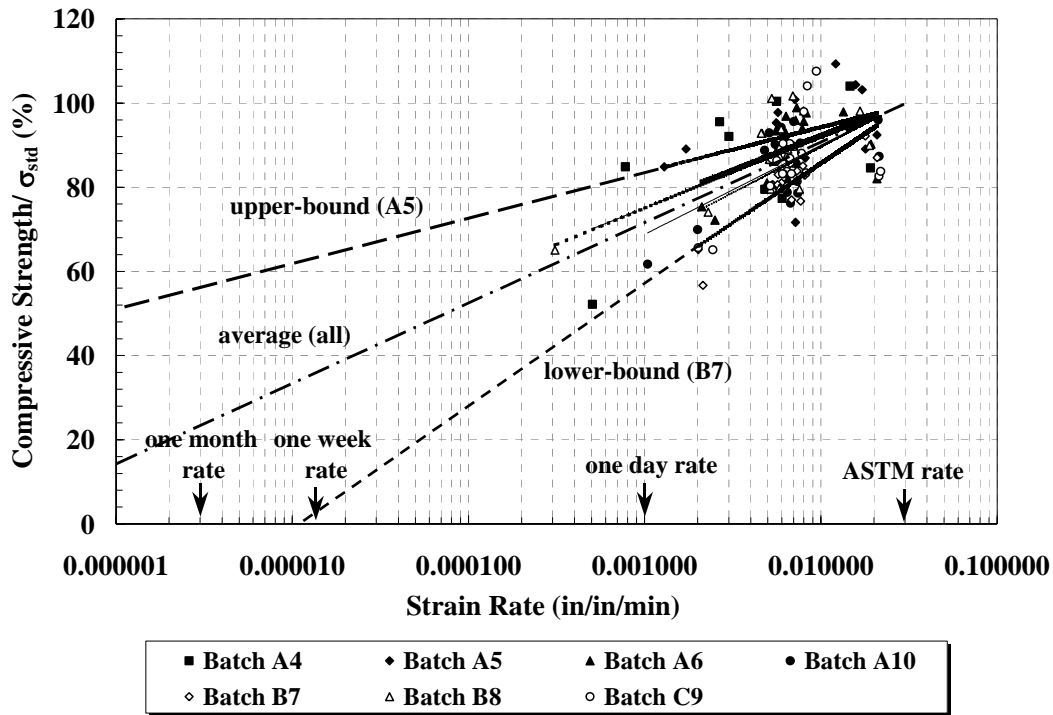


Figure 4.12 Ratio of compressive strength to standard compressive strength versus strain rate for RPPs.

Strain rates have particular significance in developing a suitable specification for recycled plastics in the slope stabilization application. Several ASTM standards have recently been developed specifically for testing plastic lumber products as summarized in Table 2.3. These standards dictate strain rates that are approximately 1.5 times greater than the highest strain rate shown in Figure 4.8, Figure 4.9, and Figure 4.10. While the value of standardized test procedures is acknowledged, current standardized tests were developed with typical building applications in mind. The loading rates specified in these standards is therefore very high. In the slope stabilization application, the members are

called upon to resist sustained bending loads over time, which may cycle from negligible load to the limit loads of the members as load is transferred from the moving soil in response to environmental conditions in the slope. In this application, the loading rate is likely to be very slow, on the order of months (seasonal). The evaluation program included tests performed at a range of loading rates to establish relationships between the properties of interest (primarily strength and stiffness) and loading rate.

4.3 Four-Point Flexure Tests

4.3.1 Flexural Stress- Center Strain Curves

Typical results of flexural stress versus center strain are observed from batches A4, A10, and B8. Specimens from batches A10 and B8 (extruded products) exhibited more than two percent center strain. Specimens from batch A4 (compression-molded) ruptured before two percent strain. Specimens from batch A10 showed a flatter curve after passing two percent strain and ruptured before reaching three percent strain, while specimens from batch B8 showed an increasing stress with increasing strain until reaching three percent strain, when the tests were stopped.

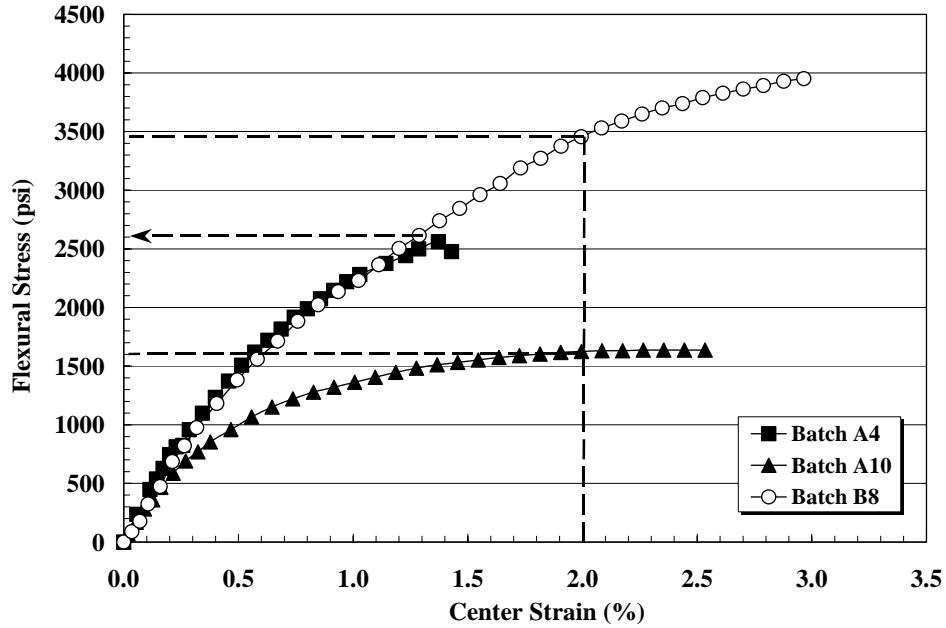


Figure 4.13 Typical flexural stresses versus center strain behavior for RPPs.

4.3.2 Flexural Strengths

Results of the four-point flexure tests are summarized in Table 4.3. Since the number of tests on batches A11 and A12 were limited, no standard deviation is reported. Extruded members showed continually increasing stress with increasing deflection/strain without experiencing rupture of the member, while the compression molded members ruptured at approximately two percent strain. The flexural strength for comparison of the different products was therefore taken to be the flexural stress at center strains of two percent or the stress at rupture for members that failed at center strains of less than two percent so that consistent strengths were established for all specimens. The measured flexural strengths for specimens loaded to failure or two percent center strain ranged from 1300 psi to 3600 psi (9 MPa to 25 MPa) under a nominal deformation rate 0.2 in/min (5.1 mm/min). The key finding from these tests is that there is significant variability, a factor of 2.8, in the flexural strength among the products tested.

Table 4.3 Results of Four-Point Flexure Tests on RPPs

Specimen Batch	# Specimens Tested	Nom. Def. Rate (in/min)	Flexural Strength ^[1] (psi)		Secant Flexural Modulus, E _{1%} (ksi)		Secant Flexural Modulus, E _{2%} (ksi)	
			Avg.	Std. Dev.	Avg.	Std. Dev.	Avg.	Std. Dev.
A1	13	-- ^[2]	1574	342	103	8	88 ^[3]	--
A4	3	0.17	2543	260	213	13	--	--
A5	5	0.23	1542	188	98	14	73	2
A6	7	0.14	1360	118	95	12	68	6
A10	6	0.18	1596	137	123	22	76	10
A11	1	0.19	1679	--	135	--	81	--
A12	1	0.19	1448	--	115	--	71	--
B 7	6	0.17	1505	112	90	7	69	4
B 8	6	0.17	3589	358	243	24	179	13
C 9	7	0.16	1696	39	107	4	83	2

^[1]: all results based on stress at 2% center strain or center strain at rupture of less than two percent

^[2]: data not available

^[3]: result of 2 specimens, others ruptured prior to reaching two percent center strain

Conversion: 1 MPa = 145 psi, 1 ksi = 6.9 MPa

A comparison the average flexural strength among all batches was plotted as a bar graph in Figure 4.14. In this plot, there is a tendency for the extruded products to have lower flexural strengths, except for batch B8 that contained reinforcing fibers. The average flexural strengths for extruded products are about 1500 psi (10 MPa) and for compression-molded products is about 2500 psi (17 MPa) (a 40 percent change); however, we must temper this conclusion with the only three tests of the batch A4. The only exception is batch B8 that has the flexural strength of approximately 3600 psi (25 MPa). The reinforced products of batch B8 showed a little increase in uniaxial compression strength (Table 4.1), but a large increase in flexural strength relative to other materials.

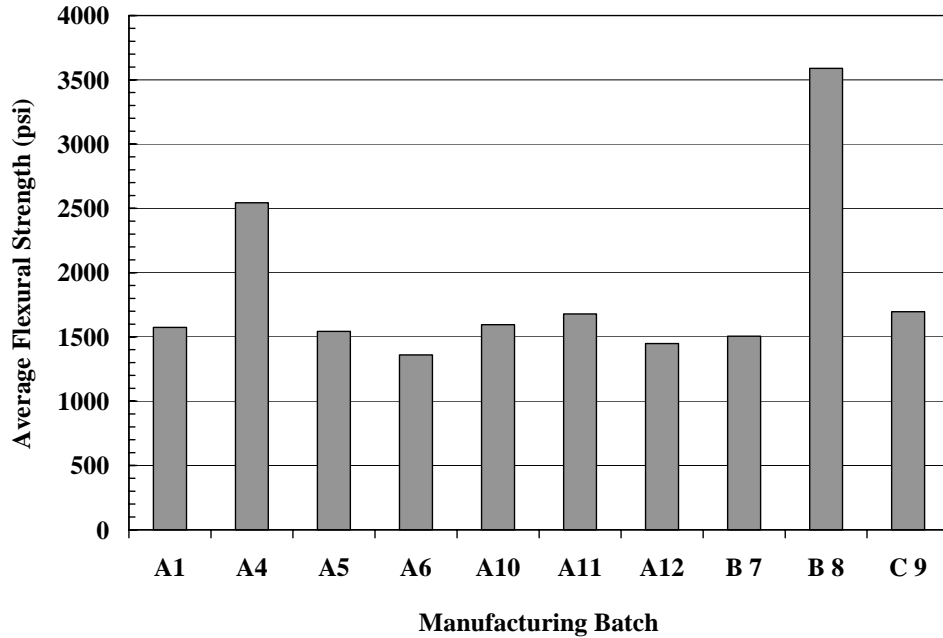


Figure 4.14 Comparison of average flexural strengths for all manufacturers.

4.3.3 Flexural Modulus

Average values of the secant flexural modulus for each batch of specimens are shown in Table 4.3. In general, the flexural moduli varied from approximately 90 ksi to 250 ksi (621 MPa to 1724 MPa) at one percent strain, similar to the values observed in the uniaxial compression tests with the exception of batch B8.

Results from batches A4 and B8 have significantly higher flexural stiffness than the other batches by a factor of two. This may potentially be a result of being compression molded or reinforced as compared to being on extruded products. Breslin et al. (1998) concluded that the use of glass and wood fiber additives significantly improves the modulus of elasticity for plastic lumber. Batch A10 (virgin specimens), batches A11 and A12 (disturbed specimens) have similar flexural strength and flexural moduli. Flexural moduli at two percent center strain were consistently lower than those

determined at one percent center strain, because the RPPs tended to soften with increasing strain. The clear difference is shown as a bar graph in Figure 4.15. Secant flexural modulus at two percent was not available for batch A4, because the specimens ruptured before two percent center strain.

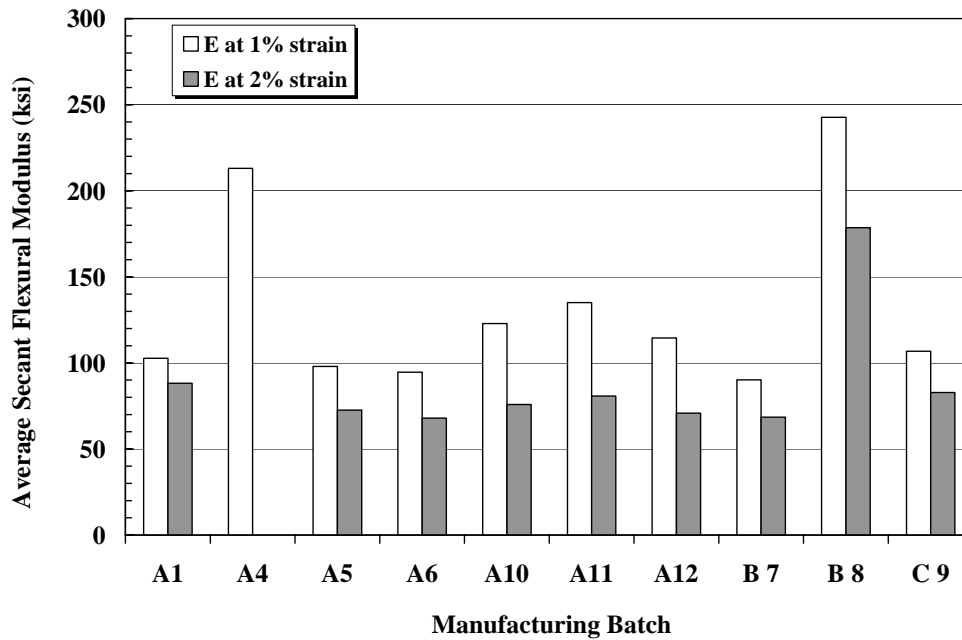


Figure 4.15 Comparison of average secant flexural modulus at one percent center strain ($E_{1\%}$) and two percent strain ($E_{2\%}$) of RPPs.

4.4 Creep Behavior

4.4.1 Flexural Creep Tests

Typical results of deflection versus time for specimens under a sustained load are shown in Figure 4.16. The behavior shown is typical of the RPPs tested at the various temperatures. The specimens were loaded with 50 lbs (23 kg) at the free end of a simple cantilever (Figure 3.6). All specimens failed after the final data point, with the exception of the specimens at 21°C (70°F), which have been under load for more than five years but have not failed.

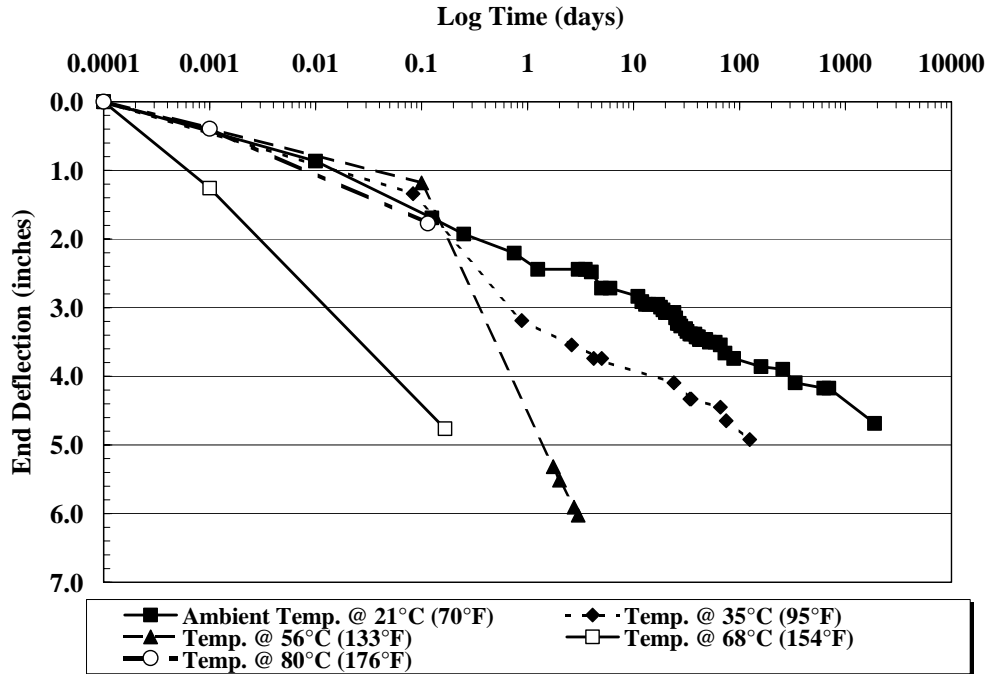


Figure 4.16 Deflection versus time response for RPP loaded with 50 lbs at the free end of a simple cantilever (Figure 3.6) under various temperatures.

Table 4.4 shows the summary results of flexural creep tests under various loading conditions and temperatures. Specimens at elevated temperatures of 56°C, 68°C, and 80°C (133°F, 154°F, and 176°F) failed under four types of loading conditions. As the temperature increased, the time to reach failure decreased for the same load condition. Results show that the loading levels, along with temperature, affect the creep behavior of the recycled plastic specimens. The higher load levels or those closer to the ultimate strength of the material, the faster the creep rate and shorter time to reach failure.

Table 4.4 Summary of Flexural Creep Tests on Recycled Plastic Specimens

# Specimens Tested	Temperature (°C)	# Specimens Tested	Average Time to Reach Failure (days)	Comments ^[2]
10 lbs @ 5 points	21	2	1185 ^[1]	Not failed
	56	2	194.5	Failed
	68	2	3.5	Failed
	80	2	0.8	Failed
21 lbs single load	21	2	1185 ^[1]	Not failed
	56	2	574	Failed
	68	2	17.5	Failed
	80	2	8.5	Failed
35 lbs single load	21	2	1185 ^[1]	Not failed
	56	2	71.5	Failed
	68	2	0.6	Failed
	80	2	0.75	Failed
50 lbs single load	21	2	1185 ^[1]	Not failed
	35	4	200	Failed
	56	2	3.1	Failed
	68	2	0.4	Failed
	80	2	0.75	Failed

^[1]: the last day of testing, specimens have not ruptured

^[2]: failure is defined as breakage of the specimens

An example of an Arrhenius plot for the RPPs is shown in Figure 4.17. The plot includes data for tests at 35°C, 56°C, 68°C, and 80°C (95°F, 133°F, 154°F, and 176°F) with a 50-lbs (23 kg) single load at the end of a simple cantilever. Results showed the RPPs were all broken when the temperature was increased at 35°C, 56°C, 68°C, and 80°C (95°F, 133°F, 154°F, and 176°F) with a 50-lbs (23 kg) single load condition, except for the RPPs that were tested at 21°C (70°F), which have been under load for more than five years. Therefore, the data point of the 21°C (70°F) didn't show in the Arrhenius plot (Figure 4.17).

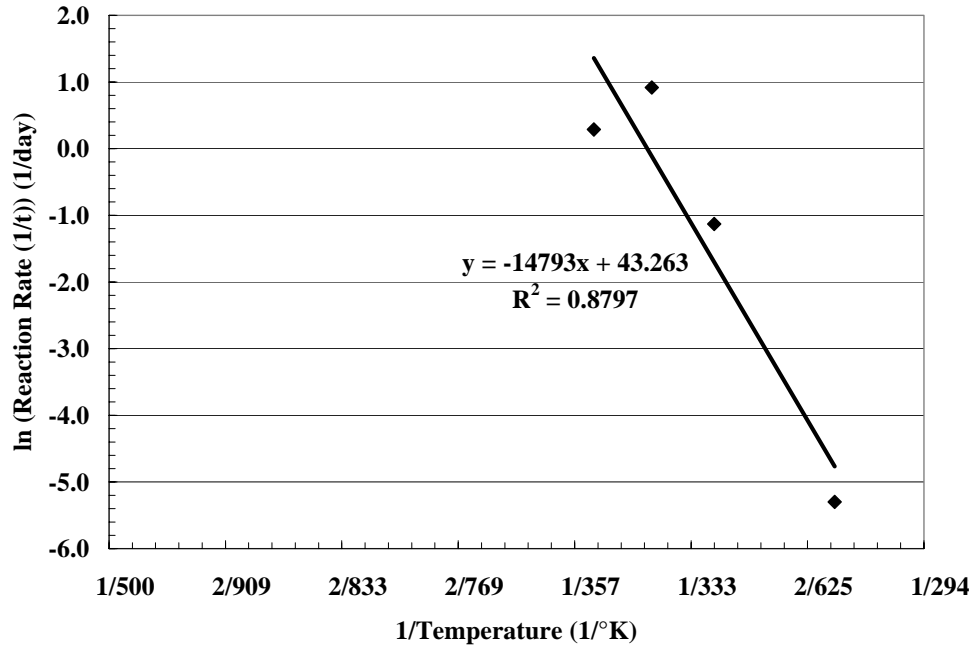


Figure 4.17 Typical Arrhenius Plot for flexural creep test on 2 in. x 2 in. x 24 in. RPP loaded with a 50-lbs weight at the end of a simple cantilever under various temperatures.

Again, as the test temperature increased, the time to reach the failure point is reduced. From the slope of the line in Arrhenius plot, we estimate the time for the RPP to creep to the failure point under field temperature condition (assume $T_{site} = 21^{\circ}\text{C} = 294^{\circ}\text{K}$).

$$\ln\left(\frac{1}{t}\right) = -14793\left(\frac{1}{T_{site}}\right) + 43.263 \quad (\text{From Eq 3.6})$$

Therefore, the time required for the RPP to creep to the failure point is approximately 1157 days (3.2 years). However, based on observations from the laboratory testing shows that the RPPs don't show any cracks on the specimens, and have steady creep rate. Thus the Arrhenius modeling underestimates the time to reach failure. Plots for other loading conditions are included in the appendix C.

Table 4.5 Loading Conditions and Results of the Flexural Creep Tests on the RPPs

Loading Condition	Moment of the Specimens, M_{test} ^[1] (in-lb)	Tensile Stress in Creep ^[2] , σ_{Tcreep} (psi)	Ratio of Tensile Stress in Creep to Tensile Strength ^[3] ($\sigma_{Tcreep}/\sigma_{TRPP}$) (%)	Time to Reach Failure Due to Flexural Creep at 21°C ^[4] (years)
50 lb Single Load	950	714	40	3.2
35 lb Single Load	665	500	28	290
21 lb Single Load	399	300	17	2317
Five 10 lb loads @ Equal Spacing	590	444	25	6515

^[1]: moment arm = 19 inches

^[2]: use Eq 4.2 to calculate stress

^[3]: average tensile strength = 1800 psi (measured in laboratory)

^[4]: calculation shown in the appendix

The loading conditions, maximum moments, and time to reach failure as predicted from the Arrhenius method for four different loading conditions are shown in Table 4.5. For example, the moment of the specimen for 50-lbs single load:

$$M_{test} = 50 \text{ lbs} * 19 \text{ in} = 950 \text{ in} - \text{lb}$$

The tensile stress in creep, σ_{Tcreep} :

$$\sigma_{Tcreep} = \frac{M_{test} * y}{I} = \frac{950 \text{ in} - \text{lbs} * 1 \text{ in}}{1.33 \text{ in}^4} = 714 \text{ psi}$$

From the result of average tensile strength (Loehr et al., 2000a), $\sigma_{TRPP} = 1800$ psi,

Therefore, the ratio of tensile stress in creep to the average tensile strength,

$$\frac{\sigma_{Tcreep}}{\sigma_{TRPP}} = \frac{714}{1800} = 0.396 \cong 40\%$$

In addition, the ratio of tensile stress due to the applied loads to the average tensile strength (1800 psi) is shown in the table. Specimens were loaded to 40 percent, 28 percent, and 17 percent of the average tensile strength for the point loading condition.

Specimens were loaded 25 percent of the average tensile strength and the time to reach failure was determined to be approximately 6500 years due to the flexural creep for the five 10-lbs loads distributed evenly. It is much longer than that for single point loaded specimens.

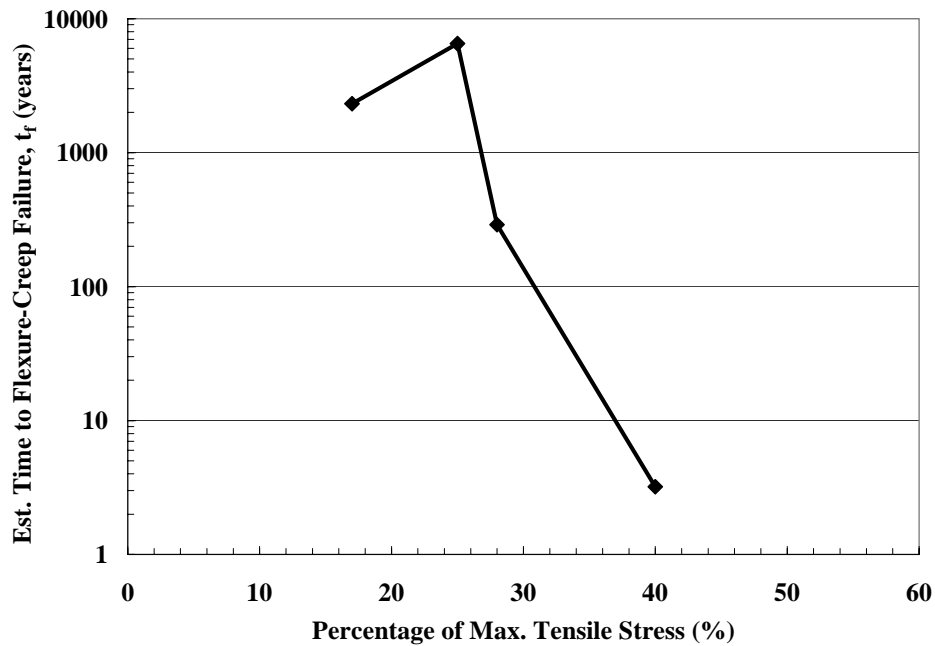


Figure 4.18 Method for estimating time to failure resulting from flexural creep of RPP.

The time to failure under flexural creep loading at field temperature (assumed 21°C) versus the load levels, i.e., the percentage of the tensile stress in creep to the average tensile strength that measured from laboratory results is plotted in Figure 4.18. The data in this plot provides the information needed to predict the effective creep lifetime of an RPP in the field. The following steps illustrate the method:

Steps to Estimate Creep Life in the Field (RPPs)

Step 1: Measure the strain on an instrument pin in the field and calculate the bending moment (M_b) for the pin.

Example: Figure 4.19 shows the maximum bending moments determined from the strain gages on instrumented pin C (slide 2) and pin G (slide 1) at the I70-Emma site. As shown in the figure, the pin G showed a steady increase in bending moment up to 350 lb-ft (475 N-m) before May 2001, assumed that it would keep steady increased. The pin C showed a steady increasing bending moment up to of 150 lb-ft (203 N-m) after July 2002.

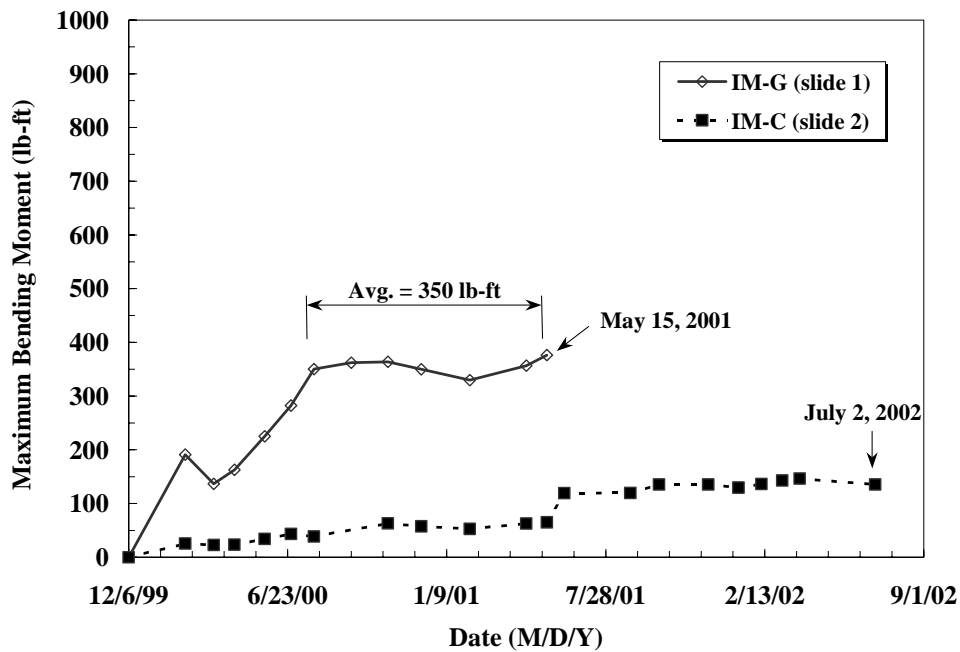


Figure 4.19 Maximum mobilized bending moments from instrumented RPPs at I70-Emma site (Parra et al., 2003).

Step 2: Use the calculated moment to compute the tensile stress (σ_T) in the extreme fiber of the RPP as:

$$\sigma_T = \frac{M_b * y}{I} \quad (4.2)$$

where y is the distance from the neutral axis to the extreme fiber, and I is the moment of inertia for a given section.

Example: for pin G at Emma site, $M_b = 350$ lb-ft (475 N-m), $y = 1.75$ in, and $I = 12.5$ in⁴, thus $\sigma_T = 588$ psi (4 MPa). For pin C at Emma site, $M_b = 150$ lb-ft (203 N-m), $y = 1.75$ in, and $I = 12.5$ in⁴, thus $\sigma_T = 252$ psi (1.7 MPa).

Step 3: Check the ratio of the calculated tensile stress in the field to the maximum tensile stress for the pin and given section.

$$Ratio = \frac{\sigma_{T \text{ field}}}{\sigma_{T \text{ max}}} \quad (4.3)$$

Example: the average tensile strength, $\sigma_{t \text{ max}} = 1800$ psi (12 MPa), and the ratio of tensile stresses is 33 percent for pin G. The ratio of tensile stresses is 14 percent for pin C.

Step 4: Figure 4.18 shows the time to failure (t_f) versus percentage of maximum tensile stress based on Arrhenius method. Locate the calculated percentage of maximum tensile stress and find the corresponding time to failure.

Example: for pin G at the I70-Emma slide 1, the percentage of maximum tensile is 33 percent and the resulting time to flexure-creep failure is found to be approximately 45 years. For pin C at the I70-Emma slide 2, the percentage of

maximum tensile is 14 percent and the resulting time to flexure-creep failure is found to be more than 2000 years.

The above procedure can be used to estimate the design life of the RPPs in slope stabilization application. If the estimated time to failure is too low, the engineer can modify the design to reduce the stress level of the pins in order to increase the design life. Options for reducing the stress include increasing the number of pins, increasing the size of the pins, changing the constituent blend in the RPPs to make less creep susceptible or changing the cross-section to increase their moment of inertia.

It is possible that the method shown above to predict flexure-creep failure is conservative, since it is entirely based on laboratory tests and the Arrhenius method, which underestimates the time to reach failure. In the testing program various single point loads were used to generate the creep deformation with breakage time. The data in Table 4.5 shows that for similar specimens, loaded with five 10 lb at equally spacing, the time to reach failure due to flexural creep at 21°C is about 6500 years, much longer than that for single point loaded specimens. However, the loading conditions in the field are much closer to distributed loading than to point loading. Thus, the proposed method could be conservative in predicting the lifetime of the RPPs in the field.

4.4.2 Compression Creep Tests

The typical plot of deflection versus time for compression creep tests is shown in Figure 4.20. Primary creep was completed within one day after the load was applied for all specimens. Secondary creep occurred after the primary creep and continued for about a year. Results show that the specimens remained in the secondary creep stage and

continued to creep at a steady rate. This might be due to the low creep stresses applied, which was calculated by dividing the spring loads by the original cross-sectional area.

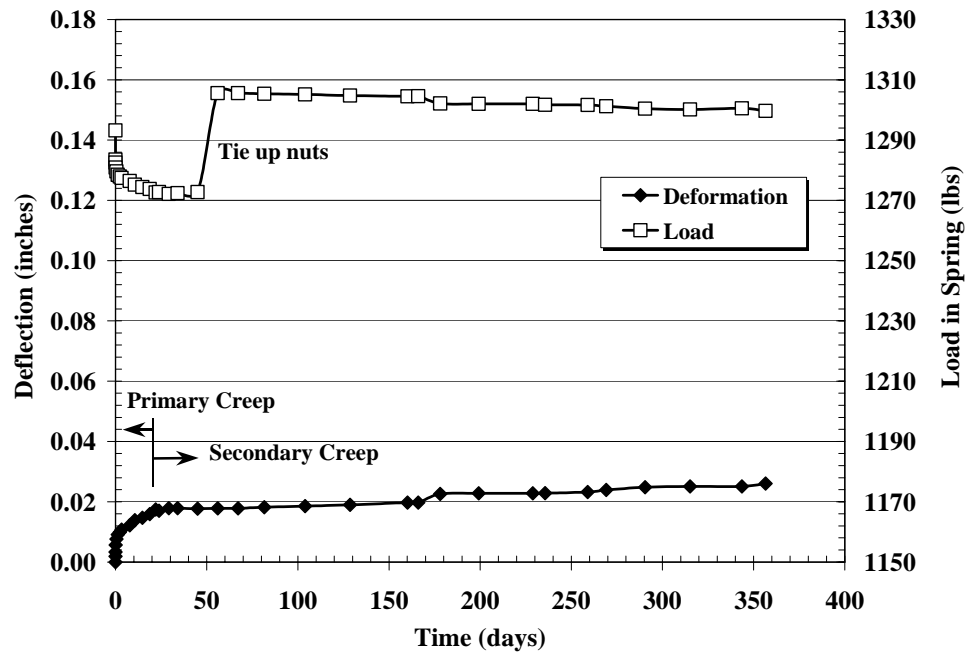


Figure 4.20 Typical deflection under constant axial stress versus time of a recycled plastic specimen from batch B7.

The creep stresses ranged from 100 psi to 120 psi (690 KPa to 827 KPa) for the RPP specimens. The ratio of creep stress to the compressive strength, ranged from four percent to six percent, a very low creep stress. Due to the low creep stress applied, no specimens has ruptured. Summary results from the compressive creep tests are shown in Table 4.6. A maximum creep strain was computed by dividing the maximum deflection to the initial height of the specimen. The maximum creep strain for batch B7 and C9 was about 0.4 percent, and for batch A3 and A6 was about 0.1 percent.

Table 4.6 Summary Results of the Compressive Creep Tests on the RPPs

Mftg	# Specimens	Creep Stress (psi)	Ratio of Creep Stress to Compressive strength^[1] (%)	Maximum Creep Strain (%)
A3	2	105	3.7	0.1
A6	2	100	6.3	0.08
B7	1	110	5.3	0.38
C9	1	120	5.1	0.36

^[1]: based on the average compressive strength from the uniaxial compression tests.

Figure 4.21 shows the deflections versus time of the compressive creep tests on the RPPs. It is clear that the primary and secondary creep behavior among the four batches varies. Specimens from batches B7 and C9 are a little more creep susceptible than specimens from batches A3 (compression molded) and A6 (extruded). Specimens from batches B7 and C9 are made from extruded processes with unreinforced material and the creep behavior is identical. However, only one test was performed for batches B7 and C9. Specimens from batches A3 and A6 are from the same manufacturer, but different manufactured process. The batch A6 shows the lowest creep rate in the first stage. The maximum stress level of these springs was used; however, the creep stresses in the RPPs are only five percent of compressive strength.

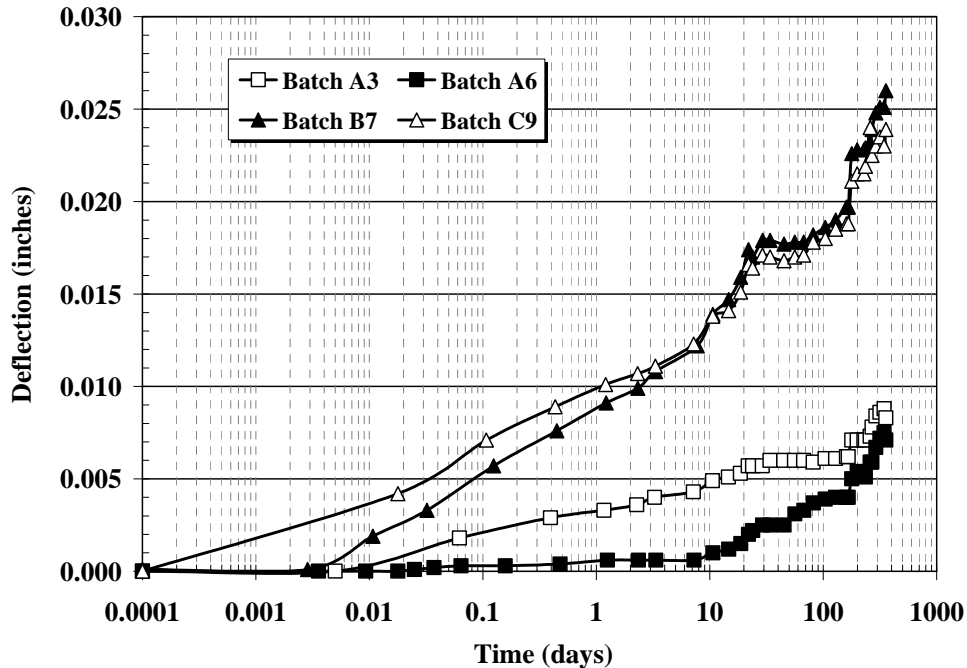


Figure 4.21 Deflections versus time of the compressive creep tests on RPPs.

4.5 Field Installation Behavior

4.5.1 Introduction

In addition to being able to resist the loads imposed by the slope, it is critical that RPPs have sufficient strength and stiffness to resist the stresses imposed during installation. The technique employed for installation of RPPs to date has been to utilize a percussion hammer mounted on the mast of track mounted drilling rigs (Loehr et al., 2000a). One such rig, used at the I70-Emma slide 1 and slide 2, is shown in Figure 3.12. The primary advantage of using rigs similar to the one shown in Figure 3.14 is that the mast of the rig maintains the alignment of the hammer and reinforcing member thereby minimizing the lateral loads imposed on the unsupported length of the member during driving.

It is logical to expect that the penetration rate of reinforcing members should increase with increasing strength and stiffness of the RPPs, since stiffer members are expected to dissipate less input energy thereby transferring more energy to penetrating the reinforcement. To investigate this hypothesis and to provide accurate data on possible installation rates, the installation records at each of the field sites were monitored and the time to drive the pins their full depth (8 feet), or to refusal, was recorded. Shorter pins, denoted as less than 8 feet (2.4 m), typically indicate difficult driving conditions. The 8-foot (2.4 m) RPPs could not penetrate the full length and the stick up portion was cut off at the ground after installation. A total of seven slides (Table 3.3) were stabilized using the RPPs obtained from three manufacturers and an additional slide was stabilized with 3.5-inch (90 mm) diameter steel pipe to provide for a wider range of reinforcing member properties.

4.5.2 I70-Emma Site

Table 4.7 shows a summary of penetration performance for the I70-Emma site. The soils at this site consist of mixed lean and fat clay with scattered cobbles and construction rubble. RPPs were installed approximately perpendicular to the slope face at the slide 1. Penetration rates were monitored for 90 of the 199 RPPs at the site. The average penetration rate for all monitored RPPs was 4.6 ft/min (1.4 m/min). RPPs were installed with a vertical orientation at the slide 2. Penetration rates were monitored for 150 of the 163 RPPs at the site. The average penetration rate for all monitored RPPs was 3.9 ft/min (1.2 m/min). The average penetration rate increased approximately 18 percent for RPPs installed perpendicular to the slope. Limitations of the Davey-Kent drilling rig necessitated the RPPs to be installed in a vertical alignment, and were driven with the rig

being backed up the slope. While not critical, this feature did result in slightly lower penetration rates for RPPs driven vertically as compared to RPPs driven perpendicular to the face of the slope (Table 4.7).

Penetration rates were monitored for 173 of the 195 RPPs. All were installed at a vertical orientation at the slide 3. The average penetration rate for all monitored RPPs from batch A10 was 6.5 ft/min (2 m/min). Twenty-five of the 32 RPPs were monitored and installed by the Daken Farm King hitter series (impact-hammer equipment- Figure 3.14). The average penetration rate was 4.2 ft/min (1.3 m/min), which decreased approximately 35 percent compared to the percussion hammer from the Ingersoll Rand CM350, track mounted drilling rig (Figure 3.13) used to drive the rest of the RPPs. A reason for the difference is that the current impact machine requires additional labor (and time) to keep the RPP and drop-weight hammer aligned. This shows in the driving rate.

An 8-foot long, 3.5 diameter timber pile was used for trial installation with the Ingersoll Rand ECM350, track mounted drilling rig (Figure 3.13). Three timber piles that are used for landscape purposes were driven in the top, middle, and bottom of the slope at the slide 3. The average penetration rate was 6.9 ft/min (2.1 m/min), which is close to the average driving rate of RPPs from batch A10 (6.5 ft/min) at the Slide 3.

If the subset of RPPs that were installed less than full length (refusal) is considered separately, the average penetration rate was 4.1 ft/min (1.2 m/min) while the rate for RPPs driven to their full length was 10.1 ft/min (3.1 m/min) at the slide 3. This means that difficult driving conditions can reduce the rate by as much as 60 percent. The same situation occurred for the slide 1 and slide 2.

Table 4.7 Penetration Performance of RPPs at I-70 Emma Site

Stabilized Slope (Working Period)	Specimen Batch	Installed length	# Pins Monitored	Penetration Rate (ft/min)			
				Min.	Max.	Avg.	Std Dev.
Slide 1 (10/18/1999~11/12/1999)	A1	8 ft	79	0.7	10.2	5.0	2.2
		< 8 ft	11	0.7	2.7	1.6	0.7
		ALL ^[1]	90	0.7	10.2	4.6	2.4
Slide 2 (11/17/1999~11/22/1999)	A1	8 ft	107	1.5	8.7	4.5	1.6
		< 8 ft	43	0.4	7.0	2.4	1.4
		ALL	150	0.4	8.7	3.9	1.8
Slide 3 (1/6/2003~1/7/2003)	A10	8 ft	60	2.0	18.5	10.1	4.4
		< 8 ft	88	0.1	17.0	4.1	2.8
		ALL	148	0.1	18.5	6.5	4.6
	A10 ^[2]	ALL	25	1.2	15.0	4.2	2.9
	Timber Pile	ALL	3	2.8	12.3	6.9	4.9

^[1]: average results for all monitored pins.

^[2]: using drop-weight hammer driving machine.

4.5.3 I435-Wornall Site and Holmes Site

A summary of penetration performance for the I435-Wornall site and Holmes site is shown in Table 4.8. The soils at the I435-Wornall site consist of a 3 feet to 5 feet (1 m to 1.5 m) thick surficial layer of soft, lean clay overlying stiffer compacted clay shale. Penetration rates were monitored for 499 of the 616 RPPs installed at the site. Of all monitored RPPs, 186 were driven their full length. The penetration rate for this subset of RPPs was 6.6 ft/min (2 m/min). In addition, 313 of the monitored pins reached refusal before the full 8 ft (2.4 m) length was embedded into the subsurface. In these cases, the average penetration rate was 4.7 ft/min (1.4 m/min), which indicates that penetration rates were reduced when stiffer soils were encountered.

Table 4.8 Penetration Performance of RPPs at I-435 Wornall and Holmes Site

Stabilized Slope (Working Period)	Specimen Batch	Installed length	# Pins Monitored	Penetration Rate (ft/min)			
				Min.	Max.	Avg.	Std Dev
I435 Wornall (10/18/2001~12/7/2001)	A4	< 8 ft	251	1.0	13.4	4.4	2.1
		ALL ^[1]	384	1.0	13.7	5.2	2.4
	A5	8 ft	49	3.8	9.7	6.6	1.4
		< 8 ft	61	2.2	13.0	6.0	2.0
		ALL	110	2.2	13.0	6.3	1.8
	B7	< 8 ft	1	--	--	6.0	--
	B8	8 ft	1	--	--	3.3	--
I435 Holmes (12/14/2001~12/20/2001)	C9	< 8 ft	3	3.5	12.0	6.7	4.6
	Steel Pipe	8 ft	3	4.8	6.9	5.9	1.0
	A5	< 8 ft	6	3.1	5.8	4.6	1.0
	Steel Pipe	< 8 ft	216	0.4	13.2	5.0	2.1

^[1]: average results for all monitored pins.

Figure 4.22 shows a frequency distribution for the penetration rates determined for the I435-Wornall site. As shown in Figure 4.22, the penetration rate varied from a low of about 1.0 ft/min (0.3 m/min) to a high of about 13.7 ft/min (4.0 m/min) and the average value was 5.4 ft/min (1.6 m/min) with a standard deviation of 2.4 ft/min (0.7 m/min). Considering all RPPs from batches A4 and A5, the average penetration time was 1.5 minutes for the 8-foot (2.4 m) long RPPs. The observed variability in the rate is primarily attributed to variability in the in situ soil conditions across the site.

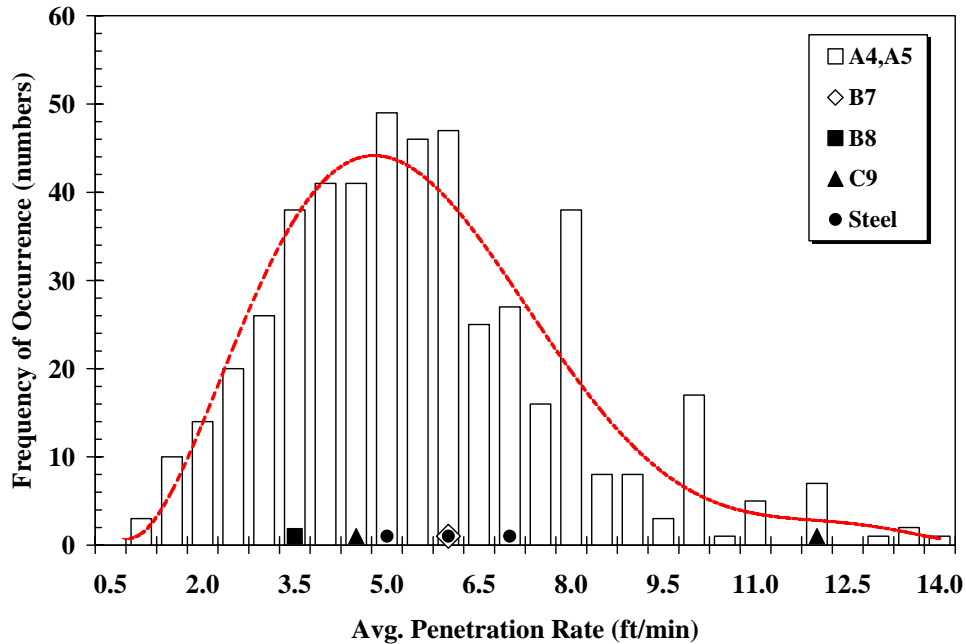


Figure 4.22 Penetration rate frequency distribution for RPPs and trial steel pipe reinforcements in slope stabilization site, I435-Wornall.

Of the 499 RPPs monitored at the I435-Wornall site, 384 were from batch A4 (compression molded) and 110 were from batch A5 (extruded). The penetration rates and strength properties for these members are summarized in Table 4.9. The average penetration rates for these two products are similar, 5.2 ft/min (1.6 m/min) of batch A4 and 6.3 ft/min (1.9 m/min) in spite of the significant differences in the strength and stiffness of the members. Several “test” drives using RPPs from batches B7, B8, and C9, and three specimens of steel pipe, were also performed at the I435-Wornall site. The penetration rates observed for these members are also shown in Figure 4.22 and summarized in Table 4.8. Penetration rates for these members ranged from 3.3 ft/min to 6.7 ft/min (1.0 m/min to 2 m/min). Only a single member from each of batches B7 and B8 was installed, so no conclusions are drawn about these materials. Three RPPs from batch C9 were driven with an average penetration rate of 6.7 ft/min (2.0 m/min). The

steel pipe, with a much greater stiffness than any of the RPPs, yielded a penetration rate of 5.9 ft/min (1.8 m/min). All of these penetration rates fall well within the range observed for the RPPs from batches A4 and A5, which suggest that penetration rates are not significantly affected by the strength and stiffness of the pins.

Table 4.9 Penetration Rates and Material Properties for RPPs Installed at I435-Wornall and I435-Holmes Sites

Stabilized Slope	Specimen Batch	# Pins Monitored	Avg. Penet. Rate (ft/min)	Avg. Compression Strength ^[1] (psi)	Avg. Secant Modulus in Compression ^[1] , E _{1%} (ksi)	Avg. Flexural Strength (psi)	Avg. Secant Modulus, E _{1%} (ksi)
I435 Wornall	A4	384	5.2	2621	186	2543	213
	A5	110	6.3	1634	84	1542	98
	B7	1	6.0	2080	87	1505	90
	B8	1	3.3	2500	138	3589	243
	C9	3	6.7	2315	87	1696	107
	Steel Pipe	3	5.0	-- ^[2]	--	--	--
I435 Holmes	A5	6	4.6	1634	84	1542	98
	Steel Pipe	216	5.0	--	--	--	--

^[1]: use original cross-sectional area (A_0) to calculate stresses

^[2]: data not available

The slide at the I435-Holmes site, which has soil conditions similar to those at the I435-Wornall site, was stabilized using 254 steel pipes (Table 4.9). Of that number, penetration rates were recorded for 216 steel pipes. The average penetration rate for these members was 5.0 ft/min (1.5 m/min) with a standard deviation of 2.1 ft/min (0.6 m/min). Six RPPs from the batch A5 were also installed in this slope. The pins produced an average penetration rate of 4.6 ft/min (1.4 m/min), only slightly lower than that observed for the steel members, again suggesting that strength or stiffness plays a minor role in determining the penetration rates.

In order to try to discount the variability of the subsurface conditions, the penetration rates of the test pins were compared to the average rate for the “nearest

neighbors” of the test pins. The idea of taking average penetration rates of the nearest neighbors that surround the test pins is illustrated in Figure 4.23. The penetration rates of the “test” drives using RPPs from batches B7, B8, and C9, and three specimens of steel pipe with their “nearest neighbors” were calculated and are shown in Table 4.10.

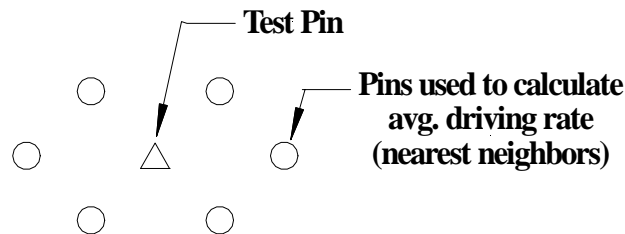


Figure 4.23 Analysis of penetration rate “test pin” to the average driving rate for its “nearest neighbors”.

Penetration rate analysis of RPPs from batch B7 shows that they penetrated the slope approximately 37 percent faster than its nearest neighbor from batch A4. RPPs from batch B8 were installed approximately 12 percent slower than the nearest neighbors for batch A4. This might indicate that RPP’s from batch B7 material can be more efficiently driven into the slope. However, observations from the field show batch B7 was hardly penetrating after 5 feet (1.5 m) of installation and there was significant lateral bending of the pins prior to refusal occurring. Batch B8 was installed its full length and had slight lateral bending refusal. We must temper this conclusion with the observations in the field and the fact that only one test pin from batch B7 and B8 were installed. More RPPs from batches B7 and B8 must be installed in the field in order to confirm this observation.

Table 4.10 Penetration Rates of “Test Pins” and “Nearest Neighbors”

	# Pins Monitored	Driving rate (ft/min)	# Surrounding Pins Monitored	Avg. Driving rate of Surrounding Pins (ft/min)	Percent of Difference ^[1] (%)
B7	1	6.0	6	4.4	37
B8	1	3.3	6	3.8	-12
C9	3	6.7	12	7.1	-6
Steel Pipe	3	5.9	10	4.7	26

^[1]: values based on average driving rate of surrounding pins

Three RPPs from batch C9 were installed at the top and middle of the slope face. The average penetration rate was 6.7 ft/min (2 m/min), which is approximately 6 percent slower than the average penetration rate of the nearest neighbors (batch A4). Thus, the average penetration rate of RPPs from batch C9 is similar to its nearest neighbors (batch A4).

Three steel pipes were all installed at the toe of the slope. The average penetration rate was 5.9 ft/min (1.8 m/min). This rate was approximately 26 percent faster than the average penetration rate of the nearest neighbors (batch A5).

4.5.4 US36-Stewartsville and US54-Fulton Site

The US36-Stewartsville test site is also composed of a soft surficial layer of lean clay overly stiff, fat clay with some gravel. This site is approximately 27-feet (8.2 m) height with 2.2:1 (Horizontal:Vertical) side slope. The slide area at this site was stabilized using 306 RPPs from batch A6 and all were installed a vertical orientation. Of that number, 206 were monitored for penetration and the rates determined for those RPPs are summarized in Table 4.11. The average penetration rate for all monitored pins was 5.2 ft/min (1.6 m/min) with a standard deviation of 3.2 ft/min (1.0 m/min). If the subset

of RPPs that were driven to refusal (less than full length) is considered separately, the penetration rate averaged 4.4 ft/min (1.3 m/min) while the rate for RPPs driven to their full depth was 8.3 ft/min (2.5 m/min). This again illustrates that difficult driving conditions can reduce the penetration rate by approximately 50 percent.

Table 4.11 Driving Performance of RPPs at US36-Stewartsville and US54-Fulton Site

Stabilized Slope (Working Period)	Specimen Batch	Installed length	# Pins Monitored	Penetration Rate (ft/min)			
				Min.	Max.	Avg.	Std Dev
US36 Stewartsville (4/30/2002~5/7/2002)	A6	8 ft	40	2.7	16.0	8.3	4.1
		< 8 ft	166	1.7	16.9	4.4	2.3
		ALL ^[1]	206	1.7	16.9	5.2	3.2
US54 Fulton (1/10/2003~1/15/2003)	A10	8 ft	143	1.4	27.6	9.6	5.8
		< 8 ft	223	0.6	14.5	4.7	2.5
		ALL	366	0.6	27.6	6.6	4.8
	Timber Pile	< 8 ft	3	3.6	9.6	6.4	3.0

^[1]: average results for all monitored pins.

The US54-Fulton site is approximately 43 feet (13.1 m) in height with 3.2: 1 (Horizontal:Vertical) side slope. This slope consists of a 2 feet to 7 feet thick surficial soft to stiff lean gravelly clay overlying very stiff to hard fat clay with sand and gravel. Penetration rates were monitored for 366 of the 400 RPPs installed at the site. The average penetration rate for all RPPs was 6.6 ft/min (2.0 m/min) with a standard deviation of 4.8 ft/min (1.5 m/min). Again, considering the subset of RPPs that were driven to refusal (less than full length), the penetration rate averaged 4.7 ft/min (1.4 m/min) while the rate for RPPs driven to their full depth was 9.6 ft/min (2.9 m/min). This shows that the penetration rates were reduced when stiff layer were encountered. Three timber piles, similar to those used at the I70-Emma Slide 3, were installed in the top,

middle, and bottom of the slope at the US54-Fulton site. The average penetration rate was 6.4 ft/min (1.95 m/min), which is similar to the averaged driving rate of RPPs from batch A10 (6.6 ft/min) at the same site.

It can be concluded that the difficult driving conditions can reduce the average penetration rate as much as a factor of two, when compared to the pins driven their full length from these seven slopes. The driving data confirms the observation that there is little correlation between the achievable penetration rates and the strength or stiffness of the RPPs installed, at least for the range of materials considered.

4.5.5 Installation Performance for all Demonstrated Sites

The drivability for all seven slopes and the pins penetration rate distribution from top of slope to the toe of slope were considered and analyzed. Figure 4.24 shows the calculation of subdividing the RPPs as four groups from the top to the bottom of the slope. The results of these analyses are shown in Table 4.12

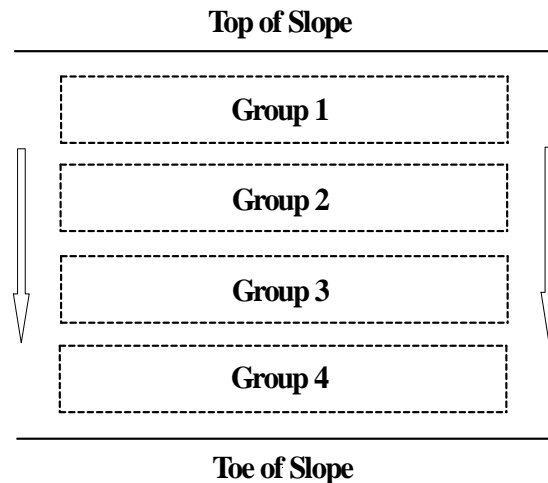


Figure 4.24 Penetration rate analysis by subdividing RPPs as four groups from top to bottom of slope.

Table 4.12 shows that the average penetration rate decreases from top of slope to the toe of slope, except the I435-Holmes site and the US54-Fulton site. The average penetration rates were similar from top of slope to the toe of slope at I435-Holmes site. This indicates that the soil conditions are similar from top of slope to the toe of slope. The RPPs may encounter the layer of sand and gravel at the top of slope, and shows that the smallest penetration rate occurred at the top of slope (Table 4.12) at the I435-Holmes site. Observations from the field installation at the US54-Fulton site show that RPPs were much easier driven on the top of slope than toe of slope. The soils on the top of slope usually push and compact the soils at the toe of slope, especially the slide failure has happened. It usually takes more time to drive RPPs at the toe of slope.

Table 4.12 Results of Subdivided Groups for RPPs at Seven Slide Sites

Stabilized Slope	Average Penetration Rate (ft/min)			
	Group 1(#^[1])	Group 2 (#)	Group 3 (#)	Group 4 (#)
I70 Emma Slide1	6.4 (28)	5.0 (29)	4.7 (29)	3.4 (20)
I70 Emma Slide2	5.0 (37)	4.5 (40)	3.4 (41)	2.7 (32)
I70 Emma Slide3	10.6 (53)	6.1 (51)	4.3 (52)	3.6 (42)
I435 Wornall	6.2 (79)	5.7 (122)	5.5 (125)	4.7 (168)
I435 Holmes	4.8 (59)	4.1 (68)	5.5 (53)	6.0 (38)
US36 Stewartsville	6.8 (57)	4.2 (49)	4.7 (48)	4.6 (51)
US54 Fulton	4.8 (68)	6.2 (69)	10.1 (88)	5.6 (152)

^[1]: number of RPPs monitored

Figure 4.25 shows the average penetration rates for the seven stabilized slopes. The slopes are listed in chronological order (from the first project to the most recent one). The average penetration rate (y-axis) increased with time. Note that, the I435-Wornall site (batch A5), the I70-Emma slide3 and the US54-Fulton site (batch A10) have the

highest penetration rates (exceeding 6.0 ft/min (1.8 m/min)). These RPPs were installed using the percussion hammer from the Ingersoll Rand CM150 (Figure 3.14) and Ingersoll Rand CM350 (Figure 3.13), track mounted drilling rig. Furthermore, the strength and stiffness of the RPPs decreased as installation progressed in the chronological order. Therefore, it might indicate that with this type of equipment makes the pins installation more efficiency. A possible explanation is that the installation crew has improved their skill in installation rather than because of using different materials.

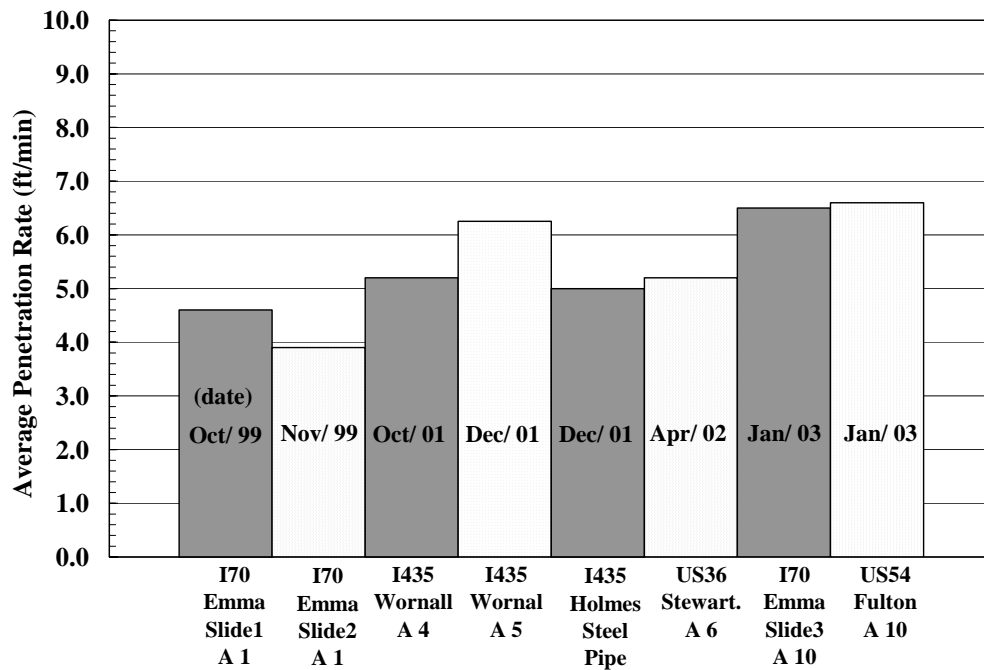


Figure 4.25 Average penetration rate versus installation sequence of seven slopes.

CHAPTER 5: DRAFT SPECIFICATION FOR RPPs TO BE USED IN THE SLOPE STABILIZATION

5.1 The Need for a Specification

A material and engineering property specification for RPP's used in the slope stabilization application is necessary for several reasons. First, Departments of Transportation (DOT's) and other agencies rely on specifications to ensure proper materials are used on their applications. Second, in slope stabilization applications, minimum engineering properties of the RPPs are required to facilitate a satisfactory design. Finally, there are numerous manufacturers of RPP materials and each use slightly different constituents and manufacturing processes, leading to RPPs with a range of engineering and material properties.

In this development program, we obtained RPP materials from multiple manufacturers. The manufacturers provided several types of RPPs or at least their product changed over time and multiple materials were obtained from different manufacturing periods. In addition, field performance data and slope stability design requirements were collected and assessed in order to establish a draft specification for the RPPs to be used in slope stabilization.

5.2 Draft Specification

A draft specification (Table 5.1) for RPPs to be used in the stabilization of slopes has been developed based upon the results of the laboratory testing, field-testing and analysis of the field performance at seven demonstration sites. The draft is presented as a provisional specification prepared in the format of the American Association of Highway and Transportation Officials (AASHTO) in Appendix E. The draft specification is based

on the design compressive strength (≥ 1500 psi at less than or equal to five percent strain measured at a strain rate of 0.00003 in/in/min) and design flexural strength (≥ 1200 psi at less than or equal to two percent center strain measured at a crosshead motion rate of 0.02 in/in/min).

Table 5.1 Draft Specification For RPPs to Be Used in Slope Stabilization Applications

Property	Minimum Requirements	
Uniaxial Compression Strength, σ_c (ASTM D6108)	A. $\sigma_c \geq 1500$ psi, axial strain \leq five percent, strain rate = 0.00003 in/in/min, or	
	Alt A1. Develop expression for the strain rate effects and correct measured strength to the design strain rate, or	
	Strain Rate (in/in/min)	No. of Compression Tests
	0.03	2
	0.003	2
	0.0003	2
	Alt A2. $\sigma_c \geq 3750$ psi, axial strain \leq five percent, strain rate = 0.03 in/in/min.	
Flexural Strength, σ_f (ASTM D6109)	B. $\sigma_f \geq 1200$ psi, center strain \leq two percent, rate of crosshead motion = 0.02 in/min, or	
	Alt B1. $\sigma_f \geq 2000$ psi, center strain \leq two percent, rate of crosshead motion = 1.9 in/min.	
Durability - Environmental Exposure	C. Polymeric Constituent $>$ 60% of mass of product, or	
	Alt C1. Less than 10% reduction in compressive strength after 100 days exposure.	
Durability - Creep	D. No bending failure during 100 days under a constant load that produces an extreme fiber stress not less than 50% of the design compressive stress, or	
	Alt D1. Testing and Arrhenius modeling showing that the RPPs do not fail during the desired design life for the facility.	

As shown in Figure 4.12, the measured strengths of RPPs are greatly influenced by the strain rate. We have assumed our field strain rate to be on the order of 0.00003 in/in/min (0.00003 mm/mm/min), which correlates with a compressive failure of a standard 3.5-in. x 3.5-in. (90-mm x 90-mm) RPP under a continuous rate of deformation for one week. The standard strain rate for the ASTM D6108 compression test is 0.03

in/in/min (0.03 mm/mm/min). As shown in Figure 4.12, the measured compressive strengths of the RPP decreases as the strain rate used in the test decreases. The rate of decrease in strength is a function of the material type. For the RPPs tested in this program, the average decrease in strength was about 20 percent per log cycle decrease in the strain rate, i.e., an RPP with a compressive strength of 1000 psi (6.9 MPa) at a strain rate of 0.03 in/in/min (0.03 mm/mm/min) will show a compressive strength of 600 psi (4.1 MPa) if tested at a strain rate of 0.0003 in/in/min (0.0003 m/mm/min). Due to the dependence on strain rate, it is imperative to make the required minimum strength a function of the testing strain rate in the draft specification.

The “design” compressive (1500 psi) and flexural (1200 psi) strengths presented in Table 5.1, represent the required minimum mechanical properties for RPPs to be used in stabilization of slopes. The values are used in design of the stabilized field slopes and are determined at the field strain rate of 0.00003 in/in/min (0.00003 mm/mm/min). Ideally, all RPP specimens should be tested at the field strain rate; however, from a practical perspective testing at this strain rate requires about one week per compression specimen which is not practical for production facilities. Therefore, alternatives for qualifying an RPP material include: (Alt A1) - establishing a compressive strength versus strain rate behavior and estimating the compressive strength at the field strain rate, or (Alt A2) a compressive strength of 3750 psi (25.9 MPa) or better when tested at the ASTM D6108 strain rate of 0.03 in/in/min (0.03 mm/mm/min). The latter value represents the increase in strength realized by the 3-order of magnitude increase in strain rate, i.e., above the field strain rate of 0.00003 in/in/min (0.00003 mm/mm/min), using a reasonable upper-bound for strain rate effects. Because Alt. A2 uses an upper-bound most

manufacturers will find that they can meet the specification more easily by establishing strain rate effects for their specific products rather than using the default relation assumed for Alt. A2.

The second part of the specification for mechanical properties is the required minimum flexural strength of 1200 psi (8.3 MPa) at less than or equal to two percent center strain, when tested in four-point flexure using a crosshead displacement rate of 0.02 in/min (0.51 mm/min) (results in a strain rate of 0.00003 in/in/min, the assumed field rate). An alternate requirement is available (Alt B1) if the ASTM D6109 crosshead deformation rate of 1.9 in/min (48.3 mm/min) is used. In Alt. B, the required flexural strength is 2000 psi (13.8 MPa) at less than or equal to two percent center strain. Again, the increase in required strength for the higher deformation rate is due to the effect that loading rate has on the resulting strength of the RPP.

In addition to mechanical properties, durability criteria must be included in the specification. Recycled plastic materials can have significant variability with respect to constituents and manufacturing processes. The durability of the finished product will influence its suitability for application to slope stabilizations. Two durability facets, environmental degradation and creep, must be considered. The proposed durability criteria are presented in the draft specification in Table 5.1. The polymeric content should be greater than 60 percent of the mass to reduce the effect of environmental exposures (Loehr et al., 2000a). The RPP should not fail (break) under a cantilever bending load that generates an extreme fiber stress of at least 50 percent of the design compressive strength when subjected to the load for 100 days. Exposure testing and Arrhenius modeling are offered as alternate means to qualify a material.

It should be noted that in any slope stabilization design using RPPs, the designer can vary the stabilization scheme through variation of the number, location, strength and stiffness of the RPPs. The designer can also change the parameters by changing the factor of safety desired for the stabilized slope. Thus, the designer has numerous options for stabilization schemes and as such the required engineering properties of the RPPs could vary considerably.

CHAPTER 6: CONCLUSIONS AND RECOMMENDATIONS

6.1 Conclusions

The use of recycled plastic pins (RPPs) to stabilize earthen slopes is a promising technology. Seven successful demonstration projects have been completed. One obstacle to widespread use of RPP technology remains the absence of a standard specification for the engineering properties of the RPPs to be used in stabilization of slopes. This project was undertaken to develop a database on the engineering properties of RPPs from various manufacturers and to combine that knowledge with the field installation and performance information available from the field demonstrations in order to develop a draft specification for RPPs to be used to stabilize slopes.

The following results were realized during the course of work performed to develop the specification:

- Compressive strengths of RPPs ranged from 1600 psi to 3000 psi (11 MPa to 21 MPa) with no cross-sectional area correction and tested at a nominal strain rate of 0.006 in/in/min (0.006 mm/mm/min).
 - The average compressive strengths of the extruded RPP products (2200 psi) are approximately 20 percent lower than the compressive strength of the compression-molded products (2800 psi).
 - Manufacturers of extruded products can modify their processes and constituent mixtures to produce materials with comparable strengths to the compression molded products.

- There is no discernable change in the average compressive strength between specimens in the virgin condition (before installation) and those in the disturbed condition (after installation) indicating that the installation process does not have a deleterious effect on the compressive strength of RPPs.
- There was close agreement in the compressive strengths for both failure criteria. This indicates that using the strength at five percent strain without correcting the cross-sectional area provides a reasonable value for the peak strength.
- There was little correlation between the compressive strengths and unit weights of the RPPs.
- Compression moduli determined at one percent strain ranged from 80 ksi to 190 ksi (552 MPa to 1310 MPa). The compression moduli of the extruded products (90 ksi) was generally on the order of one half that determined for the compression-molded products (180 ksi).
 - The unreinforced material had a secant modulus of 90 ksi (621 MPa) while the reinforced material had a secant modulus of 140 ksi (965 MPa). Obviously, the reinforcing fibers significantly stiffened the material.
- Strain rate has a significant impact on the measured strength of the RPP products.
 - For each order of magnitude decrease in strain rate, the measured compressive strength was found to decrease about 20 percent.

- A relationship was developed to allow testing at any strain rate and subsequent calculation of the compressive strength for any desired strain rate.
- Flexural strengths for specimens loaded to failure or two percent center strain ranged from 1300 psi to 3600 psi (9 MPa to 25 MPa) under a nominal deformation rate 0.2 in/min (5.1 mm/min).
 - There is significant variability, a factor of 2.8, in the flexural strength among the products tested.
 - Extruded members showed continually increasing stress with increasing deflection/strain without experiencing rupture of the member. The compression molded members ruptured at approximately two percent strain.
- The flexural capacity was limited to the maximum flexural strength or the capacity achieved at 2 percent or less center strain.
- Flexural moduli varied from 90 ksi to 250 ksi (621 MPa to 1724 MPa) at one percent strain, similar to the values observed in the uniaxial compression tests with the exception of the fiberglass-reinforced material.
- Flexural creep tests revealed RPPs to be creep sensitive.
 - Creep tests were highly dependent on the temperature and stress level in the RPP.
 - The laboratory flexural creep test, at 21°C and a stress ratio at 40 percent has not reached failure after more than five years.

- Arrhenius modeling showed that under current field stress levels, the RPPs would not reach creep failure for 45 years to 2000 years.
- The average RPP penetration rate during field installation ranged from 4.0 ft/min to 6.6 ft/min (1.2 ft/min to 2.0 ft/min) for the seven stabilized slopes.
 - There is little correlation between the achievable penetration rates and the strength or stiffness of the RPPs. Penetration rates are not significantly affected by the strength and stiffness of the pins, at least for the range of materials considered.
 - The average penetration rate increased with each successive installation indicating that the installation crew improved their skill with each job and the RPP material type was not the controlling factor.

- Based on the findings from this work, a draft specification for RPPs to be used in stabilization of slopes is as follows:

Table 6.1 Draft Specification for RPPs to Be Used in Slope Stabilization Applications

Property	Minimum Requirements	
Uniaxial Compression Strength, σ_c (ASTM D6108)	A. $\sigma_c \geq 1500$ psi, axial strain \leq five percent, strain rate = 0.00003 in/in/min, or	
	Alt A1. Develop expression for the strain rate effects and correct measured strength to the design strain rate, or	
	Strain Rate (in/in/min)	No. of Compression Tests
	0.03	2
	0.003	2
	0.0003	2
	Alt A2. $\sigma_c \geq 3750$ psi, axial strain \leq five percent, strain rate = 0.03 in/in/min.	
Flexural Strength, σ_f (ASTM D6109)	B. $\sigma_f \geq 1200$ psi, center strain \leq two percent, rate of crosshead motion = 0.02 in/min, or	
	Alt B1. $\sigma_f \geq 2000$ psi, center strain \leq two percent, rate of crosshead motion = 1.9 in/min.	
Durability - Environmental Exposure	C. Polymeric Constituent $>$ 60% of mass of product, or Alt C1. Less than 10% reduction in compressive strength after 100 days exposure.	
Durability - Creep	D. No bending failure during 100 days under a constant load that produces an extreme fiber stress not less than 50% of the design compressive stress, or Alt D1. Testing and Arrhenius modeling showing that the RPPs do not fail during the desired design life for the facility.	

6.2 Recommendations

The following recommendations are based on the findings and results of the work reported herein:

➤ Database Development

Additional materials and tests results should be added to the materials properties database in order to strengthen the conclusions used to establish the draft specification.

- Additional uniaxial compressive tests at different strain rates should be performed to provide more information for a better trend line for strain rate effects on compressive strength.
 - Additional RPPs from various manufacturers should be tested and installed in the field in order to provide a wide range of the material properties and field performance of RPPs.
 - Determine how the engineering properties (compressive and flexural strength, modulus, and creep) change when RPPs are subjected to various potentially detrimental environments.
- Specification Development
- Develop ranges of required flexural strength for RPPs in various stabilization configurations, by performing parametric analyses using slope stability modeling.
 - Use reliability analyses to determine the lowest allowable strength for RPPs that will keep specific slopes stable.
 - Use the results of field monitoring to assess the “working” loads mobilized in the RPPs in the field under different conditions, i.e., seasonal. These data will permit more rigorous identification of the appropriate stress levels to avoid creep problems in the future.

Appendix A

Test Results for Uniaxial Compression Tests

Table A.1. Summary Results of Uniaxial Compression Tests for RPPs from Batches A1 to A4

Specimen Batch	Strain rate (in/in/min)	Test time (min)	At 5 % strain			Corrected Cross-sectional area			
			Strength (psi)	Secant Modulus (E _{1%} , ksi)	Secant Modulus (E _{5%} , ksi)	Strength (psi)	Strain at Peak (%)	Secant Modulus (E _{1%} , ksi)	Secant Modulus (E _{5%} , ksi)
A1	--	--	2916	129.1	53.5	--	--	--	--
A1	--	--	2819	144.6	54.6	--	--	--	--
A1	--	--	2749	133.5	53.1	--	--	--	--
A1	--	--	2701	140.6	53.3	--	--	--	--
A1	--	--	2475	129.8	--	--	--	--	--
A1	--	--	2831	118.7	57.2	--	--	--	--
A1	--	--	2902	132.2	56.4	--	--	--	--
A1	--	--	2877	129.0	57.4	--	--	--	--
A1	--	--	2778	140.8	58.4	--	--	--	--
A1	--	--	2791	138.5	65.4	--	--	--	--
A2	0.004	25	2891	186.0	50.1	--	--	--	--
A2	0.004	28	3005	193.6	59.1	--	--	--	--
A2	0.004	28	2711	186.0	55.6	--	--	--	--
A2	0.007	17	3054	178.4	53.9	--	--	--	--
A2	0.003	29	2960	166.9	53.5	--	--	--	--
A2	0.007	21	3013	190.3	55.5	--	--	--	--
A2	0.005	22	3005	190.0	54.9	--	--	--	--
A3	0.005	25	2802	176.5	58.0	--	--	--	--
A3	0.007	15	2685	160.0	53.4	--	--	--	--
A3	0.005	26	2786	172.0	61.7	--	--	--	--
A3	0.005	21	2837	107.7	53.2	--	--	--	--
A3	0.006	22	2926	186.0	55.6	--	--	--	--
A3	0.006	20	2910	183.2	59.2	--	--	--	--
A4	0.006	18	3012	174.0	54.1	2855	3.9	172.1	50.1
A4	0.003	40	2866	225.3	58.7	2713	3.6	224.0	55.1
A4	0.003	31	2762	167.4	55.4	2594	4.1	166.1	51.9
A4	0.005	21	2384	181.5	50.0	2272	3.6	180.3	47.0
A4	0.005	23	2384	188.1	49.1	2264	3.6	186.6	46.1
A4	0.006	17	2320	181.6	47.5	2216	3.6	180.5	44.7
A4	0.0008	125	2546	156.8	46.4	2396	3.9	167.0	46.1
A4	0.015	7	3120	182.7	52.0	2976	4.0	122.6	37.4
A4	0.019	4	2537	190.1	48.0	2428	3.3	189.5	45.1
A4	0.0005	172	1566	119.6	--	1561	2.3	118.4	--

Table A.2 Summary Results of Uniaxial Compression Tests for RPPs from Batches A5 and A6

Specimen Batch	Strain rate (in/in/min)	Test time (min)	At 5 % strain			Corrected Cross-sectional area			
			Strength (psi)	Secant Modulus (E _{1%} , ksi)	Secant Modulus (E _{5%} , ksi)	Strength (psi)	Strain at Peak (%)	Secant Modulus (E _{1%} , ksi)	Secant Modulus (E _{5%} , ksi)
A5	0.006	30	1744	84.8	33.8	1701	8.0	84.1	32.0
A5	0.007	22	1846	111.4	36.8	1771	7.2	110.4	34.9
A5	0.006	22	1522	68.3	29.1	1469	7.8	67.7	27.5
A5	0.006	25	1789	92.5	36.6	1721	7.3	91.8	34.7
A5	0.008	22	1591	77.4	33.2	1527	7.3	76.7	31.4
A5	0.007	25	1311	71.4	27.0	1277	7.6	70.9	26.8
A5	0.0017	109	1630	84.0	31.8	1592	7.3	83.2	30.1
A5	0.0013	112	1552	86.0	32.3	1518	7.9	85.3	30.6
A5	0.017	8	1888	96.8	38.3	1795	7.1	95.9	36.0
A5	0.012	9	2001	121.6	38.4	1874	6.1	120.3	35.9
A5	0.016	10	1910	105.6	36.9	1815	5.9	104.5	34.5
A5	0.018	8	1630	120.8	37.5	1533	4.6	119.7	35.3
A5	0.021	9	1691	92.6	33.9	1615	8.7	91.7	32.0
A6	0.006	23	1617	85.9	31.8	1549	7.5	85.0	30.0
A6	0.006	30	1625	94.1	32.9	1553	6.7	93.2	31.1
A6	0.007	18	1669	100.3	32.8	1569	5.5	99.3	30.8
A6	0.006	20	1686	101.1	34.8	1594	5.6	100.3	32.8
A6	0.007	20	1720	104.6	33.2	1607	5.0	103.4	30.9
A6	0.008	21	1664	91.6	33.2	1598	7.9	90.7	31.3
A6	0.008	16	1634	91.7	32.4	1562	5.9	91.0	30.8
A6	0.008	24	1707	94.0	34.6	1628	7.3	93.1	32.6
A6	0.007	23	1492	77.9	29.1	1432	7.9	77.1	27.3
A6	0.007	23	1578	84.2	28.4	1492	6.5	83.2	26.5
A6	0.008	19	1699	102.6	34.2	1618	6.7	101.6	32.2
A6	0.005	29	1410	86.4	28.3	1328	6.3	85.5	26.6
A6	0.007	22	1492	96.4	30.4	1410	5.1	95.5	28.7
A6	0.006	24	1427	87.6	29.6	1346	5.5	86.7	27.9
A6	0.0021	156	1311	88.1	26.8	1245	5.6	87.6	25.4
A6	0.0025	115	1256	75.4	25.0	1204	7.2	74.7	23.7
A6	0.013	14	1703	87.0	33.0	1819	17.8	91.9	40.3
A6	0.019	8	1570	98.1	30.4	1478	5.6	97.2	28.6
A6	0.021	9	1427	87.8	29.5	1370	6.7	87.0	27.9

Table A.3 Summary Results of Uniaxial Compression Tests for RPPs from Batches A10 and A11

Specimen Batch	Strain rate (in/in/min)	Test time (min)	At 5 % strain			Corrected Cross-sectional area			
			Strength (psi)	Secant Modulus (E _{1%} , ksi)	Secant Modulus (E _{5%} , ksi)	Strength (psi)	Strain at Peak (%)	Secant Modulus (E _{1%} , ksi)	Secant Modulus (E _{5%} , ksi)
A10	0.006	29	2393	106.7	50.0	2295	6.1	106.0	47.4
A10	0.005	32	2360	127.2	48.0	2256	6.0	126.4	45.8
A10	0.005	28	2291	129.3	46.2	2193	6.5	128.3	43.8
A10	0.006	33	2274	107.1	44.5	2233	7.1	106.5	42.6
A10	0.007	27	2278	105.2	45.5	2268	7.3	104.6	43.5
A10	0.008	26	2299	107.1	45.7	2250	7.0	106.4	43.5
A10	0.007	25	2066	125.7	42.2	1967	6.1	124.7	40.0
A10	0.007	24	2180	107.1	41.8	2086	6.8	106.2	39.4
A10	0.006	25	2001	97.2	40.4	1984	7.4	96.6	38.6
A10	0.007	25	1936	96.2	39.7	1910	7.3	95.6	38.0
A10	0.007	20	1997	105.7	41.5	1971	7.6	105.2	40.0
A10	0.007	24	2428	126.1	47.6	2316	6.1	125.2	45.2
A10	0.005	28	2254	124.5	45.3	2177	6.4	123.9	43.3
A10	0.006	26	2341	130.6	47.3	2256	5.9	130.0	45.3
A10	0.007	21	2191	113.0	45.0	2124	6.8	112.4	43.0
A10	0.0020	188	1776	92.6	42.1	1686	5.3	91.9	40.3
A10	0.0010	106	1567	99.9	--	1528	2.9	99.4	--
A10	0.021	6	2438	119.0	49.0	2358	6.8	118.4	46.7
A10	0.021	7	2218	111.9	45.6	2138	8.8	111.2	43.4
A11	0.005	28	2156	127.3	45.3	2053	6.4	126.3	43.0
A11	0.006	27	2405	121.5	48.7	2323	6.4	120.8	46.5
A11	0.007	18	2409	123.3	49.3	2309	5.9	122.7	47.1
A11	0.007	22	2429	109.5	48.1	2338	5.8	108.9	46.0
A11	0.005	26	2278	136.4	47.5	2184	5.5	135.7	45.4
A11	0.007	20	2025	109.0	39.1	1955	6.1	108.2	37.1
A11	0.006	23	1989	103.3	40.4	1895	6.1	102.6	38.4
A11	0.006	23	2319	107.6	47.0	2281	6.4	107.0	45.0
A11	0.006	25	2429	128.6	49.3	2350	6.4	128.0	47.2
A11	0.007	23	2356	126.7	47.9	2259	6.1	125.8	45.6
A11	0.005	26	2364	125.2	49.1	2281	5.9	124.8	47.2
A11	0.006	23	2352	121.8	47.5	2278	6.2	121.2	45.6
A11	0.005	26	2401	131.4	48.9	2293	5.6	130.6	46.6
A11	0.007	20	2295	103.3	47.6	2215	6.1	103.0	45.7
A11	0.006	23	2311	116.7	46.8	2245	6.0	116.2	44.8
A11	0.0005	227	1846	95.7	35.8	1762	4.9	95.0	33.9
A11	0.0008	164	1985	119.1	39.0	1929	6.2	118.5	37.2
A11	0.019	7	2438	129.5	45.9	2320	5.6	128.5	43.4
A11	0.020	6	2417	130.5	45.0	2305	5.9	129.5	42.6

Table A.4 Summary Results of Uniaxial Compression Tests for RPPs from Batch A12 and A13

Specimen Batch	Strain rate (in/in/min)	Test time (min)	At 5 % strain			Corrected Cross-sectional area			
			Strength (psi)	Secant Modulus (E _{1%} , ksi)	Secant Modulus (E _{5%} , ksi)	Strength (psi)	Strain at Peak (%)	Secant Modulus (E _{1%} , ksi)	Secant Modulus (E _{5%} , ksi)
A12	0.007	25	2078	98.1	41.8	1997	6.8	97.4	40.0
A12	0.008	22	2078	106.2	42.0	1993	6.2	105.5	40.0
A12	0.008	22	2058	105.2	40.6	1987	6.1	104.5	38.4
A12	0.006	28	2209	126.4	41.4	2098	5.8	125.3	39.1
A12	0.006	27	2217	125.0	44.5	2150	6.4	124.0	42.3
A12	0.006	26	2017	101.9	41.8	1873	5.5	101.0	38.8
A12	0.005	27	2005	107.6	38.7	1924	6.1	106.7	36.5
A12	0.007	23	2017	108.1	38.8	1937	6.1	107.2	36.7
A12	0.0014	107	1478	94.3	30.3	1457	4.1	94.0	28.8
A12	0.0022	97	1711	94.3	34.1	1634	5.3	93.9	32.5
A12	0.022	6	2144	102.9	39.8	2048	5.9	102.1	37.7
A12	0.021	6	2185	121.0	42.4	2076	5.7	120.3	40.3
A13	0.008	24	1680	64.5	35.3	1642	7.8	64.0	33.5
A13	0.007	22	1819	87.3	37.9	1760	7.3	86.7	36.0
A13	0.008	18	1854	103.0	35.7	1774	6.1	102.0	33.6
A13	0.007	19	2531	134.0	51.1	2409	5.5	133.1	48.5
A13	0.006	22	2613	98.5	54.6	2512	6.4	98.0	52.2
A13	0.008	18	2482	118.6	48.1	2393	6.7	117.7	45.5
A13	0.008	16	2552	129.1	50.6	2446	5.9	128.3	48.2
A13	0.005	26	2495	129.0	49.1	2402	6.1	128.1	46.6
A13	0.007	19	2478	111.9	48.9	2422	7.0	111.1	46.5
A13	0.006	22	2760	140.0	55.9	2665	6.1	139.3	53.4
A13	0.006	23	2597	132.6	52.2	2524	6.7	131.8	49.8
A13	0.007	19	2707	120.5	53.5	2623	6.7	119.5	50.7
A13	0.007	21	2380	95.7	47.5	2369	7.0	95.3	45.6
A13	0.006	25	2360	90.9	46.0	2352	7.3	90.5	44.1
A13	0.007	20	2393	98.0	46.2	2363	6.9	97.2	43.9
A13	0.0018	120	1960	113.4	38.2	1877	5.0	112.7	36.4
A13	0.0004	200	1846	90.6	37.4	1767	5.3	90.2	35.8
A13	0.018	6	2425	130.9	46.6	2307	5.6	130.0	44.3
A13	0.014	8	2552	125.0	53.1	2468	6.1	124.2	50.7

Table A.5 Summary Results of Uniaxial Compression Tests for RPPs from Batches B7 and B8

Specimen Batch	Strain rate (in/in/min)	Test time (min)	At 5 % strain			Corrected Cross-sectional area			
			Strength (psi)	Secant Modulus (E _{1%} , ksi)	Secant Modulus (E _{5%} , ksi)	Strength (psi)	Strain at Peak (%)	Secant Modulus (E _{1%} , ksi)	Secant Modulus (E _{5%} , ksi)
B7	0.008	51	1956	69.1	38.5	2496	25.9	68.5	34.4
B7	0.006	60	2066	76.2	40.6	2691	27.1	67.6	32.7
B7	0.007	37	2123	89.5	42.6	2298	16.3	88.8	40.7
B7	0.008	36	2112	65.0	40.0	2417	17.2	64.4	38.1
B7	0.005	48	2055	92.6	42.1	2245	17.8	91.9	40.3
B7	0.005	48	2055	92.6	42.1	2250	17.8	91.8	40.2
B7	0.007	44	2183	98.5	43.3	2404	18.6	97.7	41.4
B7	0.007	44	2139	91.0	43.3	2313	13.4	90.1	41.4
B7	0.007	39	1963	80.2	39.1	2165	14.6	79.5	37.3
B7	0.006	51	2117	92.0	41.2	2341	15.7	91.3	39.8
B7	0.006	44	2147	100.5	43.4	2335	13.4	99.7	41.5
B7	0.006	45	2033	82.7	41.6	2213	14.6	82.2	40.0
B7	0.008	35	2169	91.3	44.2	2362	15.7	90.7	42.4
B7	0.006	46	2055	92.4	41.3	2228	18.6	91.7	40.0
B7	0.006	41	2029	84.8	40.8	2207	18.0	84.1	39.1
B7	0.018	14	2350	110.6	46.3	2446	14.3	109.7	44.1
B7	0.021	12	2219	107.6	43.8	2319	12.3	106.8	42.1
B7	0.0020	105	1662	83.5	32.9	1599	4.9	83.0	31.6
B7	0.0021	58	1445	85.0	31.2	1507	4.3	84.5	30.2
B8	0.006	64	2236	87.4	45.1	2733	25.5	86.7	43.3
B8	0.006	52	2449	93.3	43.0	2897	25.4	92.5	41.1
B8	0.006	43	2451	124.8	50.3	2414	8.2	124.0	48.6
B8	0.005	52	2603	160.0	53.0	2489	4.7	158.1	50.5
B8	0.005	60	2603	155.0	53.5	2476	5.3	153.7	51.0
B8	0.005	43	2231	122.0	43.9	2241	11.0	121.2	42.5
B8	0.006	35	2497	153.0	48.3	2393	5.0	151.8	46.2
B8	0.005	41	2430	133.8	51.0	2328	5.3	132.8	49.0
B8	0.006	43	2633	157.5	51.8	2600	9.9	156.7	50.3
B8	0.005	41	2836	171.2	56.3	2723	3.9	170.0	53.6
B8	0.007	24	2853	181.0	51.4	2764	3.3	179.2	48.7
B8	0.005	44	2417	127.7	47.8	2412	9.9	127.0	46.4
B8	0.006	42	2514	136.0	50.7	2413	5.9	135.0	48.5
B8	0.007	37	2519	144.3	47.1	2407	4.8	143.0	44.8
B8	0.008	35	2231	116.0	45.5	2277	11.7	115.2	43.8
B8	0.0023	87	2077	124.6	41.4	2005	3.3	123.8	39.7
B8	0.0003	237	1825	119.3	--	1773	3.3	118.5	--
B8	0.019	12	2523	141.9	46.6	2376	5.0	140.1	43.7
B8	0.017	13	2751	149.1	55.4	2635	5.3	148.0	53.0

Table A.6 Summary Results of Uniaxial Compression Tests for RPPs from Batch C9

Specimen Batch	Strain rate (in/in/min)	Test time (min)	At 5 % strain			Corrected Cross-sectional area			
			Strength (psi)	Secant Modulus (E _{1%} , ksi)	Secant Modulus (E _{5%} , ksi)	Strength (psi)	Strain at Peak (%)	Secant Modulus (E _{1%} , ksi)	Secant Modulus (E _{5%} , ksi)
C9	0.008	38	2547	70.8	50.2	3063	25.4	70.0	48.1
C9	0.008	34	2705	81.1	56.3	3189	22.4	80.3	54.1
C9	0.009	28	2797	92.6	42.1	3212	24.3	91.0	54.3
C9	0.006	49	2178	71.4	42.9	2358	18.1	70.9	41.0
C9	0.008	45	2169	81.0	43.3	2354	15.7	80.4	41.5
C9	0.007	51	2350	92.9	46.5	2490	14.3	92.1	44.4
C9	0.007	54	2259	114.9	46.9	2429	13.5	113.9	44.8
C9	0.008	40	2290	83.8	47.2	2480	15.6	83.1	45.1
C9	0.005	52	2088	71.8	43.1	2287	15.0	71.3	41.4
C9	0.006	46	2164	90.3	44.7	2332	13.2	89.7	42.8
C9	0.007	43	2164	94.0	44.4	2377	16.1	93.3	42.5
C9	0.006	40	2350	86.5	48.9	2622	16.6	85.8	46.7
C9	0.005	49	2254	107.9	46.6	2395	13.2	107.0	44.6
C9	0.006	47	2246	84.5	46.0	2441	21.3	83.8	43.9
C9	0.006	51	2163	84.1	43.2	2315	13.1	83.5	41.3
C9	0.0020	137	1707	75.8	35.6	1652	5.5	75.3	34.2
C9	0.0024	157	1694	94.2	35.3	1629	4.2	93.8	33.8
C9	0.021	12	2147	91.4	44.1	2293	13.5	90.7	42.3
C9	0.022	11	2178	95.4	44.2	2308	14.0	94.7	42.3

Appendix B

Test Results for Four-Point Flexure Tests

Table B.1. Summary Results of Four-Point Flexure Tests for RPPs from Manufacturers A

Specimen Batch	Deformation rate (in/min)	Test time (min)	Flexural Strength at 2% Strain (psi)	Secant Flexural Modulus ($E_{1\%}$, ksi)	Secant Flexural Modulus ($E_{2\%}$, ksi)
A1	--	--	2429	117.0	88.5
A1	--	--	2195	110.8	88.0
A1	--	--	1594	113.9	Failed
A1	--	--	1531	112.1	Failed
A1	--	--	1387	96.4	Failed
A1	--	--	1471	94.4	Failed
A1	--	--	1462	94.6	Failed
A1	--	--	1533	98.5	Failed
A1	--	--	1407	95.1	Failed
A1	--	--	1299	97.0	Failed
A1	--	--	1461	99.0	Failed
A1	--	--	1368	100.2	Failed
A1	--	--	1321	105.8	Failed
A4	0.16	12	2275	206.7	Failed
A4	0.14	14	2561	228.3	Failed
A4	0.20	21	2795	204.1	Failed
A5	0.07	71	1362	99.7	70.2
A5	0.41	10	1848	72.6	Failed
A5	0.26	18	1573	107.0	75.5
A5	0.17	52	1425	105.4	71.0
A5	0.25	36	1504	104.9	73.7
A6	0.13	62	1369	90.2	62.7
A6	0.14	56	1425	107.1	70.4
A6	0.17	44	1241	86.8	64.5
A6	0.12	72	1256	89.4	65.1
A6	0.10	57	1233	78.0	62.0
A6	0.18	38	1475	98.7	71.3
A6	0.17	37	1519	112.3	79.4
A10	0.16	36	1707	131.3	80.8
A10	0.19	33	1539	117.1	74.6
A10	0.20	33	1609	130.8	77.1
A10	0.19	34	1350	80.7	57.1
A10	0.17	33	1716	144.0	84.9
A10	0.19	33	1652	133.3	80.8

Table B.2 Summary Results of Four-Point Flexure Tests for RPPs from Manufacturers B and C

Specimen Batch	Deformation rate (in/min)	Test time (min)	Flexural Strength at 2% Strain (psi)	Secant Flexural Modulus ($E_{1\%}$, ksi)	Secant Flexural Modulus ($E_{2\%}$, ksi)
B7	0.16	31	1295	78.9	61.7
B7	0.17	38	1530	87.6	66.5
B7	0.17	36	1522	86.7	66.5
B7	0.19	35	1438	94.5	72.8
B7	0.15	40	1569	97.8	71.7
B7	0.19	35	1647	96.0	72.8
B7	0.18	38	1535	89.2	67.9
B8	0.19	37	3449	233.0	175.0
B8	0.18	35	3415	240.3	176.9
B8	0.16	36	4296	291.0	204.5
B8	0.18	34	3520	236.1	167.7
B8	0.16	42	3560	228.2	177.0
B8	0.17	38	3295	227.7	170.0
C9	0.13	39	1686	105.9	81.4
C9	0.13	34	1761	100.6	84.8
C9	0.18	37	1678	106.9	81.9
C9	0.19	35	1741	113.7	85.8
C9	0.18	36	1670	107.7	81.1
C9	0.16	40	1654	106.1	81.4
C9	0.16	42	1685	106.3	83.3

Appendix C

Test Results for Flexural Creep and Compressive Creep Tests

Flexural Creep

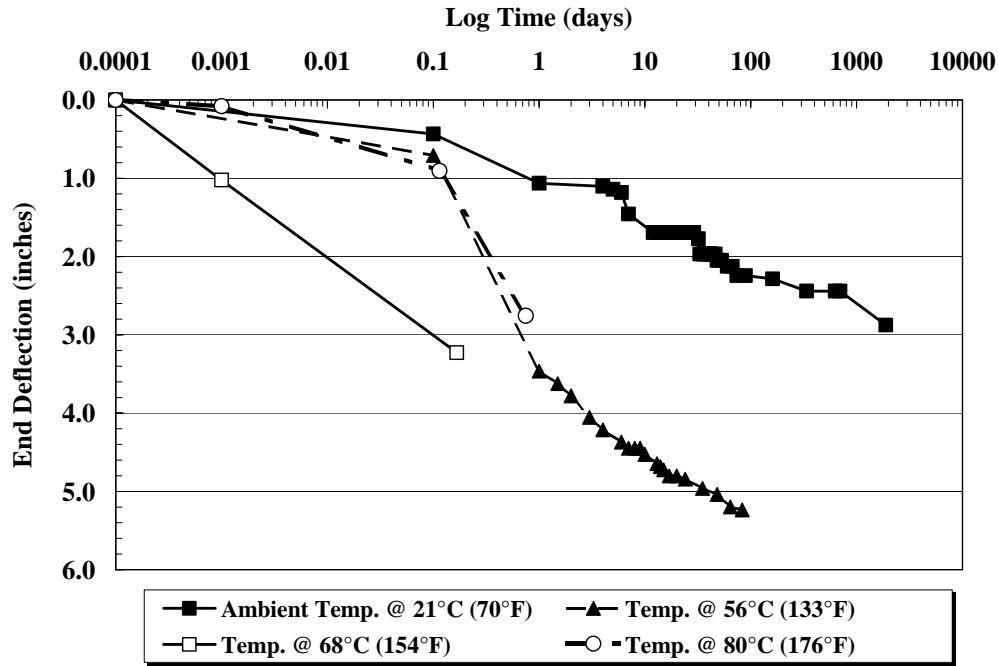


Figure C.1 End deflection versus time response for RPPs loaded with 35-Lb single load under various temperatures.

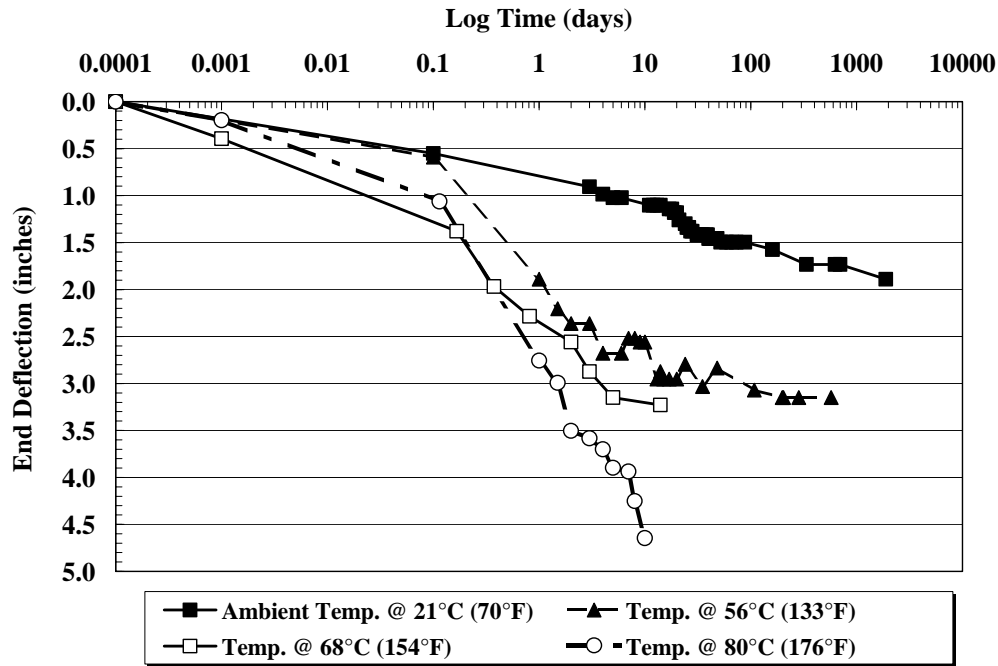


Figure C.2 End deflection versus time response for RPPs loaded with 21-Lb single load under various temperatures.

Flexural Creep

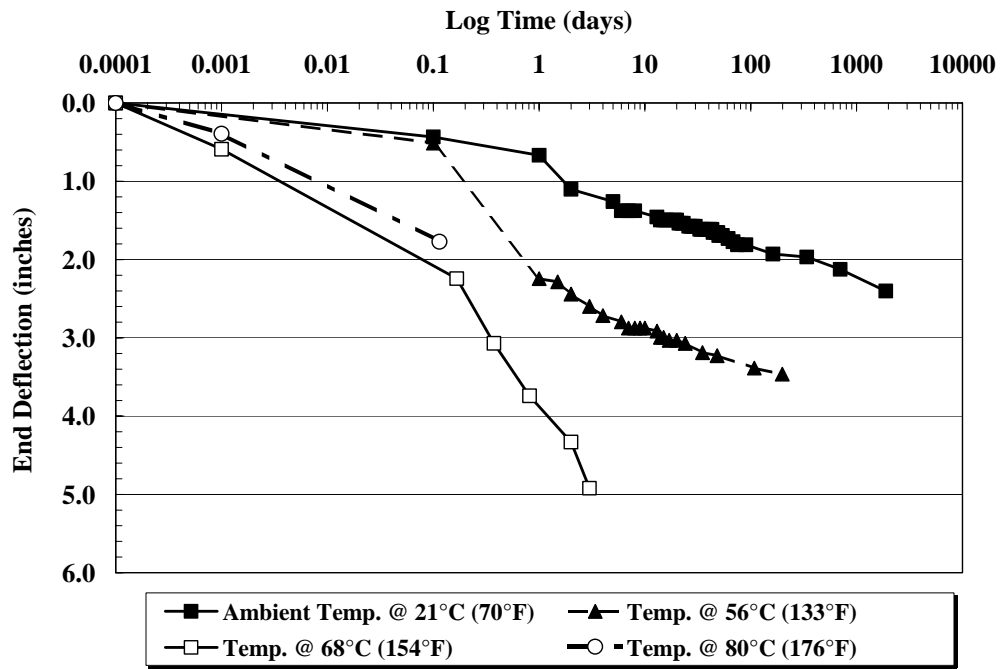


Figure C.3 End deflection versus time response for RPPs loaded with five 10-Lb loads under various temperatures.

Flexural Creep: Arrhenius Modeling for Long-term Bending Behavior

Data for single 35-Lb weight - Time to reach failure (breaking)

Temp (°C)	1/temp (°C ⁻¹)	Temp (°K)	1/temp (°K ⁻¹)	Time (day)	Time (day)	Avg. Time (day)	1/avg. time (d ⁻¹)	ln(1/ avg. t) (d ⁻¹)	Comment
21	0.0476	294	0.0034	697	697	697	0.0014	-6.547	Not failed (July, 2003)
56	0.0179	329	0.0030	35	108	71.5	0.0140	-4.270	Failed
68	0.0147	341	0.0029	0.375	0.81	0.59	1.6878	0.523	Failed
80	0.0125	353	0.0028	0.75	0.75	0.75	1.3333	0.288	Failed

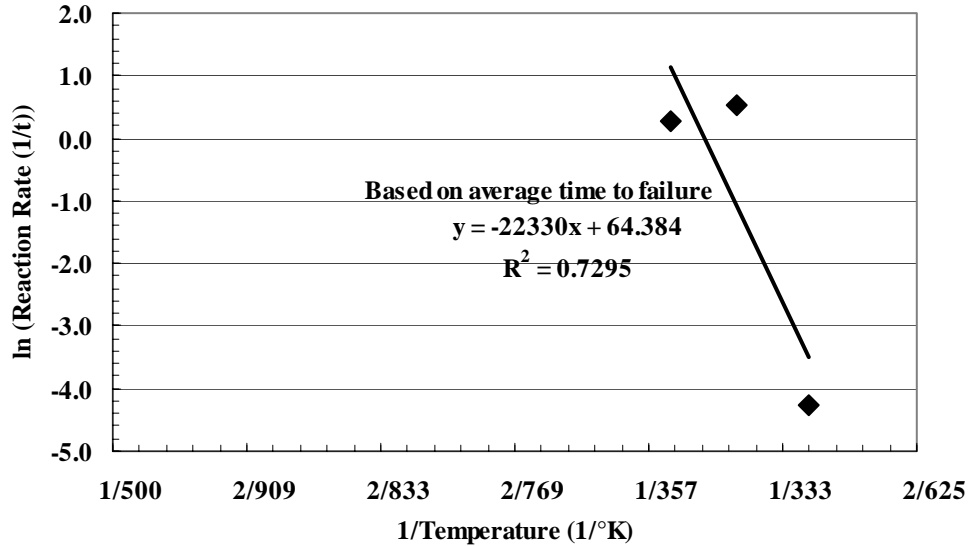


Figure C.4 Arrhenius plot for flexural creep test on 2 in.x 2 in.x 24 in. RPPs loaded with a 35-Lb weight at the end of a simple cantilever under various temperatures.

$$\ln(1/t) = -22330(1/T) + 64.384$$

where t = time to reach failure (defined here as breaking).

T = temperature (°K) at which RPP will be in the field (Assumed = 21°C = 294°K).

∴ $t = 105702$ days (290 years) (under the single 35-Lb cantilever load).

Flexural Creep: Arrhenius Modeling for Long-term Bending Behavior

Data for single 21-Lb weight - Time to reach failure (breaking)

Temp (°C)	1/temp (°C ⁻¹)	Temp (°K)	1/temp (°K ⁻¹)	Time (day)	Time (day)	Avg. Time (day)	1/ avg. time (d ⁻¹)	Ln(1/ avg. t) (d ⁻¹)	Comment
21	0.0476	294	0.0034	697	697	697	0.00143	-6.5468	Not failed (July, 2003)
56	0.0179	329	0.0030	574	574	574	0.00174	-6.3526	Not failed
68	0.0147	341	0.0029	48	49	48.5	0.02062	-3.8816	Failed
80	0.0125	353	0.0028	6	11	8.5	0.11765	-2.1401	Failed

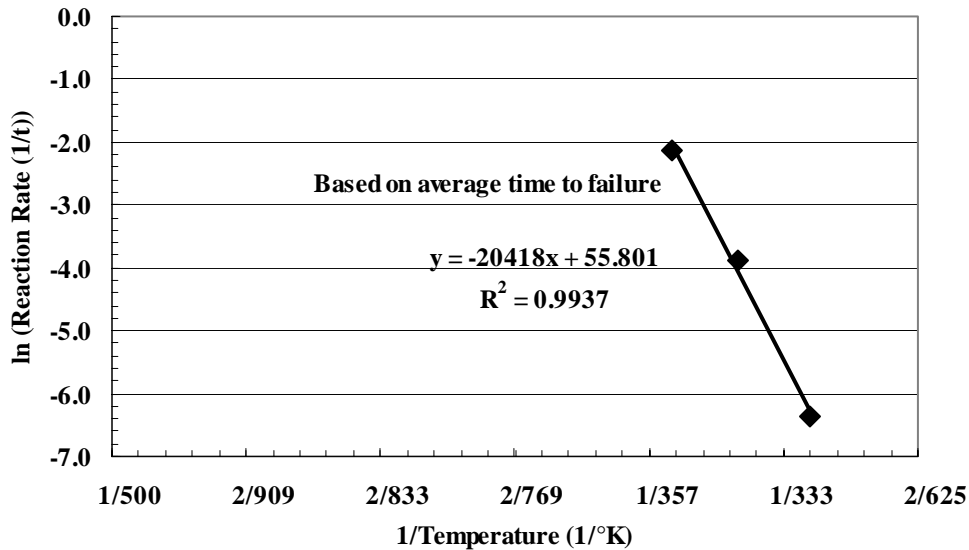


Figure C.5 Arrhenius plot for flexural creep test on 2 in.x 2 in.x 24 in. RPPs loaded with a 21-Lb weight at the end of a simple cantilever under various temperatures.

$$\ln(1/t) = -20418(1/T) + 55.801$$

where t = time to reach failure (defined here as breaking).

T = temperature (°K) at which RPP will be in the field (Assumed = 21°C = 294°K).

$\therefore t = 845750$ days (2317 years) (under the single 21-Lb cantilever load).

Flexural Creep: Arrhenius Modeling for Long-term Bending Behavior

Data for 5 @ 10-Lb weights - Time to reach failure (breaking)

Temp (°C)	1/temp (°C-1)	Temp (°K)	1/temp (°K-1)	Time (day)	Time (day)	Avg. Time (day)	1/ avg. time (d-1)	ln(1/ avg. t) (d-1)	Comment
21	0.0476	294	0.0034	697	697	697	0.00143	-6.5468	Not failed (July, 2003)
56	0.0179	329	0.0030	189	200	194.5	0.00514	-5.2704	Failed
68	0.0147	341	0.0029	2	5	3.5	0.28571	-1.2528	Failed
80	0.0125	353	0.0028	0.75	0.75	0.75	1.33333	0.2877	Failed

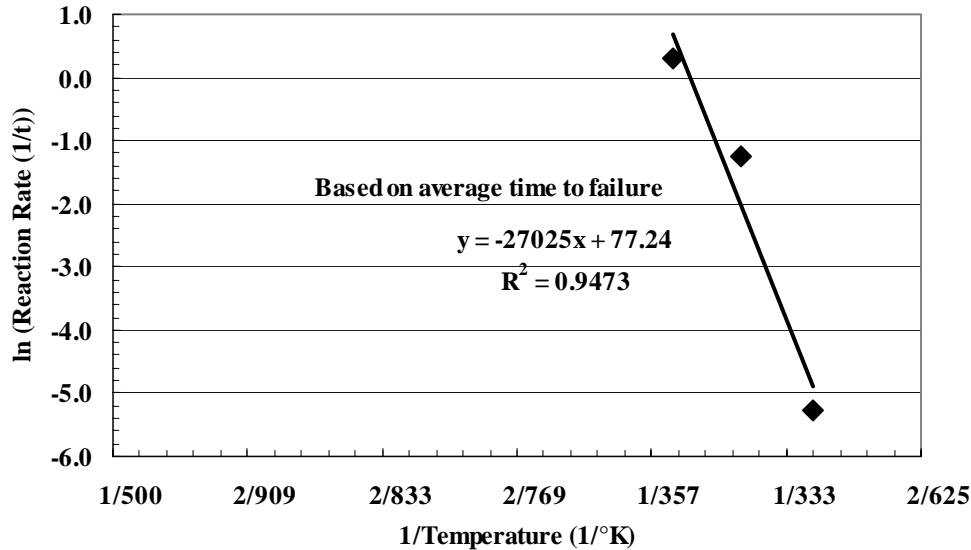


Figure C.6 Arrhenius plot for flexural creep test on 2 in.x 2 in.x 24 in. RPPs loaded with five 10-Lb loads on a simple cantilever under various temperatures.

$$\ln(1/t) = -27025(1/T) + 77.24$$

where t = time to reach failure (defined here as breaking).

T = temperature (°K) at which RPP will be in the field (Assumed = 21°C = 294°K).

$\therefore t = 2.38 \times 10^6$ days (6515 years) (under five 10-Lb evenly distributed loads on cantilever).

Compressive Creep

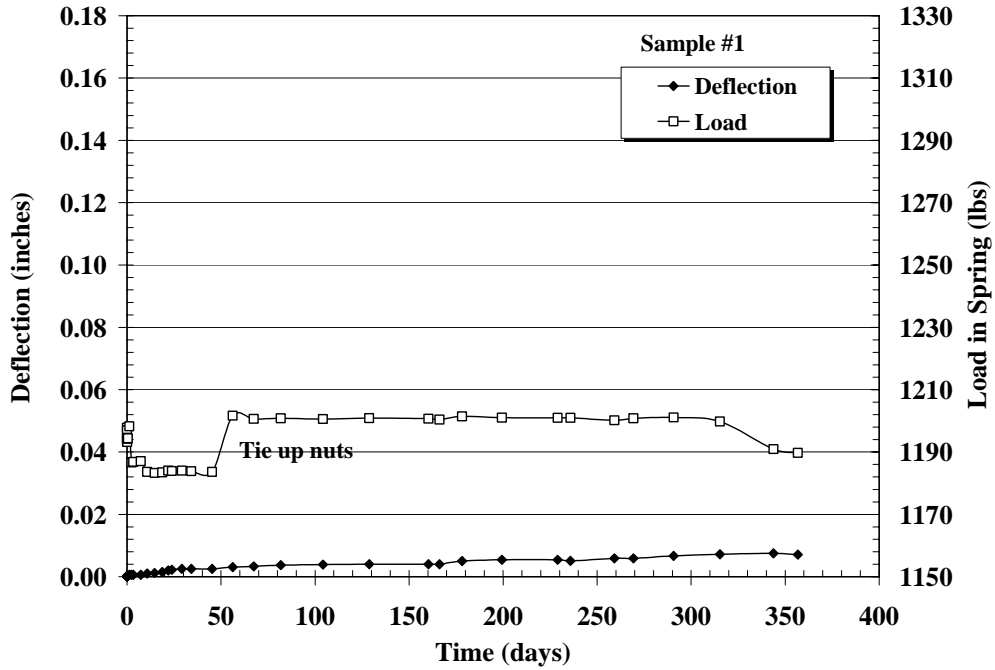


Figure C.7 Deflection versus time of the RPPs from batch A6 under constant axial stress (Sample #1).

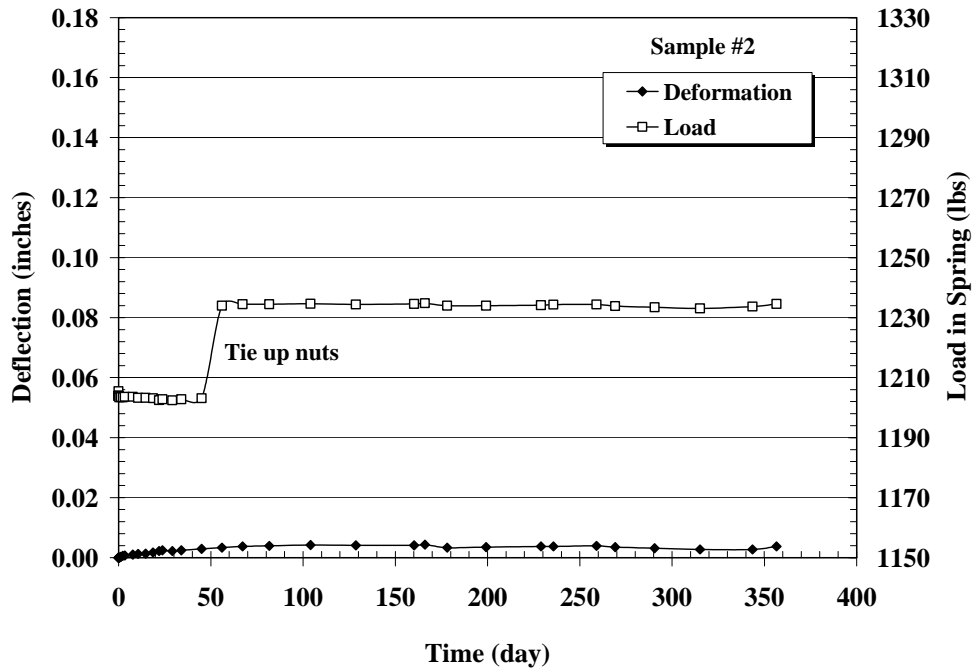


Figure C.8 Deflection versus time of the RPPs from batch A6 under constant axial stress (Sample #2).

Compressive Creep

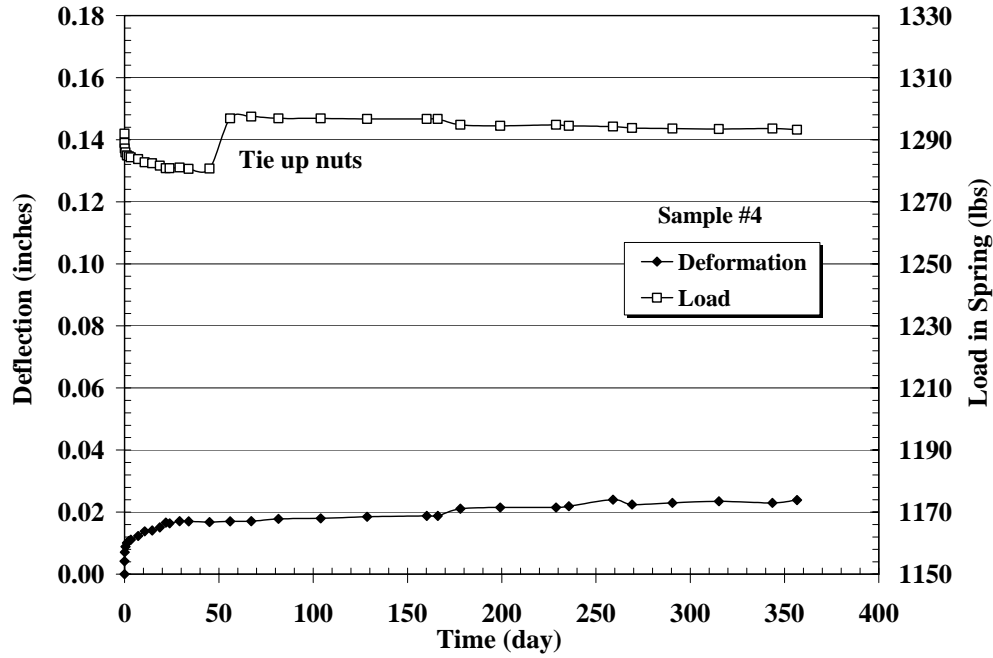


Figure C.9 Deflection versus time of the RPPs from batch C9 under constant axial stress (Sample #4).

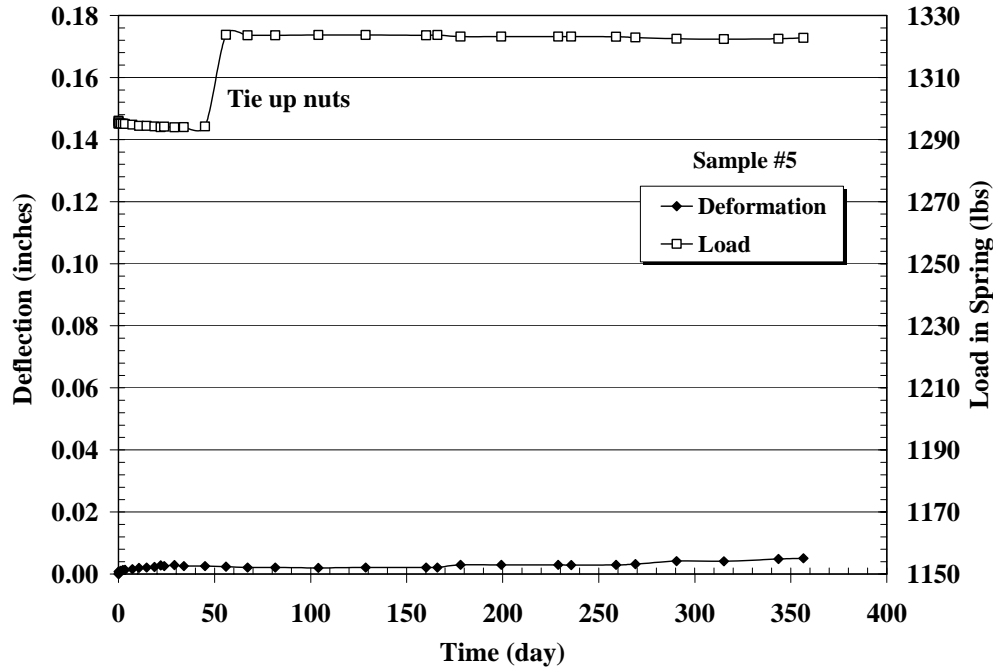


Figure C.10 Deflection versus time of the RPPs from batch A3 under constant axial stress (Sample #5).

Compressive Creep

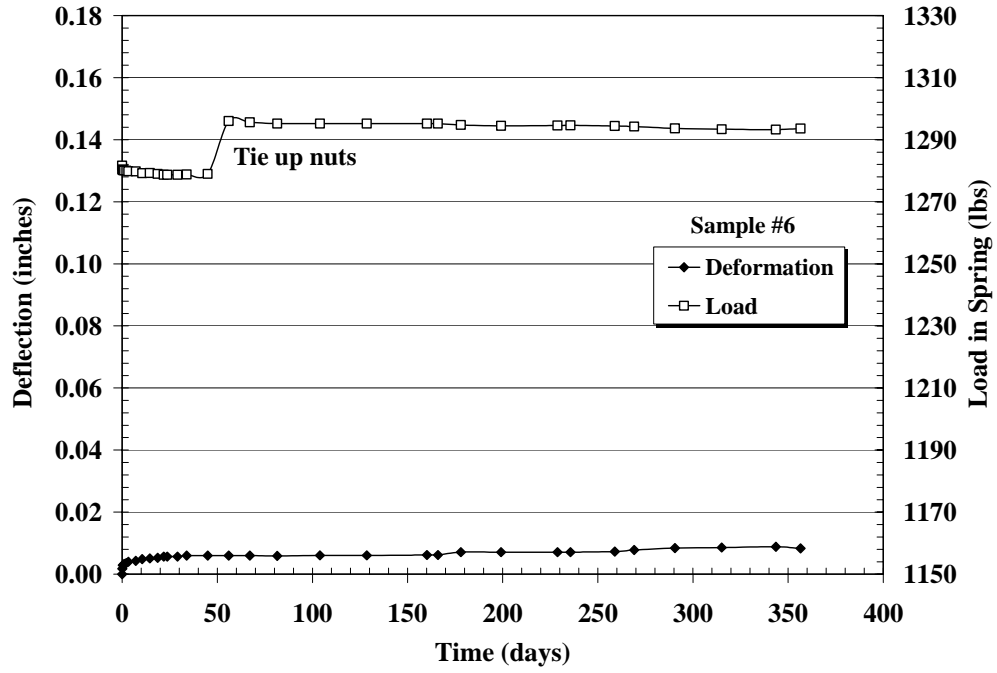


Figure C.11 Deflection versus time of the RPPs from batch A3 under constant axial stress (Sample #6).

Appendix D

RPP Penetration Rate Frequency Distribution for Field Installations

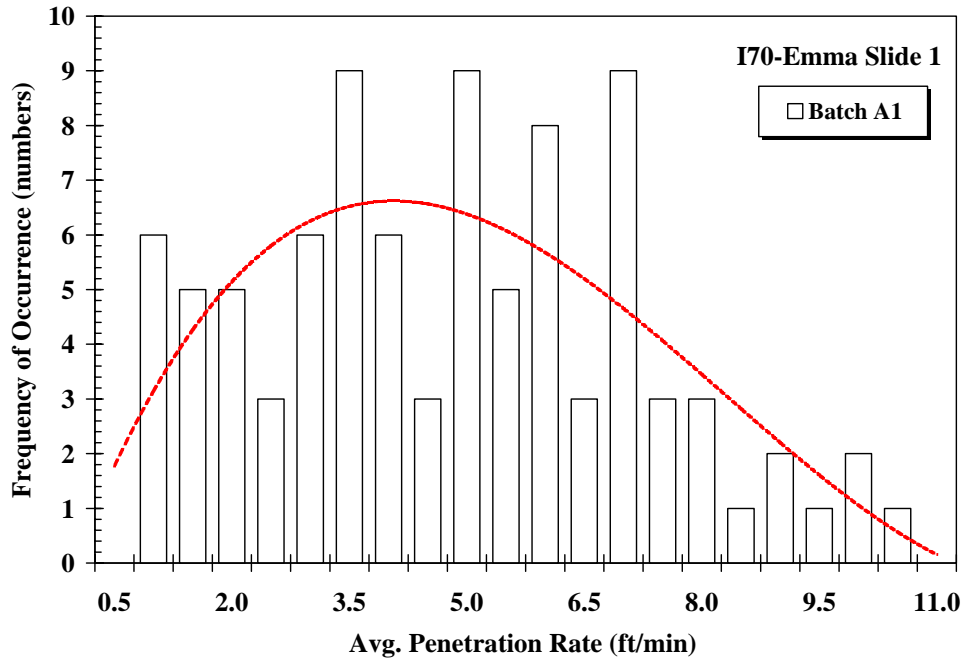


Figure D.1 Penetration rate frequency distribution for RPPs installed at the I70-Emma slide 1.

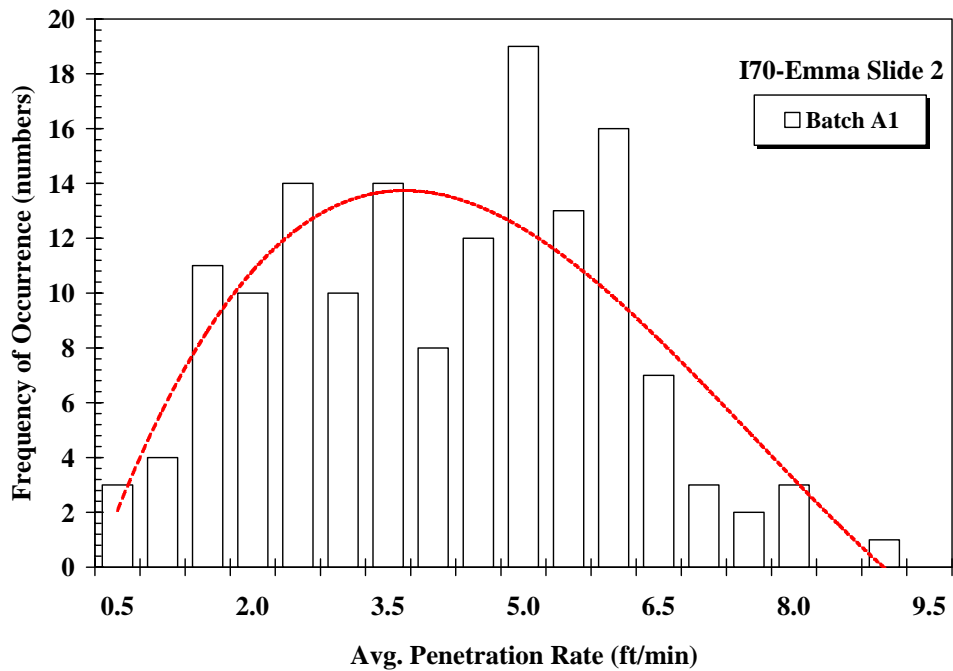


Figure D.2 Penetration rate frequency distribution for RPPs installed at the I70-Emma slide 2.

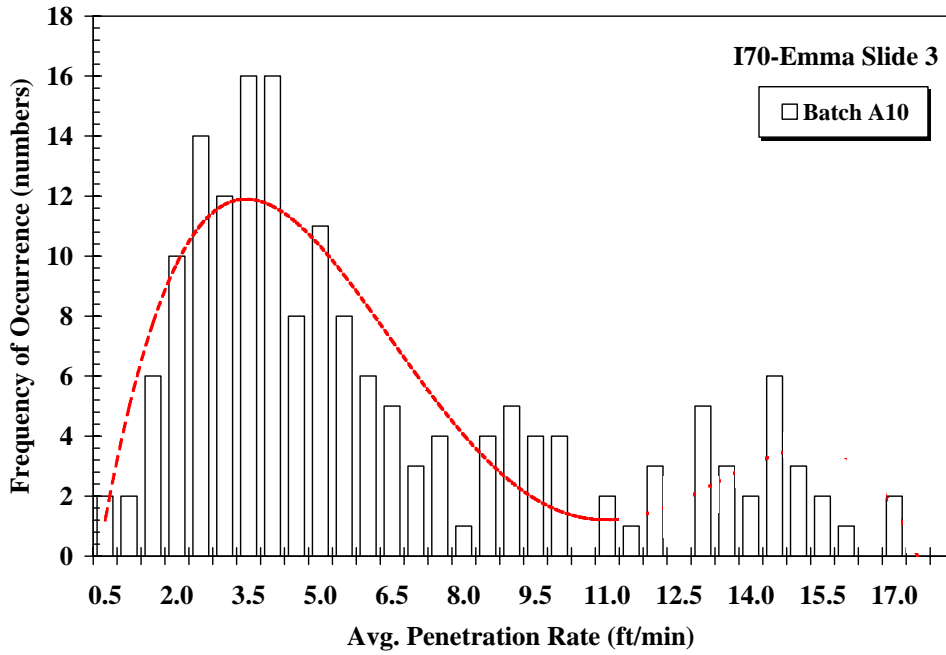


Figure D.3 Penetration rate frequency distribution for RPPs installed at the I70-Emma slide 3.

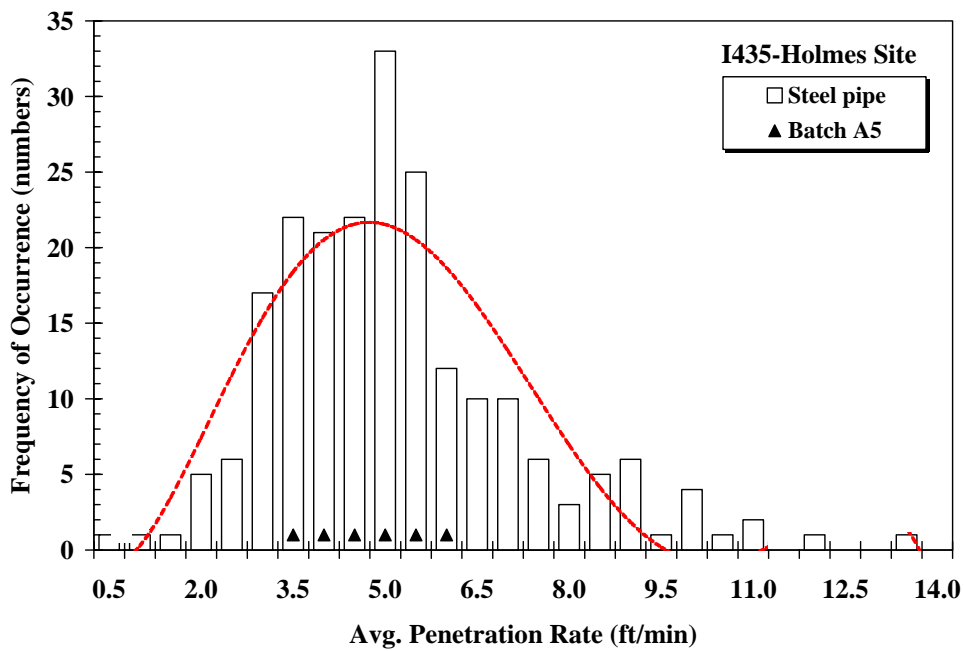


Figure D.4 Penetration rate frequency distribution for RPPs installed at the I435-Holmes site.

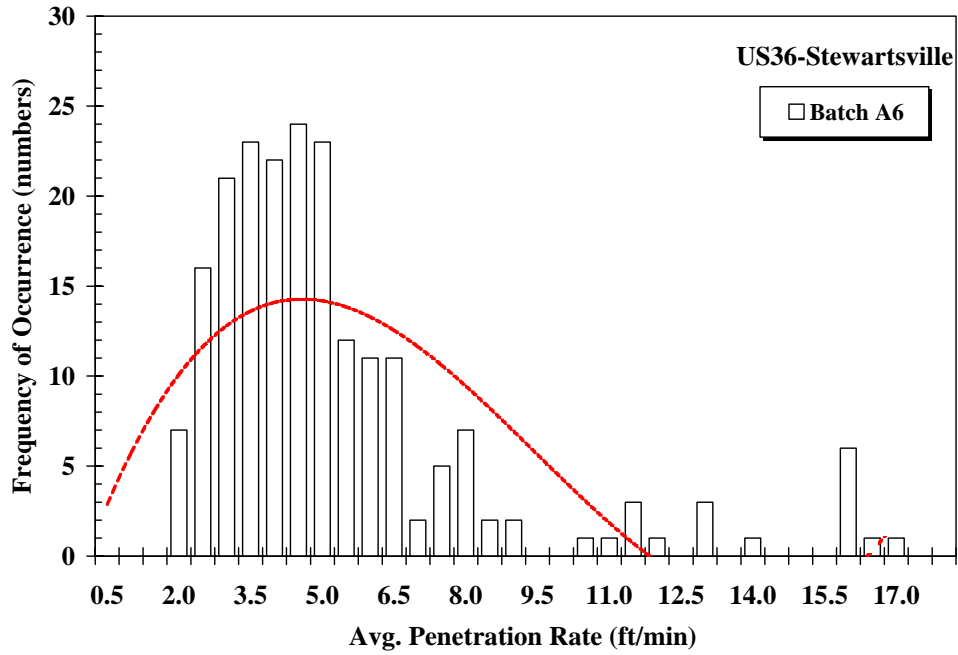


Figure D.5 Penetration rate frequency distribution for RPPs installed at US36-Stewartsville site.

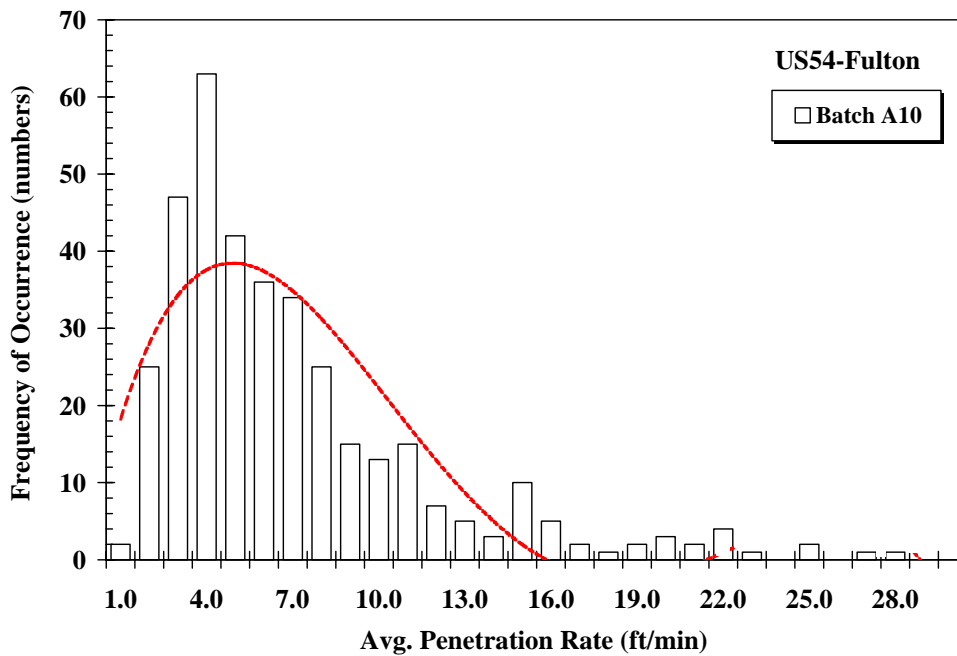


Figure D.6 Penetration rate frequency distribution for RPPs installed at US54-Fulton site.

Appendix E

Draft AASHTO Provisional Specification for Recycled Plastic Pins Used to Stabilize Slopes

Standard Specification for**Recycled Plastic Pins Used to Stabilize Slopes****AASHTO Designation: MP ##-##**

1. SCOPE

- 1.1 This specification covers recycled plastic lumber produced from industrial by products and post-consumer waste materials, for use as slender member units for stabilization of earthen slopes.
- 1.2 This specification provides minimum engineering properties for the recycled plastic members to be considered for use in slope stabilization. Also provided are the testing protocols to be used to determine the engineering properties of candidate recycled plastic members. Alternative methods are provided for qualifying the recycled plastic members.

2. REFERENCED DOCUMENTS**2.1 *ASTM Standards:***

- ASTM D6108 (1997a), "Standard Test Method for Compressive Properties of Plastic Lumber and Shapes," Section 8, Vol. 8.03.
- ASTM D6109 (1997b), "Standard Test Method for Flexural Properties of Unreinforced and Reinforced Plastic Lumber," Section 8, Vol. 8.03.
- ASTM D6111 (1997c), "Standard Test Methods for Bulk Density and Specific Gravity of Plastic Lumber and Shapes by Displacement," Section 8, Vol. 8.03.
- ASTM D6112 (1997d), "Standard Test Methods for Compressive and Flexural Creep and Creep-Ruptured of Plastic Lumber and Shapes," Section 8, Vol. 8.03.

2.2 *Other Documents*

- Loehr JE, Bowders JJ and Salim H (2000) "Slope Stabilization Using Recycled Plastic Pins – Constructability," *Final Report*, RDT 00-007, Research Investigation 98-007, Missouri Department of Transportation, 74pp.
- Loehr JE, Bowders JJ (2003) "Slope Stabilization Using Recycled Plastic Pins: Phase II - Assessment in Varied Site Conditions" *Final Report*, RDT 03-016, Research Investigation 98-007B, Missouri Department of Transportation.

3. GENERAL DESCRIPTION

- 3.1 Slender recycled plastic pins (RPPs) can be used to stabilize earthen slopes by driving the RPPs into the face of the slope to intercept the sliding surface and "pin" the slope.

- 3.2 Recycled plastic pins (RPPs) are manufactured from industrial by-products or post-consumer waste consisting predominantly of polymeric materials (usually high or low density polyethylene).
- 3.3 Typically, recycled plastic pins are composed of the following: High Density Polyethylene (HDPE) (55 percent to 70 percent), Low Density Polyethylene (LDPE) (5 percent to 10 percent), Polystyrene (PS) (2 percent to 10 percent), Polypropylene (PP) (2 percent to 7 percent), Polyethylene-terephthalate (PET) (1 percent to 5 percent), and varying amounts of additives (sawdust, fly ash, and other by-products) (0 percent to 5 percent).
- 3.4 Two main processes are commonly used to produce recycled plastic pins: compression molding and extrusion forming.
 - 3.4.1 In compression molding, the constituent waste streams are pulverized, blended together, heated until partially melted, and then compression formed in molds. In this process, the raw material is compressed into desired shapes and dimensions and is cured with heat and pressure.
 - 3.4.2 Extrusion forming includes steps similar to compression molding; however, the molten composite material is forced through a die of the desired cross-section for the member being produced in lieu of compression into a mold. An advantage of the extrusion process is that it is relatively easy to manufacture members of any desired length while the compression molding process requires different molds for each different member length.
- 3.5 Recycled plastic pins acceptable for slope stabilization applications must meet the strength, flexure and durability criteria outlined in Section 4.

4. REQUIRED PROPERTIES

- 4.1 Recycled plastic pins specified for slope stabilization application must meet the criteria specified in Table 1. The parameters must be determined in accordance with the testing protocols listed and described in Section 5.
- 4.2 The design compressive strength must be equal to or greater than 1500 psi at less than or equal to five percent strain measured at a strain rate of 0.00003 in/in/min.
- 4.3 The design flexural strength must be equal to or greater than 1200 psi at less than or equal to two percent center strain measured at a crosshead motion rate of 0.02 in/in/min.

5. TEST METHODS

- 5.1 The measured strengths of RPPs are greatly influenced by the strain rate. The assumed field strain rate is on the order of 0.00003 in/in/min, which correlates

with a compressive failure of a standard 3.5-in. x 3.5-in. RPP under a continuous rate of deformation for one week. Measured compressive strength of the RPP decreases as the strain rate used in the test decreases. The rate of decrease in strength is a function of the material type. For the RPPs tested in one program, the average decrease in strength was about 20 percent per log cycle decrease in the strain rate, i.e., an RPP with a compressive strength of 1000 psi at a strain rate of 0.03 in/in/min will show a compressive strength of 600 psi if tested at a strain rate of 0.0003 in/in/min. Due to the dependence on strain rate, it is imperative to make the required minimum strengths a function of the testing strain rate.

Table 1 – Minimum Properties for Recycled Plastic Pins Utilized in Slope Stabilization Applications.

Property	Minimum Requirements	
Uniaxial Compression Strength, σ_c (ASTM D6108)	A. $\sigma_c \geq 1500$ psi, axial strain \leq five percent, strain rate = 0.00003 in/in/min, or	
	Alt A1. Develop expression for the strain rate effects and correct measured strength to the design strain rate, or	
	Strain Rate (in/in/min)	No. of Compression Tests
	0.03	2
	0.003	2
	0.0003	2
	Alt A2. $\sigma_c \geq 3750$ psi, axial strain \leq five percent, strain rate = 0.03 in/in/min.	
Flexural Strength, σ_f (ASTM D6109)	B. $\sigma_f \geq 1200$ psi, center strain \leq two percent, rate of crosshead motion = 0.02 in/min, or	
	Alt B1. $\sigma_f \geq 2000$ psi, center strain \leq two percent, rate of crosshead motion = 1.9 in/min.	
Durability - Environmental Exposure	C. Polymeric Constituent $>$ 60% of mass of product, or	
	Alt C1. Less than 10% reduction in compressive strength after 100 days exposure.	
Durability - Creep	D. No bending failure during 100 days under a constant load that produces an extreme fiber stress not less than 50% of the design compressive stress, or	
	Alt D1. Testing and Arrhenius modeling showing that the RPPs do not fail during the desired design life for the facility.	

- 5.2 The “design” compressive (1500 psi) and flexural (1200 psi) strengths (measured at field strain rates, presented in Table 5.1, represent the required minimum mechanical properties for RPPs to be used in stabilization of slopes. The values are used in design of the stabilized field slopes and are determined at the field strain rate of 0.00003 in/in/min. Ideally, all RPP specimens should be tested at the field strain rate; however, from a practical perspective testing at this strain rate

- requires about one week per compression specimen which is not practical for production facilities.
- 5.3 Alternatives for qualifying an RPP material include:
- 5.3.1 (Alt A1) - Establish a compressive strength versus strain rate behavior and estimate the compressive strength at the field strain rate, or
- 5.3.2 (Alt A2) - A compressive strength of 3750 psi (25.9 MPa) or better when tested at the ASTM D6108 strain rate of 0.03 in/in/min (0.03 mm/mm/min). The latter value represents the increase in strength realized by the 3-order of magnitude increase in strain rate, i.e., above the field strain rate of 0.00003 in/in/min, using a reasonable upper-bound for strain rate effects.
- 5.3.2.1 Because Alt. A2 uses an upper-bound most manufacturers will find that they can meet the specification more easily by establishing strain rate effects for their specific products rather than using the default relation assumed for Alt. A2.
- 5.4 The second part of the specification for mechanical properties is the required minimum flexural strength of 1200 psi at less than or equal to two percent center strain, when tested in four-point flexure using a crosshead displacement rate of 0.02 in/min (results in a strain rate of 0.00003 in/in/min).
- 5.4.1 (Alt B1) - If the ASTM D6109 crosshead deformation rate of 1.9 in/min is used, the required flexural strength is at least 2000 psi at less than or equal to two percent center strain. Again, the increase in required strength for the higher deformation rate is due to the effect that loading rate has on the resulting strength of the RPP.
- 5.5 In addition to mechanical properties, the candidate RPPs must meet several durability criteria. Recycled plastic materials can have significant variability with respect to constituents and manufacturing processes. The durability of the finished product will influence its suitability for application to slope stabilizations. Two durability facets, environmental degradation and creep, must be considered.
- 5.5.1 To address environmental degradation, the polymeric content of the RPPs should be greater than 60 percent of the mass to reduce the effect of environmental exposures.
- 5.5.2 To address the issue of creep, the RPP should not fail (break) under a cantilever bending load that generates an extreme fiber stress of 75 percent of the ultimate tensile strength when subjected to the load for 100 days.
- 5.5.3 Exposure testing and Arrhenius modeling are offered as alternate means to qualify a material's durability properties.

- 5.6 It should be noted that in any slope stabilization design using RPPs, the designer can vary the stabilization scheme through variation of the number, location, strength and stiffness of the RPPs. The designer can also change the parameters by changing the factor of safety desired for the stabilized slope. Thus, the designer has numerous options for stabilization schemes and as such the required engineering properties of the RPPs could vary considerably.

6 KEYWORDS

- 6.1 Slope Stabilization, Embankments, Highways, Cuts, Excavations, Recycled Plastic Lumber, Plastic By-Products, Post-Consumer Waste, Compressive Strength, Flexural Strength, Durability, Creep.

REFERENCES

1. American Plastics Council (2002), "2001 National Post-consumer Plastics Recycling Report," R. W. Beck, Inc. Washington, D.C.
2. ASTM D6108 (1997a), "Standard Test Method for Compressive Properties of Plastic Lumber and Shapes," Section 8, Vol. 8.03.
3. ASTM D6109 (1997b), "Standard Test Method for Flexural Properties of Unreinforced and Reinforced Plastic Lumber," Section 8, Vol. 8.03.
4. ASTM D6111 (1997c), "Standard Test Methods for Bulk Density and Specific Gravity of Plastic Lumber and Shapes by Displacement," Section 8, Vol. 8.03.
5. ASTM D6112 (1997d), "Standard Test Methods for Compressive and Flexural Creep and Creep-Ruptured of Plastic Lumber and Shapes," Section 8, Vol. 8.03.
6. Birley A.W., B. Haworth, and J. Batchelor (1991), "Physics of Plastics," Oxford University Press, New York.
7. Breslin, V.T., U. Senturk, and C.C. Berndt (1998), "Long-term Engineering Properties of Recycled Plastic Lumber Used in Pier construction," *Resources Conservation and Recycling*, Vol. 23, pp. 243-258.
8. Bruce, A.H., G.R. Brenniman, and W.H. Hallenbeck (1992), *Mixed Plastics Recycling Technology*, Noyes Data Corporation, Park Ridge.
9. Koerner, R.M., Y.H. Halse, and A.E. Lord (1990), "Long-term Durability and aging of geomembranes," *Waste Containment Systems: Construction, Regulation, and Performance, Geotechnical Special Publication*, No. 26, pp. 106-137.
10. Koerner, R.M. (1998), *Designing with Geosynthetics*, 4th Ed, Prentice Hall, New Jersey.
11. Lampo, R.G. and T.J. Nosker (1997), Development and Testing of Plastic Lumber Materials for Construction Applications, Report TR 97/95, US Army Construction Engineering Research Laboratories, Champaign, Illinois.
12. Loehr, J.E., J.J. Bowders, and H. Salim (2000a), *Slope Stabilization Using Recycled Plastic Pins- Constructability*. Report RDT 00-007, RI 98-007, Missouri Dept of Transportation, Jefferson City, Missouri.

13. Loehr J.E., J.J. Bowders, L. Sommers, J.W. Owen, and W. Liew (2000b), "Stabilization of Slopes Using Recycled Plastic Pins," *Transportation Research Record: Journal of the Transportation Research Board*, No. 1714, Paper No. 00-1435, pp. 1-8.
14. McLaren, M.G. (1995), "Recycled Plastic Lumber and Shapes, Design and Specifications. *Proceeding of the 13th Structures Congress*, Vol. 1, ASCE, pp. 819-833.
15. National Research Council Special Report (1996), "Landslides: Investigation and Mitigation," Report No. 247, A.K. Turner and R.L. Schuster, editors, Transportation Research Board, pp. 673.
16. Osman, H.E., D.J. Elwell, G. Glath, and M. Hiris (1999), "Noise Barriers Using Recycled-Plastic Lumber," *Transportation Research Record: Journal of the Transportation Research Board*, No. 1670, Paper No. 99-2100, pp. 49-58.
17. Parra, J.R., J.E. Loehr, D.J. Hagemeyer, and J.J. Bowders (2003) "Field Performance of Embankments Stabilized with Recycled Plastic Reinforcement," Presented at 82nd Annual Meeting of the Transportation Research Board, Washington, D.C.
18. Sommers L., J.E. Loehr, and J.J. Bowders (2000), "Construction Method for Slope Stabilization Using Recycled Plastic Pins," *Proceedings of the Mid-continent Transportation Symposium*, May 15-16, Iowa State University, pp. 254-258.
19. Timoshenko S.P., and J.M. Gere (1972), "*Mechanics of Materials*," VanNostrand, New York.